https://doi.org/10.5194/egusphere-2025-6290
Preprint. Discussion started: 29 December 2025

Pleistocene Benthic Foraminifer Bioevents in the Central Arctic Ocean: stratigraphic and paleoceanographic implications

Jutta Wollenburg[1], Jens Matthiessen[1]

[1]Wegner Institute Helmholtz Centre for Polar and Marine Research, Bremerhaven, 27515, Germany

Correspondence to: Jutta Wollenburg (jutta.wollenburg@awi.de)

Abstract. Benthic foraminifers show distinct temporal and spatial distribution patterns in the Central Arctic Ocean (CAO) demonstrating their potential to provide robust age constraints and to address paleoceanographic change in the Pleistocene. Several benthic foraminifer bioevents have been previously reported from the upper and middle Pleistocene that are here critically evaluated by studying three sediment cores from the Mendeleev and Lomonosov ridges and analysing published data sets. Based on this data bioevents are defined by using absolute abundances of species in the >63 µm grain size fraction, whereas relative abundances are considered not reliable because taphonomic processes such as disintegration and/or dissolution overprint the original assemblage composition. Bioevents are calibrated to lithological horizons and then linked to Quaternary subseries and marine isotope stages based on available independent stratigraphic data.

Three calcareous bioevents can be defined in the Brunhes Chron (Middle Pleistocene): (1) the highest common occurrence of *Bolivina arctica* (~MIS 9) at the top of lithological unit L in brown bed B 7, (2) the lowest common occurrence of *Oridorsalis umbonatus* at the base of brown bed ?B 4 (~MIS 7), and (3) the acme of *Bulimina aculeata* (~MIS 7) in brown bed ?B 4 in water depths of less than ~2000 m. The lowest common occurrence of *Oridorsalis umbonatus* is coeval with the base of the acme of *Bulimina aculeata* at shallow sites (<2000 m). The proposed correlation to marine isotope stages should be considered provisional and subject to modifications as additional age tie-points become available. So far numerical ages for these bioevents are too imprecise due to the limited number of biostratigraphic and radiometric ages.

Further benthic foraminifer bioevents may be useful for stratigraphic correlation on a regional to supra-regional scale but require evaluation of previous taxonomic identifications and additional sediment core studies. The extinct agglutinated species *Haplophragmoides obscurus* disappeared on Lomonosov Ridge in the Middle Pleistocene but the complex taxonomy and the few data on the occurrence in arctic sediment cores currently prohibits the application as biostratigraphic marker. The assemblage turnover from agglutinated to calcareous benthic foraminifera occurred close to the first downcore change of normal to reverse magnetic polarity and might be a synchronous event in the eastern Arctic Ocean in middle Pleistocene sediments older than MIS 11 indicating a possible relation to the mid-Brunhes event. This fundamental change in assemblage composition is time-transgressive because it probably occurred in the Amerasian Basin in the Early Pleistocene. However, there is sedimentological evidence for a significant gap in the sedimentary sequences on Lomonosov Ridge at the stratigraphic level of the assemblage turnover. Since stratigraphic tie-points are not available for the sequences below this event, it remains

https://doi.org/10.5194/egusphere-2025-6290
Preprint. Discussion started: 29 December 2025

speculative if the ages are closer to each other in both basins.

In the Late Pleistocene the identification of bioevents is hampered by sporadic occurrences of benthic foraminifera, and the disputable chronostratigraphy due to possible hiati and/or condensed sections in MIS 2 to MIS 5 sediments. The identification of MIS 5 is a controversial issue, and it might be missing in some cores from Lomonosov Ridge, possibly due to extensive carbonate dissolution, while certain brown layers in the Amerasian Basin are potential candidates for this interglacial. The acme of *Siphotextularia rolshauseni* that was previously described as stratigraphic marker for MIS 2 sediments in the Norwegian-Greenland Sea can only be used in the Fram Strait area and at the upper continental slope of the northern Barents Sea. *Pullenia bulloides*, frequently used to identify MIS 5a in polar to subpolar sediments, is only sporadically present in Pleistocene sediments from the CAO and is not confined to a specific stratigraphic interval. Since this species shows variable abundances in cores from water depths less than 2000 m in the Fram Strait area and at the northern Barents Sea continental margin in the Pleistocene, it is not anticipated that it is a stratigraphically useful species.

The bioevents in the CAO are caused by a complex interplay of various biological processes. Apart from *B. arctica* and *H. obscurus* that likely evolved in the Arctic Ocean, the species characterizing these bioevents such as B. aculeata and *O. umbonatus* must have invaded the Arctic Ocean from subpolar latitudes. Since an unrestricted exchange of water masses with subpolar latitudes is only facilitated through Fram Strait, these intermediate to deep-water species had to be transported as juvenile specimens (propagules) by Atlantic Water to CAO sites during time periods favourable for their propagation. The possible time span of a vital transport, and thus the maximum reachable location for settlement within the Arctic Ocean, depends on the species, the vitality of a respective specimen, the local environmental conditions, and the strength of Atlantic water advection. The environmental conditions, in particular the availability of food, play then a major role for the successful colonization at a particular site, not only for the invading species but also the species endemic to the CAO (*H. obscurus*, *B. arctica).* These sites must face a high (*H. obscurus*, *B. arctica*, *O. umbonatus*), or significantly higher particulate organic carbon export to the sea floor than today (*B. aculeata*). Such environmental conditions must have occurred basin-wide to trigger the synchronous and coincident changes in assemblage compositions. Moreover, external forcing may have triggered environmental change. The onset of a massive discharge of detrital dolomite-rich ice-rafted debris might have caused the abrupt collapse of a *Bolivina arctica* dominated fauna and almost disappearance of *Haplophragmoides obscurus*. The most conspicuous change in the environment is expressed in the turnover from predominance of agglutinated to calcareous foraminifer which was probably caused by a fundamental change in food supply and its quality. However, the formation of bioevents cannot be attributed alone to biological processes. Due to selective dissolution of thin-shelled epifaunal taxa, assemblages are enriched in robust epifaunal and/or infaunal calcareous species, or may consist only of a agglutinated taphocoenosis.

1 Introduction

The Pleistocene biostratigraphy and paleoceanography of the Arctic Ocean is rather challenging because ecologic and

https://doi.org/10.5194/egusphere-2025-6290
Preprint. Discussion started: 29 December 2025

taphonomic processes such as temperature gradients, dissolution and degradation in the water column and sediments limit the applicability of the routinely used planktic microfossil groups in the Pleistocene. Calcareous microfossils (coccoliths, foraminifers) are more prominent than biosiliceous and organic-walled microfossils but assemblages have a low diversity and taxa are only discontinuously present (e.g., Herman, 1974; Herman et al., 1989; Cronin et al., 2008; Backman et al., 2009; Razmjooei et al., 2023). Biosiliceous microfossils are largely absent in Pleistocene sediments while organic-walled palynomorphs (e.g. dinoflagellate cysts) are sparse and occur only in certain stratigraphic intervals (e.g., Mudie, 1985; Herman et al., 1989; Matthiessen et al., 2018).

The existence of a permanent ice cover combined with the long polar night enables only low and extremely optional slightly increased primary production. Together with the very low surface water temperatures, these factors are critical for many fossilizable planktic organisms such coccolithophores, foraminifera, and dinoflagellates which generally prefer warmer water environments rather than arctic conditions. Thus, maximum adaptability to this harsh environment result in net catches of planktic foraminifera under the permanent ice cover consisting of >90% of the polar species *Neogloboquadrina pachyderma* (e.g., Carstens and Wefer, 1992). Since *N. pachyderma* also has the thickest shell of all planktic foraminifera encountered, thin-shelled subpolar species usually disintegrate during descent, and diagenetic processes in the surface sediment further contribute to this, resulting in a frequency of >98% *N. pachyderma* in sediment samples (Herman, 1964; O'Regan et al., 2019; Eynaud et al., 2009).

In contrast, benthic foraminifers are the most diverse and widespread microfossil group in the Arctic Ocean and its marginal shelf seas, and approx. 400 living and dead calcareous and agglutinated species have been recorded from the different environments (e.g., Lagoe, 1977; Scott and Vilks, 1991; Wollenburg, 1992; Bergsten, 1994; Ishman and Foley, 1996; Hald and Korsun, 1997; Wollenburg and Mackensen, 1998a, b; Wollenburg and Kuhnt, 2000; Polyak et al., 2002; Saidova, 2011; Husum et al., 2015; Kniazeva and Korsun, 2019). Due to their adaption to different ecological niches in outer estuarine to deep-sea sediments, benthic foraminifers have a strongly variable spatial and temporal distribution and depict pronounced changes in assemblage composition (Lee and Anderson, 1991; Gupta Sen, 2003; Murray, 2006). Based on summer field data, the distribution of living benthic foraminifera and their abundance in the Arctic Ocean are mainly determined by food availability and competition, although additional ecological aspects such as currents and temperature are also relevant for some species (Wollenburg and Mackensen, 1998a; Wollenburg and Kuhnt, 2000).

Despite the advantages of a higher diversity over planktic microfossils, benthic foraminifer species have not been thoroughly utilized as biostratigraphic and paleoceanographic proxy in the Pleistocene Arctic Ocean. The biostratigraphic applicability is limited by the low evolutionary turnover of deep-sea benthic foraminifera (Van Morkhoven et al., 1986; Thomas, 2007; Mckinney, 1987) generally leading to few appearances and extinctions of taxa in the Pleistocene (e.g., Buzas and Culver, 1989; Kawagata et al., 2005; Kawagata et al., 2007; Hayward, 2001; Hayward et al., 2007; Mancin et al., 2013; Kender et al., 2016). Therefore, most species previously used for Arctic Ocean biostratigraphy have a long stratigraphic range on a global scale (e.g., *Pullenia bulloides*, *Epistominella exigua*, *Bulimina aculeata*, *Oridorsalis umbonatus*, Holbourn et al., 2013). On the Pleistocene time scale, however, benthic records from the adjacent Norwegian-Greenland Sea up to the Barents Sea continental

https://doi.org/10.5194/egusphere-2025-6290
Preprint. Discussion started: 29 December 2025

shelf show that abundance maxima may be useful stratigraphic bioevents if these were calibrated to an independent time scale. Here, acmes of *Siphotextularia rolshauseni* and *Pullenia bulloides* mark certain time intervals in Late Pleistocene marine isotope stages (MIS) 2 and 5, respectively (e.g., Nees and Struck, 1994; Haake et al., 1990; Wollenburg et al., 2001b). In the CAO, stratigraphic occurrences of selected species have been frequently used to assign isotope stages to foraminifer-rich intervals and to correlate such layers across the Arctic Ocean (e.g., Ishman et al., 1996; Backman et al., 2004; Polyak et al., 2004; Polyak et al., 2013; Nørgaard-Pedersen et al., 2007a; Nørgaard-Pedersen et al., 2007b; Adler et al., 2009; Cronin et al., 2013; Cronin et al., 2014; Cronin et al., 2019b; Lazar and Polyak, 2016; Zhao et al., 2022; Hanslik et al., 2013; Kaufman et al., 2008; Xiao et al., 2020). However, faunal counts and quantitative data are rarely reported and therefore compilations exclusively based on presence/absence data may lead to rather inconsistent occurrences in different sediment cores (e.g., *Bulimina aculeata*, Alexanderson et al., 2014). Despite these limitations, calcareous benthic foraminifers may generally provide valuable tie points for stratigraphic correlation between Lomonosov, Mendeleev, and Northwind ridges (e.g. (Backman et al., 2004; Polyak et al., 2004; Cronin et al., 2014). Yet, their application is additionally complicated by previous age assignments of such events that are now outdated because of recent progress in $^{230}Th_{ex}$ dating and coccolith biostratigraphy (Razmjooei et al., 2023; Hillaire-Marcel et al., 2017; Song et al., 2023). Nonetheless, previous data suggest that benthic foraminifer bioevents have the potential to improve the still imprecise Pleistocene Arctic Ocean chronostratigraphy if these events had been fdefined based on stratigraphic ranges and abundance patterns of individual species, and their regional/supra-regional synchroneity been tested by calibration to an independent chronology.

The paleoceanographic applicability is strongly hampered by the variable preservation of species often leading to the enrichment of robust thick-shelled taxa (Loubere and Rayray, 2016). Moreover, agglutinated benthic foraminifera are often excluded from benthic foraminifer analysis although agglutinated species dominate in lower Pleistocene sediments (O´Neill, 1981; Scott et al., 1989; Evans and Kaminski, Cronin et al., 2008). This may result in a lower number of species, with increased relative abundance, false specimen numbers per sample weight and the loss of any faunal information on samples devoid of calcareous taxa. In practice, only a few species are often used for paleoceanographic interpretations, regardless of their proportion of the total assemblage, which is then not specified.

Here, we primarily evaluate the potential of the calcareous benthic foraminifera *Bolivina arctica*, *Bulimina aculeata, Cassidulina neoteretis*, *Epistominella arctica*, *E. exigua*, *Oridorsalis umbonatus* and *Pullenia* spp. and the agglutinated foraminifer *Haplophragmoides obscurus* as biostratigraphic and paleoceanographic markers in the Pleistocene based primarily on absolute (specimens/gram dry sediment) and secondly on relative abundances. We focus on the interval with normal magnetic polarity in the upper to middle Pleistocene where bioevents of these species have been recorded predominately in sediment cores recovered from water depths less than 1500-1700 m (e.g., O'Neill, 1981; Scott et al., 1989; Jakobsson et al., 2001; Backman et al., 2004; Polyak et al., 2004; Cronin et al., 2008; Cronin et al., 2013; Cronin et al., 2014; Lazar and Polyak, 2016). Therefore, we include sites PS72/396 and PS72/340 located in more than 2300 m water depth at the southern Mendeleev Ridge (Fig. 1) to test whether occurrence of individual species is restricted to certain water depths. Bioevents in these cores are compared with those in reference core PS2185-6 from the central Lomonosov Ridge and published data to assess the

https://doi.org/10.5194/egusphere-2025-6290
Preprint. Discussion started: 29 December 2025

temporal relationship between western and eastern Arctic Ocean. The individual bioevents are calibrated to independent chronostratigraphic data and lithological marker beds to reveal a possible synchroneity on a regional or supra-regional scale. Finally, ecological and taphonomic processes and the paleoceanographic implications are discussed that may have caused the formation of these bioevents.

2 Material and Methods

2.1 Sediment cores

Benthic foraminifera have been studied in sediment cores PS72/340-5 and PS72/396-5 from the Amerasian Basin east of the southern Mendeleev Ridge and in core PS2185-6 from the central Lomonosov Ridge (Fig. 1). Primarily, the uppermost core sections that are characterized by normal magnetic polarity (Frederichs, 1995; Bazhenova, 2012) were studied because this interval comprises the foraminiferal events used previously for stratigraphic correlation (e.g., Backman et al., 2004; Polyak et al., 2004). The sediment cores were sampled in 1 cm-thick slices at the *Polarstern* Core Repository in Bremerhaven (Germany) at variable depth intervals depending on the expected foraminifera content. The mid-depth of the sample is used in this study. The brown layers were sampled at a higher resolution because these layers are usually more productive for foraminifera. All sediment cores referred to in the text are shown in Figure 1 and the meta data are listed in Table 1. All data are stored in Pangaea and will be made available for download there after acceptance of the manuscript.

2.2 Foraminifer Analysis

2.2.1 Sample Preparation

All samples were freeze-dried, and their dry weight was determined (mean freeze-dried sample weight is 75, 89, and 96 grams for cores PS72/396-5, PS72/340-5, and PS2185-6, respectively). Thereafter, samples were washed with tap water over >2 mm and > 63 µm sieves and oven dried (50°C). The dried sand-size fraction (<2000 to >63 µm) was split into a small-size fraction >63- <125 µm (sf) and large-size fraction >125 - <2000 µm (lf) using a 125 µm-mesh. All size fractions were weighed and the dry weight-% of each grain size fraction calculated.

Benthic foraminifera were picked and identified from both sf and lf separately. With aid of a micro-splitter, grain-size fractions were split to obtain ~100 and 300 specimens picked from the whole sample splits of the sf and lf, respectively. Fragments of a particular taxon were also counted and included in the counts if the sum of fragments resulted in complete specimens (Wollenburg, 1995a). A cut off of 100 specimens of the sf in low-diverse samples was applied because picking small foraminifers is extremely time-consuming.

https://doi.org/10.5194/egusphere-2025-6290
Preprint. Discussion started: 29 December 2025

For the calculation of absolute (nos./g dry sediment) and relative (dry weight-%) abundances in the sand-size fraction, foraminifera counts per sample split were first extrapolated to 100% of the size fraction, then the counts of both size fractions were added, and abundances calculated. If benthic foraminifer counts were less than 100 specimen per sample, only absolute abundances of calcareous and agglutinated foraminifera were calculated. Actual specimen counts per sample, sample dry weight, the number of specimens per g/dry weight, and relative abundances of the individual taxa are archived in PANGAEA Tables 1-3. The foraminifera of each sample split were picked in plastic microslides and are archived in the *Polarstern* Core Repository.

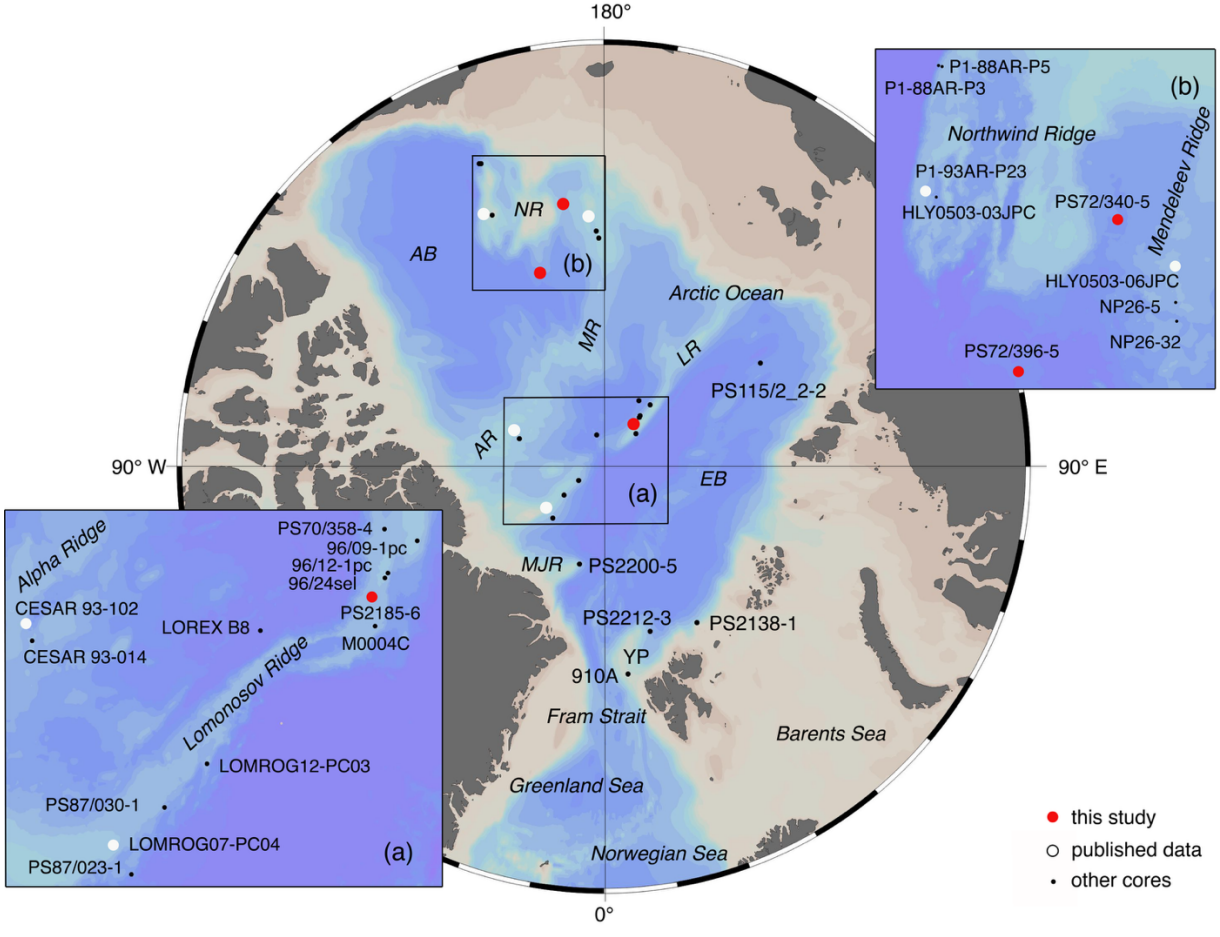

Figure 1: Location of sediment cores. Inset maps: (a), sediment cores from the western Lomonosov Ridge. (b), Sediment cores from the southern Mendeleev and Northwind ridges. AB: Amerasian Basin; AR: Alpha Ridge; EB: Eurasian Basin; MJR: Morris Jesup Rise; MR: Mendeleev Ridge; NR: Northwind Ridge; YP: Yermak Plateau. The map bases were drawn in Ocean Data View (Schlitzer, 2022).

https://doi.org/10.5194/egusphere-2025-6290
Preprint. Discussion started: 29 December 2025

180

Table 1: Sediment cores referred to in this study. GC: gravity corer; KAL: Kastenlot corer; PC: Piston Corer; HPC: Hydraulic Piston Corer; SEL: SelCorer.

Station	Type	Longitude	Latitude	Water Depth (m)	Recovery (m)
PS2138-1	GC	30.8762	81.5377	-862	6.34
PS2185-6	KAL	144.1662	87.5293	-1073	8.1
PS2200-5	KAL	-14.0220	85.3277	-1073	7.7
PS2212-3	KAL	15.6723	82.0237	-2531	8.02
PS70/358-4	KAL	152.1462	86.5263	-1462	7.9
PS72/340-5	KAL	-171.4933	77.6038	-2351	8.14
PS72/396-5	KAL	-162.3179	80.5778	-2723	7.87
PS87/023-1	KAL	-44.8997	86.6372	2445	6.98
PS87/030-1	KAL	-61.5420	88.6620	-1277	6.28
PS115/2-2-2	KAL	123.4839	81.2441	-3669	7.64
LOREX B8	GC	-167.1305	88.4953	4225	1.48
CESAR 83-014	GC	-108.3600	85.8467	-1370	4.40
CESAR 83-102	GC	-111.1183	85.6350	-1495	1.18
NP26-5	GC	-178.1500	78.9783	1435	1.48
NP26-32	GC	-178.6667	79.3233	1610	1.00
P1-88AR-P5	PC	-157.8840	74.6225	1089	4.76
P1-88AR-P3	PC	-157.6598	74.5933	1909	5.81
P1-93AR-P23	PC	-155.0650	76.9550	951	5.72
Hole 910A	HPC	6.5900	80.2647	-567	24.26
96/09-1pc	PC	143.4395	86.4087	-927	2.7
96/12-1pc	PC	144.7703	87.0918	-1003	7.81
96/24-1sel	SEL	144.6060	87.1830	-980	4.00
HLY0503-03JPC	PC	-156.0625	77.1000	594	7.25
HLY0503-06JPC	PC	-176.9862	78.2938	800	12.1
LOMROG07-PC04	PC	-53.7700	86.7000	811	5.23
LOMROG12-PC03	PC	-54.4253	87.7247	-1607	3.73
M0004C	HPC	136.1897	87.8678	-1288	25.6

185 Planktic foraminifera in the lf were also enumerated in cores PS72/340-5 and PS72/396-5 because their abundance is used to characterize brown beds in the Arctic Ocean (e.g., Polyak et al., 2004). Hereby, depending on the diversity ~100-300 specimens were picked from sample splits of the lf. Planktic foraminifer data of the size fraction > 125 to < 500 µm from core PS2185-6 have been reported by Spielhagen et al. (2004).

Foraminifera were picked and identified by JW under a ZeissSteREO Discovery.V8 stereomicroscope, equipped with a PlanS
190 1.0x FWD81 mm objective, and WPL 10x/23 Bf. foc. oculars, allowing for a magnification range of 10-80x, if needed oculars were changed to PL16x/16 Bf. foc. oculars allowing a maximum magnification of 128x. All stereomicroscope images are stacked digital images taken under a Zeiss Axio Zoom.V16 microscope equipped with 16x/16 Br. foc. oculars and the objectives PlanNeoFluar Z 1.0x (numerical aperture 0.25, FWD 56 mm, magnification 11x…179x with eyepieces PL 16x/16; object field in mm 23…1.4), and Apo Z 1.5x (numerical aperture 0.37, magnification 10.5…168x with eyepieces PL 16x/16;
195 object field in mm 15…0.95). The numerical aperture is 0.25, and the microscope used the ZEISS ZEN 2.3 (blue edition) imaging software. Images were taken with a ZEISS Axiocam 506 colour microscope camera. Scanning electron microscopy (SEM) images are performed by means of a JEOL JSM-IT100 InTouchScope™ Scanning Electron Microscope. Samples mounted on aluminium stubs using conductive double-sided carbon tape are analysed without conductive coating in low

https://doi.org/10.5194/egusphere-2025-6290
Preprint. Discussion started: 29 December 2025

vacuum mode. Shell thickness measurements were performed on SEM pictures of the broken last chamber of the respective species using the software ImageJ (Schneider et al., 2012).

A sound taxonomy is the prerequisite for the application of species in biostratigraphy and paleoceanography. Therefore, the taxonomic status of the selected species was restudied before bioevents were defined. The taxonomy follows the original descriptions deposited in the Ellis and Messina Catalogues (Ellis and Messina, 1940-2025), and deviating generic classification as depicted in The World Foraminifera Database and WoRMS (Hayward et al., 2025; Worms, 2024). A total of 236 species was identified in the sediment cores (Table A1). Specimens that could not be identified to species level are recorded under the respective genus or are listed as unidentified benthic foraminifera. White, dull or fragmented tests of calcareous foraminifera, often with enlarged pores, are interpreted as indication of progressive corrosion of calcareous shells (Poirier et al., 2021; Wollenburg et al., 2023). Fragments of agglutinated shells are indicative of progressive Fe-mobilisation and degradation of organic cement (Murray and Alve, 2011; Schroeder, 1988). Taxonomic notes and images of the stratigraphically relevant species are included in the Appendix A. The characteristic morphological features and ecological preferences of the selected species are listed in Appendix B. Here, we report only the specimen counts of the taxa relevant for this stratigraphic study (PANGAEA Tables 1-3), whereas all other taxa and unidentified specimens are listed as other benthic foraminifers. All data will be deposited in the data bank Pangaea.

2.2.2 Definition of bioevents

The bioevents were described based on absolute abundances, partly supported by relative abundances, rather than presence/absence data. Absolute abundance maxima are often more distinct and confined to shorter intervals and distinct lithological units than relative abundances (Jakobsson et al., 2001; Polyak et al., 2004) (Fig. 2). Moreover, relative abundances, generally used in arctic studies (Adler et al., 2009; Polyak et al., 2013; Lazar et al., 2016; Chauhan et al., 2014; Chauhan et al., 2015; Hanslik et al., 2013), are first of all influenced by variable abundances of the other taxa in an assemblage. Additionally, agglutinated species are often not included in benthic foraminfera studies making comparison of relative abundance data difficult.

The definition of bioevents follows the concept of biostratigraphic datums used by De Schepper and Head (De Schepper and Head, 2008). The in-situ stratigraphic occurrence of a taxon is marked by the lowest (LO) and highest (HO) occurrence. The highest and lowest sample in a sediment core in which a particular taxon is noticeably abundant, indicates the highest common occurrence (HCO) and lowest common occurrences (LCO), respectively. A particular taxon may occur in very low numbers above and below this stratigraphic level. Bell-shaped curves may indicate that bioturbation has blurred distinct absolute abundance maxima. Thus, species may have high relative abundances above and below absolute abundance maxima in sediments that originally had low benthic foraminifer contents (Fig. 2). Therefore, an LCO, HCO, and acme, based on absolute abundances appear to be more useful than an LO and HO. Chronological information was compiled from various sources to

https://doi.org/10.5194/egusphere-2025-6290
Preprint. Discussion started: 29 December 2025

assess the ages of the bioevents in the individual cores. The bioevents were assigned to the Pleistocene subseries of the Quaternary system (Head et al., 2001) and tentatively to marine isotope stages.

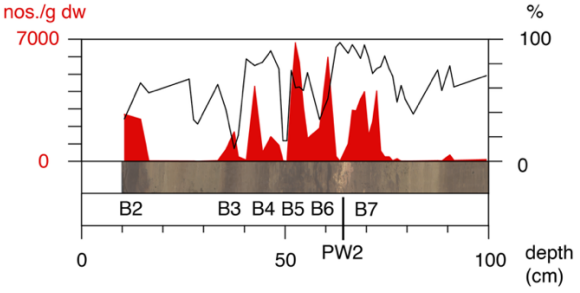

Figure 2: Digital image of core PS72/396-5 and relative (%) and absolute (numbers /g dry weight= nos./g dw) abundances of Stetsonia horvathi. This species dominates the assemblages but only shows distinct absolute abundance maxima in the brown layers. Please note that bioturbation has blurred the clear distinction between foraminifer-rich brown and foraminifer-poor gray layers, making distinction of specific brown layers difficult. Brown layers are labelled according to Polyak et al. (2004) and Stein et al. (2010b).

2.2.3 Comparison with published records

Published stratigraphic data of Arctic sediment cores were compiled to obtain a broader geographic coverage of the bioevents (Fig. 1). Comparison with previous studies is complicated by the fact that there is no common agreement on the grain-size fraction to be used in arctic foraminifer analyses. Early studies applied the CLIMAP cut off of >150 µm or >125 µm (Poore et al., 1994; Adler et al., 2009; Hanslik et al., 2013) but subsequently it was realized that smaller benthic foraminifer may account considerably to the assemblages. Schroeder et al. (1987) emphasize the importance of smaller sized species such as *Alabaminella weddellensis* or abundant small-sized offspring such as *Epistominella exigua* in benthic foraminifer assemblages. Thus, smaller specimens (>63- <125 µm) may be by one order of magnitude more abundant in samples from Arctic Ocean cores than larger benthic foraminifer (>125 µm) (Wollenburg and Mackensen, 1998a; Wollenburg et al., 2001b; Lazar and Polyak, 2016). Nevertheless, different size fractions are still used to obtain smaller foraminifers (e.g. >63 µm, >100 µm; Ishman et al., 1996; Polyak et al., 2004; Polyak et al., 2013; Chauhan et al., 2014; Lazar and Polyak, 2016). When different size fractions were used in foraminifer analyses it is sometimes not well documented from which size fraction data of a particular species has been obtained. Moreover, only relative abundances of marker species are usually shown, leading to relative abundance maxima of e.g. *Epistominella exigua* from specimen-poor samples which are depleted in thin-shelled species like *Stetsonia horvathi* or *Epistominella arctica* (Lazar and Polyak, 2016). Whether agglutinated and less common calcareous foraminifera were included in relative abundance calculations is usually not stated.

Here, we analysed the >63 µm to < 2000µm size fraction to obtain a record of the smaller sized, and usually dominant, benthic foraminifers, and compared the data with those records obtained from the same size fraction (Scott et al., 1989; Lazar and Polyak, 2016). It must be noted that Lazar and Polyak (2016) did not include agglutinated species which leads to some bias in

https://doi.org/10.5194/egusphere-2025-6290
Preprint. Discussion started: 29 December 2025

relative abundances compared to the new data. Since this work is based primarily on absolute abundances, data from Scott et al. (1989) and Lazar and Polyak (2016) could be included.

3 Results

At first the lithostratigraphy of the sediment cores is briefly described because sediments in the Arctic Ocean are generally siliciclastic in composition and show a pronounced lithological variability, and the stratigraphic occurrence of species is related to lithological units (Figs. 3-5).

3.1 Lithostratigraphy at Mendeleev and Lomonosov Ridges

For the western Arctic Ocean, Clark et al. (1980) proposed thirteen lithostratigraphic units (standard arctic lithostratigraphic units A to M) based on grain size composition and presence of detrital carbonate-rich pink-white layers. This scheme has been routinely applied in subsequent studies and slightly modified for cores from Alpha Ridge (Minicucci and Clark, 1983; Mudie, 1985; Darby et al., 1989; Clark et al., 1990; Poore et al., 1993; Poore et al., 1994; Ishman et al., 1996; Phillips and Grantz, 1997; Stein et al., 2010a; Stein et al., 2010b). In the past years, a simplified lithostratigraphy has been preferred for visual core description counting downcore the alternation of brown, calcareous foraminifer- and manganese-rich and coarser-grained grey to olive, foraminifer- and manganese-poor layers (Polyak et al., 2004). These layers were termed brown beds B1 to B7 and grey beds G1 to G6, and are interpreted to reflect interglacials/interstadials and glacials/stadials, respectively. In the western Arctic Ocean, lithological Unit M comprises brown beds B1 to B6, whereas the top of Unit L is marked by B7 (Figs. 3, 4). This scheme was extended downcore into older sediments but the number of brown beds in specific stratigraphic intervals varies between cores (Stein et al., 2010b; Wang et al., 2018; Dong et al., 2020; Park et al., 2020).

The combination of the standard lithostratigraphic units and colour stratigraphy has been applied on cores from southern Mendeleev Ridge including PS72/340-5 and PS72/396-5 (Figs. 3, 4) (Stein et al., 2010a; Stein et al., 2010b). However, the link between brown layers and calcareous foraminifer abundances is not straightforward because when sedimentation is slow as at site PS72/396, brown beds are difficult to distinguish because of extensive bioturbation blurring the record (Fig. 3) (Stein et al., 2010b). Moreover, brown bed B 5 is barren of calcareous foraminifer and contains only agglutinated foraminifers in core PS72/340-5 (Fig. 4). This is a common feature in Northwind Ridge cores (Poore et al., 1993; Poore et al., 1994; Ishman et al., 1996; Phillips and Grantz, 1997; Yurco et al., 2010). Sediments in the brown layers are sometimes coarser at the southeastern Mendeleev Ridge (Figs. 3, 4), contrary to the original definition (Polyak et al., 2004).

Thin layers enriched in pink-white and whitish lenses or clasts of detrital dolomite (PW layers) may additionally be useful for stratigraphic correlation in the western Arctic Ocean but the relative high number in sediment cores from the Northwind and Mendeleev ridges make an unequivocal correlation difficult (Clark et al., 1980; Mudie and Blasco, 1985; Minicucci and Clark, 1983; Poore et al., 1993; Poore et al., 1994; Phillips and Grantz, 1997; Polyak et al., 2004; Adler et al., 2009; Stein et al.,

https://doi.org/10.5194/egusphere-2025-6290
Preprint. Discussion started: 29 December 2025

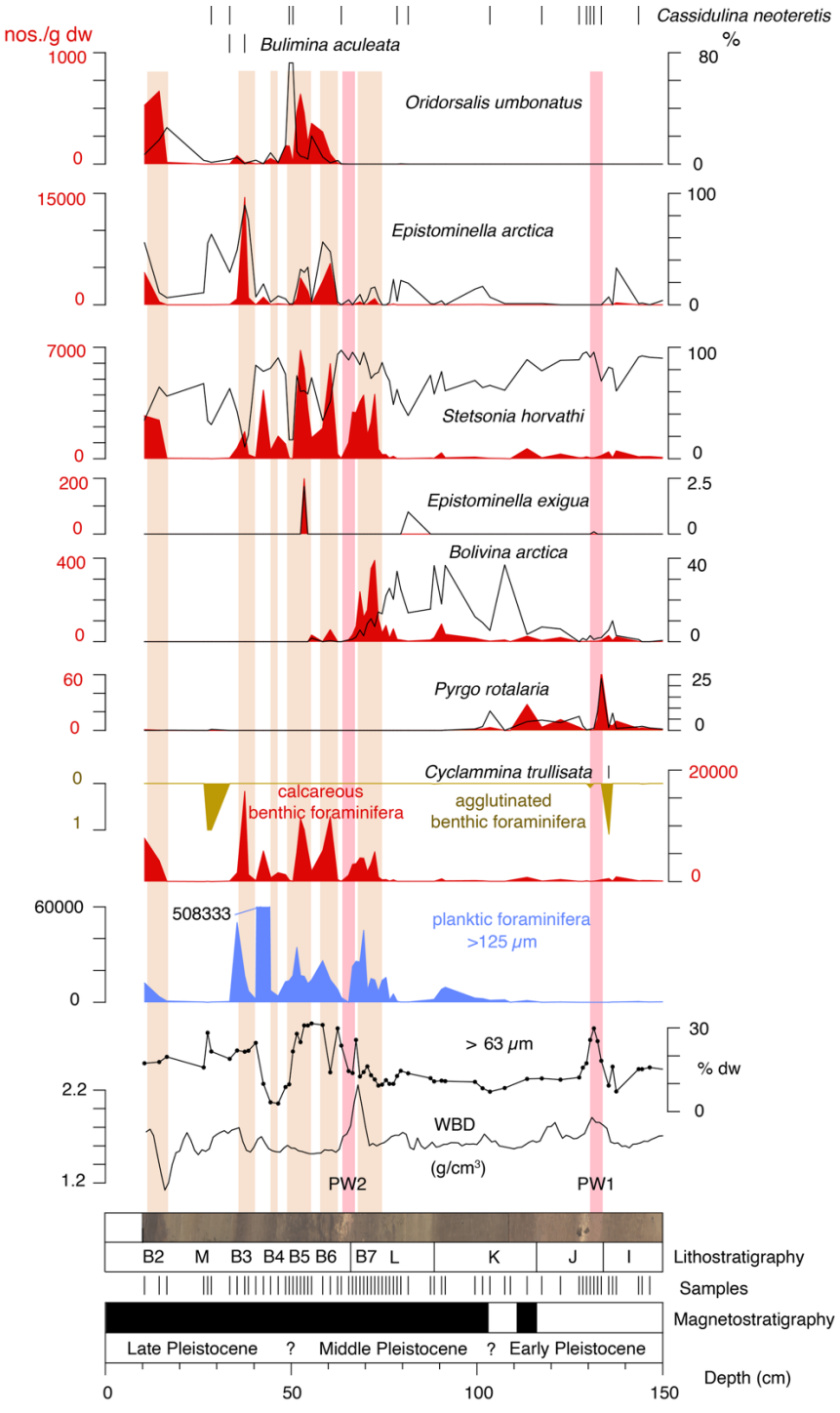

295 **Figure 3: Stratigraphic distribution of selected benthic foraminifera (> 63 µm) in sediment core PS72/396-5 from the eastern**

https://doi.org/10.5194/egusphere-2025-6290
Preprint. Discussion started: 29 December 2025

Mendeleev Ridge. Only the presence of *Bulimina aculeata* and *Cassidulina neoteretis* is noted because of consistently low relative abundances (< 2%). The first downcore change in magnetic polarity is assigned to the Brunhes/Matuyama boundary (Elkina et al., 2023) which is supported by $^{230}Th_{ex}$ data (Geibert et al., 2021). The Pleistocene is tentatively subdivided into subseries. The standard lithostratigraphic units of Clark et al. (1980) were identified by Stein et al. (2010b). Brown (B) and pink-white layers (PW) are labelled according to Polyak et al. (2004) and Stein et al. (2010b). Line scan images are from Matthiessen (2013b). Wet bulk density data (wbd) are from Niessen (2010b). Please note that brown bed B 1 was not recovered at the core top due to coring disturbance. %: relative abundances; nos/g dw: absolute abundances (number/ gram dry weight).

2010a; Stein et al., 2010b; Cronin et al., 2014; Bazhenova et al., 2017). These diamictons reflect synchronous sedimentation events because they were formed by rapid sedimentation from melting icebergs that have calved at the grounding line of the Laurentide ice sheet at the arctic margin, drifting then with prevailing currents across the arctic basins and releasing ice-rafted debris while melting (Darby et al., 2002; Polyak et al., 2004; Matthiessen et al., 2010; Stein et al., 2010a; Stein et al., 2010b; Bazhenova et al., 2017).

The lithostratigraphic scheme of Clark et al. (1980) cannot be applied on Lomonosov Ridge sediments (Sellén et al., 2008) and a separate lithostratigraphic scheme has not been developed yet for Eurasian Basin cores. Non-destructive physical property records, such as magnetic susceptibility (ms) and wet bulk density (wbd) enable correlation within similar depositional environments (Sellén et al., 2010; O'Regan et al., 2019; Vermassen et al., 2021; Razmjooei et al., 2023). Thus, Razmjooei et al. (2023) used wet bulk density maxima of two diamictons in the upper part of sediment cores from the western Lomonosov Ridge for stratigraphic correlation, including core PS2185-6 (Fig. 5).

Since foraminifer-rich brown layers are also widespread in the Eastern Arctic Ocean (e.g., Jakobsson et al., 2001; Backman et al., 2004; Polyak et al., 2004; Löwemark et al., 2014), these may be applicable for a basin-wide lithostratigraphic correlation if they were coeval across the Arctic Ocean. Visual inspection of sediment core images revealed that some intervals in core PS2185-6 with high planktic foraminifer concentrations (Spielhagen et al., 2004) and increased manganese contents (Schoster, 2005) have a brown colour (Grobe and Fütterer, 2003), comparable to those in adjacent core 96/12-1pc (Jakobsson et al., 2001; Backman et al., 2004). However, März et al. (2011) note that diagenetic processes may lead to post-depositional dissolution and/or formation of Mn-rich brown layers. Therefore, they emphasize that these layers should not be used for stratigraphic correlation without independent age control.

There are possibly some lithological marker sequences that may be used for stratigraphic correlation across the Arctic Ocean. In the Mendeleev Ridge area, the base of lithological Units M and J are marked by the dolomite-rich pink-white diamictons PW 2, and PW 1, respectively (Figs. 3, 4; Clark et al., 1980; Poore et al., 1993; Polyak et al., 2004; Adler et al., 2009; Stein et al., 2010a; Stein et al., 2010b; März et al., 2011). Pink-white layer PW 2 is interbedded in two brown layers which were correlated to foraminifer-rich brown layers in core 96/12-1pc on Lomonosov Ridge (Backman et al., 2004; Polyak et al., 2004). A similar sequence may be observed in core PS2185-6 where detrital carbonates in the 125 – 500 µm size fraction (Spielhagen et al., 2004) may represent fine-grained detrital dolomites between two foraminifer-rich brown layers in the lower

https://doi.org/10.5194/egusphere-2025-6290
Preprint. Discussion started: 29 December 2025

330

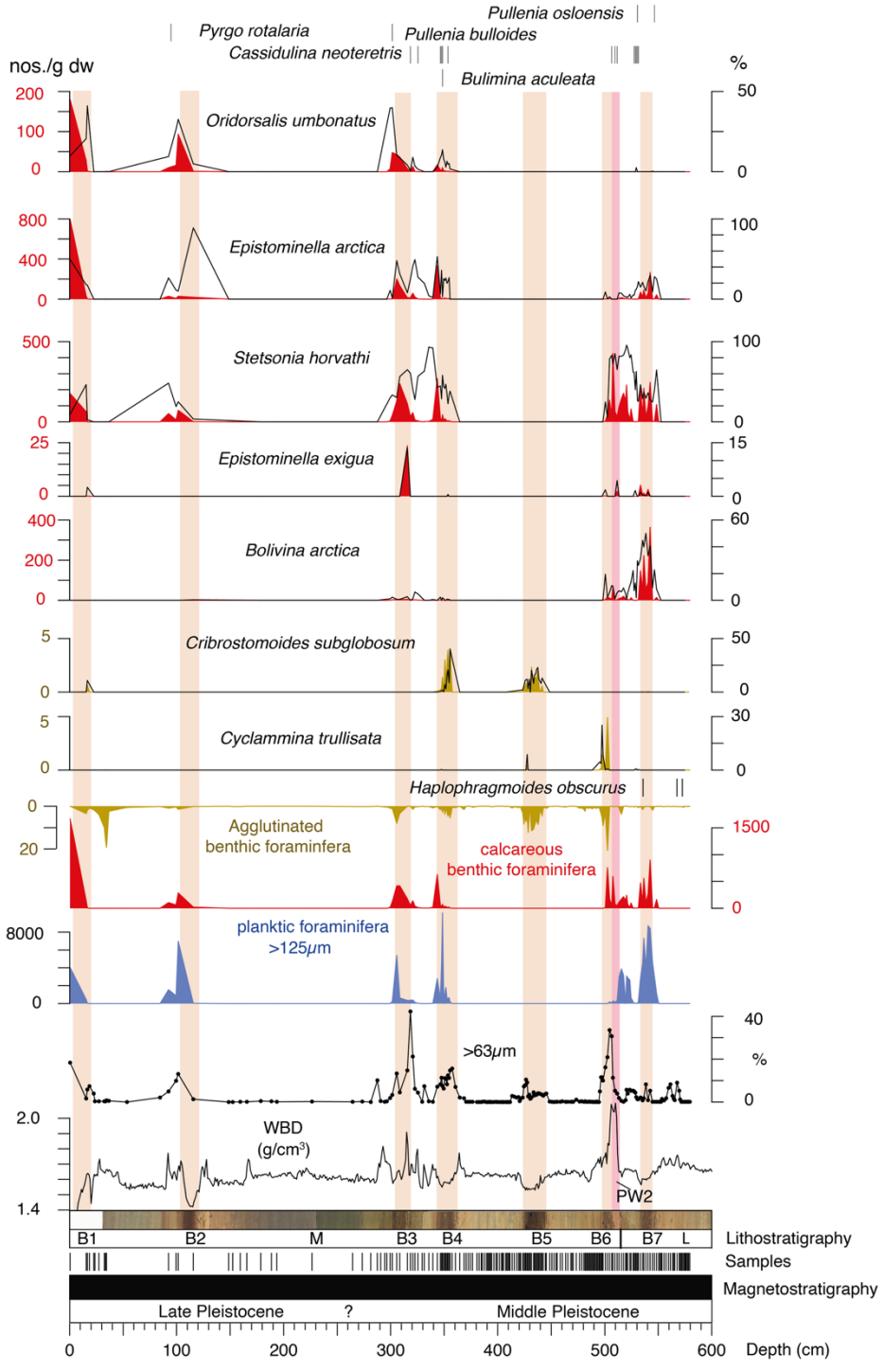

Figure 4: Stratigraphic distribution of selected benthic foraminifers in sediment core PS72/340-5 from the eastern Mendeleev Ridge

https://doi.org/10.5194/egusphere-2025-6290
Preprint. Discussion started: 29 December 2025

area. Only the presence of *Bulimina aculeata*, *Cassidulina neoteretis*, *Pullenia bulloides*, *Pullenia osloensis* and *Pyrgo rotalaria* is noted because of consistently low relative abundances (< 2%). The studied core interval was deposited in the Brunhes Chron (Bazhenova, 2012). The standard lithostratigraphic units of Clark et al. (1980) were identified by Stein et al. (2010b). Brown (B) and pink-white layers (PW) are labelled according to Polyak et al. (2004) and Stein et al. (2010b). Line scan images are from Matthiessen (2013a). Wet bulk density (wbd) data are from Niessen (2010a). %: relative abundances; nos/g dw: absolute abundances (number/ gram dry weight).

part of the uppermost interval with normal polarity (Fig. 5). Pink-white clasts in a diamicton in adjacent core PS70/358-4 (Stärz, 2008; Fig. 1) were used by Stein et al. (2010a: Fig. 9) to tentatively infer the presence of diamicton PW 2. Based on this correlation, Stein et al.(2010b) suggest that brown bed B7 must be present below this layer in cores PS70/358-4 and PS2185-6. Previously, Morris et al. (1985, p.904) used the presence of whitish blotches at the base of the Theta member of their Makarov Basin Formation in LOREX core B8 to infer the presence of the base of Unit M (see also Sellén et al., 2008). These observations suggest that sediments equivalent to the base of Unit M and the top of Unit L may also be recorded in the central Lomonosov Ridge.

However, sedimentation on the shallow Lomonosov Ridge may be disrupted by glacial erosion and/or slow sedimentation during times of extensive glacial ice cover (e.g., Jakobsson et al., 2001; Jakobsson et al., 2010; Frank et al., 2008) complicating the construction of age models. Thus, an erosional unconformity is observed below a pink layer in core 96/09-1pc that is correlated by wbd and ms to core PS2185-6 (Jakobsson et al., 2001; Razmjooei et al., 2023). This correlation suggests that this pink layer is synchronous with the inferred pink-white layer PW 2 above brown bed B 7 in PS2185-6 (Fig. 5).

3.2 Stratigraphic occurrence of selected species in the Arctic Ocean

The discontinuous occurrence of foraminifera in in the studied cores is related to the lithology (Figs. 3-5). Planktic and calcareous benthic foraminifera show absolute abundances maxima rather in brown layers than in the grey to olive layers, as it has been previously observed (e.g., Polyak et al., 2004; Backman et al., 2004). Core PS72/396-5 at the western Mendeleev Ridge comprises older sediments than core PS72/340-5, showing orders of magnitude lower absolute foraminifer abundances in brown layers below brown bed B 7 than in younger sediments. On Lomonosov Ridge, only some brown layers in the uppermost interval with normal magnetic polarity are rich in calcareous foraminifers. The few calcareous shells in the gray to olive layers of the three cores may be bioturbated from the brown layers, as indicated by extensive brown mottling (see digital images and x-radiographs (Fütterer and Grobe, 2003; Matthiessen and Stein, 2008a, 2008b; Matthiessen, 2013a, 2013b), or may be of allochthonous origin (Geibert et al., 2021). Coarse-grained intervals, such as the diamictons in core PS2185-6 are barren (Fig. 5).

Planktic foraminifer assemblages in cores PS72/340-5 and PS72/396-5 are almost exclusively composed of *Neogloboquadrina pachyderma* (Wollenburg, unpubl.). Benthic foraminifer assemblages are generally dominated by *Stetsonia horvathi* in the

https://doi.org/10.5194/egusphere-2025-6290
Preprint. Discussion started: 29 December 2025

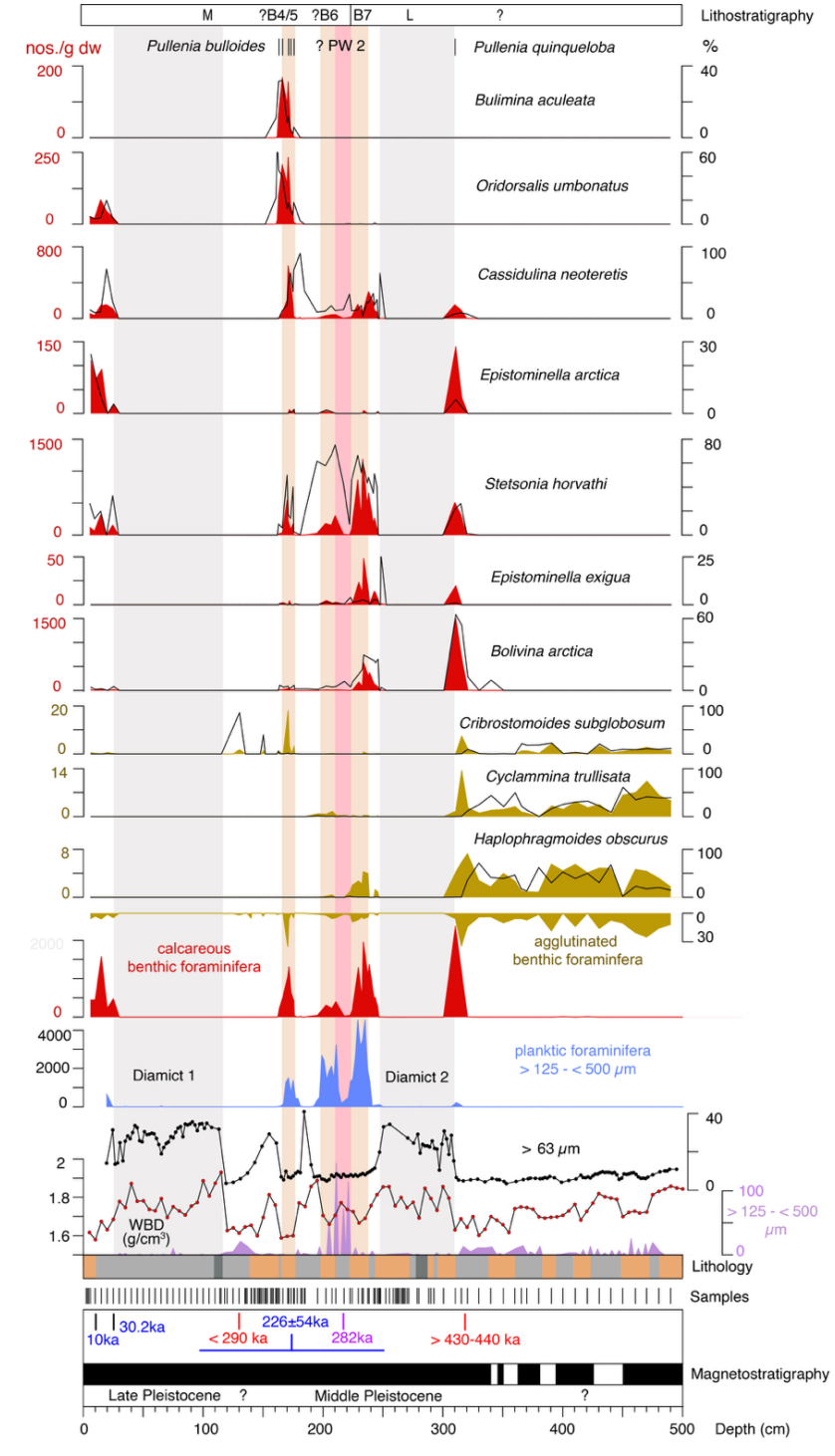

Figure 5: Stratigraphic distribution of selected benthic foraminifers in sediment core PS2185-6 from Lomonosov Ridge. Only the

https://doi.org/10.5194/egusphere-2025-6290
Preprint. Discussion started: 29 December 2025

presence of *Pullenia bulloides* and *P. quiqueloba* is noted because of consistently low relative abundances (< 2%). The numerical ages (blue colour) in the interval with normal magnetic polarity (Frederichs, 1995) are based on two AMS ^{14}C ages at the core top (selected from a radiocarbon data set of Wollenburg et al., 2023) and a $^{230}Th_{ex}$ extinction age (depth range is depicted by a bar; Song et al., 2023). This core is correlated to adjacent cores by distinct wet bulk density (wbd) maxima (Bergmann, 1995) representing diamict 1 and 2 enabling to transfer ages of coccolith events (red colour) to core PS2185-6 (Razmjoeei et al, 2023). The pink age is assigned to a detrital carbonate-rich interval based on the correlation to pink-white layer PW 2 (Stein et al., 2010b, 2025). The simplied lithology characterized by brown, olive grey, and grey layers is taken from photographic images (Grobe and Fütterer, 2003). Planktic foraminifer concentrations, relative abundance of coarse sediment fraction, and detrital carbonate contents (no >125 - <500 µm) are from Spielhagen et al. (1997). %: relative abundances; nos/g dw: absolute abundances (number/ gram dry weight).

intervals with calcareous taxa (Figs. 3-5), whereas stratigraphically important taxa such as *Bolivina arctica* are rarely abundant to dominant. Calcareous foraminifer bioevents occur in Unit M and in the upper part of Unit L brown bed B7.

Agglutinated benthic foraminifera do not show a consistent distribution in the three cores. Where calcareous and agglutinated foraminifera are preserved, absolute abundances of agglutinated foraminifera are generally two orders of magnitude lower than those of the calcareous taxa. Brown layers in the lower part of core PS2185-6, and brown bed B5 in core PS72/340-5 comprise exclusively agglutinated foraminifera. In core PS72/340-5 the thick interbedded grey to olive layers contain few to no calcareous foraminifers but sometimes low abundances of agglutinated foraminifers. Core PS72/396-5 is almost devoid of agglutinated taxa. Below the magnetic polarity change, only agglutinated foraminifers are present in core PS2185-6 (Fig. 5).

Selected benthic taxa which are important for biostratigraphy and ecology are shown in figures 3, 4, and 5. Additionally, the stratigraphic occurrence of selected stratigraphically important taxa in cores from Alpha Ridge, Northwind Ridge, Mendeleev Ridge, and Lomonosov Ridge (this study; Scott et al., 1989; Lazar and Polyak, 2016) is compiled to evaluate the spatial distribution of bioevents.

The agglutinated benthic foraminifer *Siphotextularia rolshauseni*, a stratigraphic marker for MIS 2 in Norwegian-Greenland Sea sediments, has not been observed in the sediment cores from the CAO but it occurs sporadically in the Fram Strait area and the adjacent Barents Sea continental slope (Wollenburg et al., 2001b). This species has not been observed in any other study on agglutinated foraminifer from the Arctic Ocean (e.g., O´Neill, 1981; Scott et al., 1989; Evans and Kaminski, 1998).

Bulimina aculeata is abundant only in core PS2185-6 where an absolute abundance maximum is restricted to a short interval in a brown layer (Fig. 5). It is present in very low numbers at the deep-water sites, in a single sample in brown bed B 4 in core PS72/340-5, and in two samples in brown bed B 3 in core PS72/396-5 (Figs. 3, 4). A distinct acme of absolute abundances has been previously observed in cores from relatively shallow water depths (<1800 m), occurring usually above pink-white layer 2 in lithological Unit M in the western Arctic Ocean (Fig. 6).

https://doi.org/10.5194/egusphere-2025-6290
Preprint. Discussion started: 29 December 2025

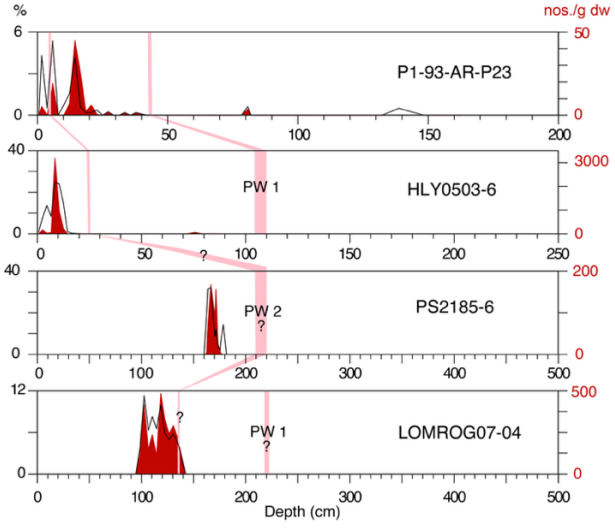

405 **Figure 6: Stratigraphic occurrence of *B. aculeata* across the Arctic Ocean. A distinct acme is observed above PW 2 in all cores from relatively shallow water depths, except for core P1-93-AR-P23. Core locations are shown in Figure 1. Absolute abundances (>63µm) of cores P1-93-AR-P23, HLY0503-6, and LOMROG07-04 are from Lazar and Polyak (2016). The depth intervals of the pink-white layers in these cores are from Cronin et al. (2014). %: relative abundances; nos./g dw: absolute abundances (numbers/ gram dry weight).**

410

Species of *Pullenia* are present at different stratigraphic levels in the studied sediment cores. *Pullenia bulloides* only occurs in the *B. aculeata* acme core PS2185-6 (Fig. 5), and in core PS72/340-5 in brown bed B 3 (Fig. 4). *Pullenia quinqueloba* and *P. osloensis* occur sporadically in cores PS2185-6 and PS72/340-5, respectively. *Pullenia bulloides* shows a variable distribution in sediment cores from the Arctic Ocean (Fig. 7), and appears not to be a useful stratigraphic marker.

415 *Oridorsalis umbonatus* (often referred to *O. tener*, see Appendix A) has a distinct lowest maximum of absolute abundances above PW 2 in a brown layer across the Arctic Ocean (Figs. 3, 4, 5, 8). A distinct relation to a specific brown layer is not observed in the western Arctic Ocean where the oldest maximum occurs in brown beds B 3 and B 6 in cores PS72/340-5 and PS72/396-5, respectively. However, brown beds B 4, B 5 and B 6 are difficult to distinguish in core PS72/396-5 because of intensive bioturbation, and at site PS72/340 brown bed B 5 is barren in calcareous foraminifera. The oldest abundance

420 maximum coincides with that of *B. aculeata* in cores from shallow water depths (Figs. 5, 8, see also Polyak et al., 2004). Below the oldest maximum, *O. umbonatus* may be sporadically abundant but never reach high absolute abundances. *Cassidulina neoteretis* occurs in certain brown layers in core PS2185-6 and is particularly abundant in the *B. aculeata* acme above the lowest maximum of absolute abundances of *O. umbonatus* (Fig. 5). A comparable assemblage has been observed in the composite NP26 record from the shallow Mendeleev Ridge (Polyak et al., 2004). In cores PS72/340-5 and PS72/396-5

425 from deeper waters, *C. neoteretis* is only rare in some intervals (Figs. 3, 4). This species might be a good additional marker

https://doi.org/10.5194/egusphere-2025-6290
Preprint. Discussion started: 29 December 2025

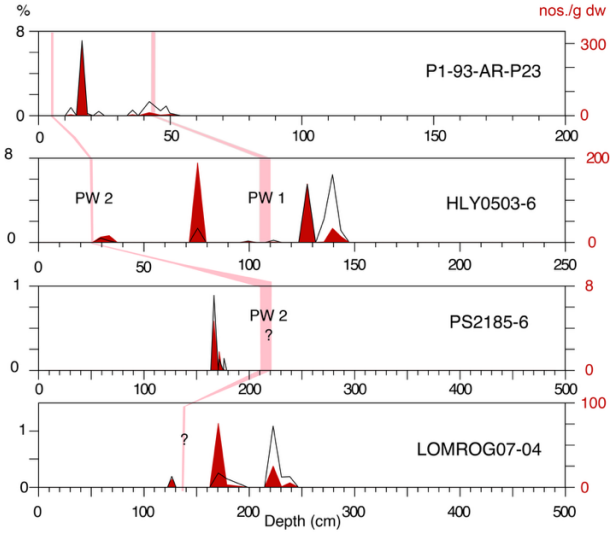

Figure 7: Stratigraphic occurrence of *P. bulloides* across the Arctic Ocean. Core locations are shown in Figure 1. Absolute abundances (>63µm) of cores P1-93-AR-P23, HLY0503-6, and LOMROG07-04 are from Lazar and Polyak (2016). The depth intervals of the pink-white layers in these cores are from Cronin et al. (2014). %: relative abundances; nos./g dw: absolute abundances (numbers/ gram dry weight).

for the *B. aculeata* acme in shallow water cores, but *C. neoteretis* has not been consistently distinguished from *C. teretis* making it currently difficult to assess its stratigraphic potential (Appendix A).

Epistominella arctica and *E. exigua* do not show a consistent stratigraphic occurrence in the studied sediment cores (Figs. 3-5). *Epistominella arctica* is more abundant than *E. exigua* and occurs with variable absolute and relative abundances in certain brown layers. Hereby, high absolute abundances of *Epistominella arctica* are more frequent above PW 1, whereas *E. exigua* is more abundant below PW 2 (Figs. 9, 10).

Bolivina arctica occurs in variable absolute and relative abundances through the cores (Figs. 3-5). Absolute abundance maxima are generally restricted to the lower part of the interval with normal magnetic polarity. The youngest pronounced absolute abundance maximum is terminated by a pronounced decline to low abundances. This is located at the top of Unit L in brown bed B7 just below pink-white layer PW 2 in the western Arctic Ocean, and at the same stratigraphic level on Lomonosov Ridge based on the proposed lithostratigraphic correlation (Fig. 11, Stein et al., 2010b).

The extinct agglutinated foraminifer *Haplophragmoides obscurus* dominates the benthic faunas in the lower part of core PS2185-6 (Fig. 5) and disappeared above the top of the youngest absolute abundance maximum of *B. arctica*. This species is only observed in traces in PS72/340-5 (Fig. 4). In core PS72/396-5 *H. obscurus* is absent but likely the stratigraphic occurrence of *Pyrgo rotalaria* is comparable with that of *H. obscurus* (Fig. 3).

https://doi.org/10.5194/egusphere-2025-6290
Preprint. Discussion started: 29 December 2025

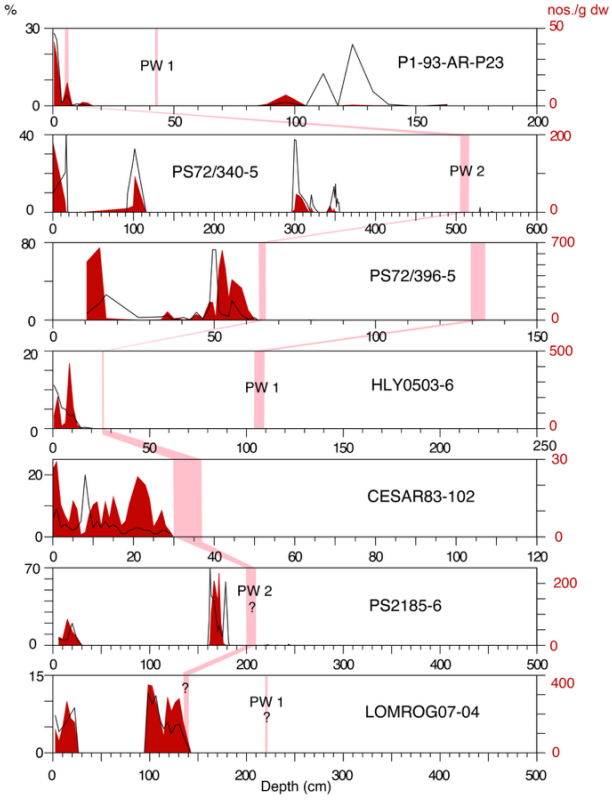

Figure 8: Stratigraphic occurrence of *O. umbonatus* across the Arctic Ocean. This species consistently shows absolute abundance maxima above PW 2. Core locations are shown in Figure 1. Absolute abundances (>63µm) of cores P1-93-AR-P23, HLY0503-6, and LOMROG07-04 are from Lazar and Polyak (2016), and CESAR83-102 from Scott et al. (1989). The depth intervals of the pink-white layers in these cores are from Cronin et al. (2014) and Scott et al. (1989). %: relative abundances; nos./g dw: absolute abundances (number/ gram dry weight). Absolute abundances in core CESAR83-102 are numbers/10ccm wet sample (Scott et al., 1989).

The changeover in predominance from agglutinated to calcareous benthic foraminifers has been observed in core PS2185-6 slightly above the change to normal magnetic polarity (Fig. 5). This substantial decline of agglutinated foraminifers has been previously described for this core (Evans et al., 1995; Evans and Kaminski, 1998). Below the changeover, assemblages only comprise foraminifers firmly agglutinated with high iron content in the cement (Schröder, 1988; Hedley, 1963; Bender, 1989). These include taxa accessory in recent assemblages (*Cribrostomoides subglobosum*, *Glomospira* spp., *Rhabdammina*

https://doi.org/10.5194/egusphere-2025-6290
Preprint. Discussion started: 29 December 2025

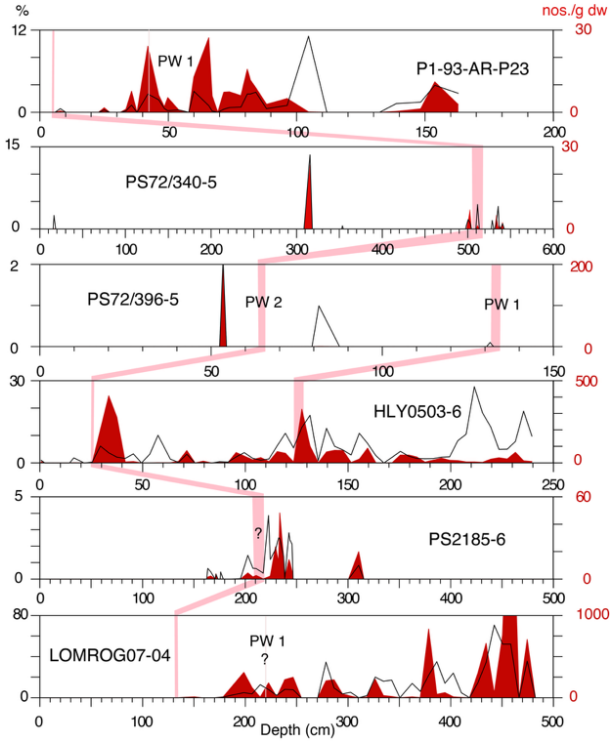

Figure 9: Stratigraphic occurrence of *E. exigua* across the Arctic Ocean. Core locations are shown in Figure 1. Absolute abundances (>63µm) of cores P1-93-AR-P23, HLY0503-6, and LOMROG07-04 are from Lazar and Polyak (2016). The depth intervals of the pink-white layers in these cores are from Cronin et al. (2014). %: relative abundances; nos./g dw: absolute abundances (numbers/ gram dry weight).

spp., *Jacullela* spp., *Hyperammina* spp., *Saccammina socialis*, *S. sphaera*, *Psammosphaera fusca*, *Reophax* spp.), and *H. obscurus* and *Cyclammina trullissata* that are unknown from the modern Arctic benthic foraminifera fauna. *Cyclammina trullissata* disappears in core PS2185-6 in a brown layer above the proposed pink-white layer PW 2, and in core PS72/340-5 in brown bed B 5. In younger sediments above the HOs of *H. obscurus* and *C. trullisata* the agglutinated fauna is dominated by modern taxa, and predominantly firmly agglutinated *Cribrostomoides subglobosum* occurs sporadically in certain intervals. Agglutinated foraminifers are almost absent in the studied interval of core PS72/396-5 whereas in core PS72/340, brown layers and some laminated interbedded sequences comprise predominantely agglutinated tubular taxa.

4 Discussion

4.1 Chronostratigraphy of studied sediment cores

A robust chronostratigraphic framework for Pleistocene sediments in the CAO has not been developed yet, and beyond the

https://doi.org/10.5194/egusphere-2025-6290
Preprint. Discussion started: 29 December 2025

range of radiocarbon dating there are few chronological tie-points because of discontinuous microfossil and sparse radionuclide records. Moreover, variable accumulation of sediments and stratigraphic breaks at the Arctic Ocean sea-floor hamper linear interpolation between tie-points and thus calculation of numerical ages for bioevents (Hillaire-Marcel et al., 2017; Matthiessen et al., 2018).

Since the turn of the century the Pleistocene chronostratigraphy in the western Arctic Ocean primarily relied on stratigraphic correlation to the central Lomonosov Ridge (e.g., Jakobsson et al., 2000; Backman et al., 2004; Spielhagen et al., 2004; Adler et al., 2009; Park et al., 2024). Three brown layers that are characterized by absolute abundance maxima of planktic foraminifera in cores PS2185-6 (Fig. 5) and 96/12-1pc have been dated to MIS 5 by coccolith biostratigraphy and optical stimulated luminescence (OSL) ages and these ages served with AMS ^{14}C dates as backbone for the Arctic Ocean MIS 1 to 6 chronostratigraphy (Jakobsson et al., 2000; Jakobsson et al., 2001; Jakobsson et al., 2003; Backman et al., 2004; Spielhagen et al., 2004). New radiocarbon, coccolith, amino acid razemisation and radiometric data from various Lomonosov Ridge cores now require a substantial revision of these age assignments (Hillaire-Marcel et al., 2017; Geibert et al., 2021; Razmjooei et al., 2023; Song et al., 2023; West et al., 2023; Wollenburg et al., 2023).

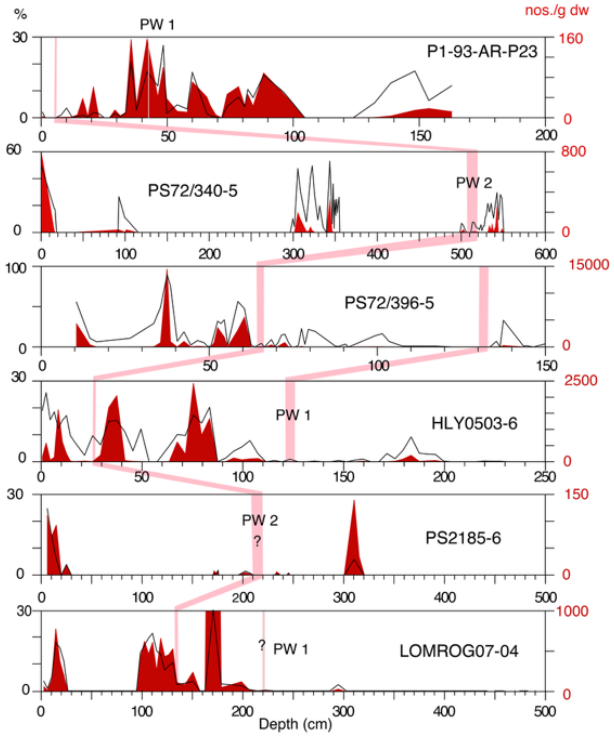

Figure 10: Stratigraphic occurrence of *E. arctica* across the Arctic Ocean. Core locations are shown in Figure 1. Absolute abundances (>63µm) of cores P1-93-AR-P23, HLY0503-6, and LOMROG07-04 are from Lazar and Polyak (2016). The depth intervals of the

https://doi.org/10.5194/egusphere-2025-6290
Preprint. Discussion started: 29 December 2025

pink-white layers in these cores are from Cronin et al. (2014). %: relative abundances; nos./g dw: absolute abundances (numbers/ gram dry weight).

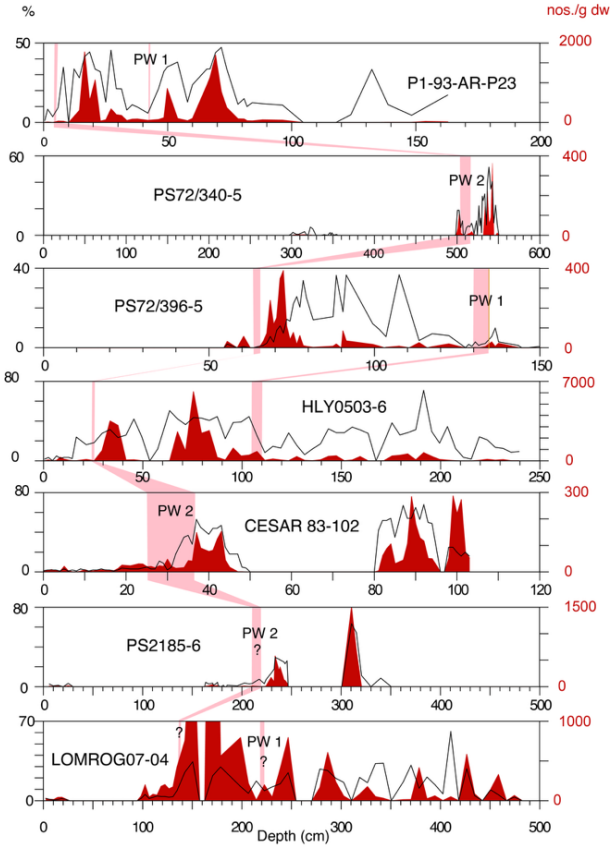

Figure 11: Stratigraphic occurrence of *B. arctica* across the Arctic Ocean. Core locations are shown in Figure 1. Absolute abundances (>63µm) of cores P1-93-AR-P23, HLY0503-6, and LOMROG07-04 are from Lazar and Polyak (2016), and CESAR83-102 from Scott et al. (1989). The depth intervals of the pink-white layers are from Cronin et al. (2014) and Scott et al. (1989). %: relative abundances; nos./g dw: absolute abundances (number/ gram dry weight). Absolute abundances in core CESAR83-102 are numbers/10ccm wet sample (Scott et al.,1989).

Chronological tie points for core PS2185-6 are provided by radiocarbon ages for the Holocene to late glacial interval and by a $^{230}Th_{ex}$ extinction age for the Middle Pleistocene (Wollenburg et al., 2023; Song et al., 2023). The radiocarbon ages indicate the presence of MIS 1 and upper MIS 3 in core PS2185-6 (Fig. 5; Wollenburg et al., 2023). Although the extinction age at the base of the upper foraminifer maximum has large uncertainties with respect to stratigraphic interval and age (Song et al., 2023), the core section with the three foraminifer maxima between 160 and 240 cm is older than MIS 6 (Fig. 5). The previous coccolith

https://doi.org/10.5194/egusphere-2025-6290
Preprint. Discussion started: 29 December 2025

biostratigraphy of Spielhagen et al. (2004) for core PS2185-6 based on the presence of *Emiliania huxleyi* (assigned to *Geophyrocapsa huxleyi* by Bendif et al., 2023) in these foraminifer maxima could not be confirmed by a detailed taxonomic restudy (Razmjooei et al., 2023).

The revision of previous age models complicates the identification of MIS 5 in Lomonosov Ridge sediments. The radiocarbon and $^{230}Th_{ex}$ extinction ages are supplemented by correlating coccolith bioevents from sediment cores on the western Lomonosov Ridge to core PS2185-6 by means of wet bulk density data (Razmjooei et al., 2023). This correlation suggests that *E. huxleyi* must have appeared below diamicton 1 in core PS2185-6 indicating an age younger than the early MIS 8 based on its global first appearance (290 ka, Backman et al., 2012; Anthonissen and Ogg, 2012) (Fig. 5). Amino acid razemization data on *N. pachyderma* and *C. wuellerstorfi* indicate a MIS 6-9 age for the LO of *E. huxleyi* in core LOMROG12-PC03 (West et al., 2023). In contrast, the extinction age of $^{231}Pa_{excess}$ of 140 ka below the correlated LO in core PS87/030-1 indicate an age younger than MIS 6 age at this stratigraphic level (Hillaire-Marcel et al., 2017; Razmjooei et al., 2023). Thus, *E. huxleyi* might have appeared in the Arctic Ocean not before MIS 5 (Razmjooei et al., 2023) but this datum should be calibrated in a core with robust independent chronostratigraphy. Unfortunately, this stratigraphic level is barren of calcareous microfossils in core PS2185-6 but if the wbd correlation is correct the correlated stratigraphic level is younger than the extinction age of 226±54 ka indicating an age younger than MIS 8 for the LO of *E. huxleyi* (Fig. 5). In contrast, a foraminifer-rich interval has been recognized in adjacent core 91/12-1pc above the former MIS 5.1 at the proposed LO of *E. huxleyi* (Jakobsson et al., 2001; Backman et al., 2004; Razmjooei et al., 2023) that might now correspond to MIS 5. Irrespective of the exact age of the LO of E. huxleyi in the Arctic Ocean, the coccolith biostratigraphy confirms that the three foraminifer maxima must be older than MIS 6. If the detrital carbonate maximum in core PS2185-6 is equivalent to a pink-white layer in core PS115/2-2-2, then the top of the lower foraminifer-rich layer, tentatively assigned to brown bed B 7, is older than 282 ka (late MIS 9) based on $^{230}Th_{ex}$ data (Stein et al., 2010a; Stein et al., 2025).

The wbd correlation indicates that *Pseudoemiliania lacunosa* must have disappeared slightly below diamicton 2 in core PS2185-6 (Fig. 5; Razmjooei et al., 2023), the former MIS 6 (Spielhagen et al., 2004). The disappearance of *P. lacunosa* indicates an age older than the uppermost MIS 12 (ca. 430-440 ka) (Backman et al., 2012; Anthonissen and Ogg, 2012) for this stratigraphic level. Razmjooei et al. (2023) suggest that *P. lacunosa* became extinct in MIS 13 (> 478 ka) because they assume that this coccolithophore disappeared rather in an interglacial than a glacial stage. However, a pronounced temperature decline in a glacial stage might have been a more likely trigger for extinction than a relatively warm interglacial. The correlated HO of *P. lacunosa* in core PS2185-6 indicates that the first downcore change in magnetic polarity occurred in the Middle Pleistocene, being younger than the Brunhes/Matuyama boundary (Fig. 5). The correlation of physical properties between the ACEX composite and PS2185-6 rather suggests that the Brunhes/Matuyama boundary is located at the base of core PS2185-6 (ca. 765 cm) (O´Regan et al., 2008; Frank et al., 2008). The stratigraphic data appear to be rather consistent for the Lomonosov Ridge, while only the OSL ages of Jakobsson et al. (Jakobsson et al., 2003) from core 96/24-1sel located close to core 96/12-1pc (Fig.1) apparently disagree with the new chronology.

The chronostratigraphy of the western Arctic Ocean cores is more debatable. Magnetostratigraphy provides the basic age

https://doi.org/10.5194/egusphere-2025-6290
Preprint. Discussion started: 29 December 2025

model for cores PS72/340-5 and PS72/396-5 (Bazhenova, 2012; Elkina et al., 2023). The entire studied core interval in PS72/340-5 can be assigned to the Brunhes Chron (Fig. 4) (Bazhenova, 2012) while the Brunhes/Matuyama boundary in core PS72/396-5 is placed in the middle part of Unit K and the Jaramillo Subchron at the transition of Unit K to J (Fig. 3, Elkina et al., 2023). This agrees with the correlation of lithological units to the magnetic polarity pattern based on the re-analysis of paleomagnetic data obtained on sediment cores recovered from ice island T-3 in the Mendeleev Ridge area (Jones, 1987). $^{230}Th_{ex}$ data support this interpretation (Geibert et al., 2021) and a MIS 5e/late Termination II age has been proposed at ca. 28 cm for core PS72/396-5, and an age older than MIS 7 and younger than MIS 9 at ca. 65 cm (Song et al., 2023). At the latter stratigraphic level the diamicton PW 2 has been assigned an age of 282 ka (top MIS 9) based on the correlation to a pink-white layer in core PS115/2-2-2 (Fig. 1; Stein et al., 2025). Both age estimates are quite close indicating a MIS 9 age for brown bed B7. In contrast, the interval which may have a MIS 5e/late Termination II age (Song et al., 2023) is barren of calcareous foraminifera in core PS72/396-5.

4.2 Foraminifer biostratigraphy

Here, we critically discuss the benthic foraminifer bioevents to select those that are useful for stratigraphic correlation in the CAO. These bioevents are tentatively calibrated to independent lithological and chronological data. We refrain from assigning numerical ages or marine isotope substages to bioevents because of a lack of a robust independent chronostratigraphy. We rather stick to marine isotope stages that implies a certain duration and not a single definite age.

4.2.1 Changeover in benthic foraminifer assemblages

A conspicuous change in benthic foraminifer assemblages occurred across the Arctic Ocean in the Pleistocene when the predominance of agglutinated benthic foraminifers was replaced by calcareous foraminifers (Fig. 5) (O´Neill, 1981; Scott et al., 1989; Evans and Kaminski, 1998; Backman et al., 2004, Polyak et al., 2004; Cronin et al., 2008). Cronin et al. (2008) suggest that this turnover may have occurred in MIS 7 to 9, but they note that the age control is based only on sites from the central Lomonosov Ridge. However, the new stratigraphic data rather suggest an older age, and a time-transgressive change in the benthic foraminifer assemblages across the CAO.

The stratigraphic level of the turnover is located close to the first downcore change from normal to reverse magnetic polarity on the western Lomonosov Ridge in cores PS87/023-1, PS2185-6, 96/12-1pc and IODP Hole M4C (Fig. 5, Frederichs, 1995; Evans and Kaminski, 1998; Jakobsson et al., 2001; Backman et al., 2004; Spielhagen et al., 2004; Cronin et al., 2008; O´Regan et al., 2008; Stein, 2015; Elkina et al., 2023). Frequent polarity changes occurred below this stratigraphic level where assemblages in most cores are almost exclusively composed of agglutinated benthic foraminifers. The *Pseudoemiliania lacunosa* event correlated to core PS2185-6 suggests an age older than top MIS 12 (Backman et al., 2012; Gradstein et al., 2012) or MIS 13 (Razmjoeei et al., 2023) for this stratigraphic level (Fig. 5).

https://doi.org/10.5194/egusphere-2025-6290
Preprint. Discussion started: 29 December 2025

Semi-quantitative shipboard data of core PS87/030-1 (Fig. 1) suggest that the downcore increase of agglutinated foraminifera commenced at the stratigraphic level of a hardground at ca. 218-222 cm core depth (Stein, 2015). The wbd correlation between both sites (Razmjooei et al., 2023) indicate that the changeover from agglutinated to calcareous foraminifers is located approximately at the same stratigraphic level in both core PS87/030-1 and PS2185-6. This hardground might be related both to the change in benthic foraminifer assemblages and the first downcore change from positive to negative magnetic polarity. A MIS 12 or older age for this hardground is likely. Interestingly, a carbonate hardground has been dredged on the Alpha Ridge that is probably not older than 400 ka (Bingham-Koslowski et al., 2025).

Formation of hardgrounds are linked to sedimentation breaks suggesting the presence of a hiatus or a condensed stratigraphic interval in core PS87/030-1. Neither a hardground nor an unconformity has been observed in core PS2185-6 (e.g. Svindland and Vorren, 2002) but a significant increase in coarse fraction content occurred slightly above this stratigraphic level (Fig. 5). Unconformities formed by glacial erosion have been observed frequently on Lomonosov Ridge (e.g., Jakobsson et al., 2001; Polyak et al., 2001; Jakobsson et al., 2010; Frank et al., 2008) complicating the establishment of age models for sediment cores. The considerable thickness of lower to middle Pleistocene sediments younger than 1.8 Ma in ACEX Hole M0004C (O´Regan et al., 2008, Frank et al., 2008), rather suggest a more continuous sedimentation close to site PS2185, probably due to being located in deeper waters than core PS2185-6.

A similiar relation to the magnetic polarity change can been observed on Morris Jesup Rise in core PS2200-5 where planktic foraminifer abundances decrease while agglutinated foraminifer abundances increase downcore at the base of the uppermost interval with normal magnetic polarity (Evans and Kaminski, 1998; Frederichs, 1995; Spielhagen et al., 2004). It might be likely that the substantial change in benthic foraminifer assemblages at the sites in the eastern Arctic Ocean was coeval and occurred before MIS 11.

In the western Arctic Ocean, there is some variability in the age of the turnover but it is apparently older than on Lomonosov Ridge. On Northwind Ridge the changeover occurred in lithological Unit I in the uppermost Early Pleistocene close to the base of the Jaramillo Subchron in core PI-88AR-P5 (Poore et al., 1993; Backman et al., 2004). At the Mendeleev Ridge, the new sediment cores have not been studied down to the turnover of calcareous to agglutinated foraminifers but preliminary shipboard data suggest that it occurred below ca. 200 cm in Unit G in core PS72/396-5, being of mid-Early Pleistocene age in the early Matuyama Chron (Wollenburg, unpubl. Data; Stein et al., 2010b; Elkina et al., 2023). This is comparable to Clark et al. (1990) who observed this change in Unit F at approximately 1.5-2 Ma. At the Alpha Ridge, the turnover occurred in core CESAR 83-14 at the base of Unit H within or at the top of the Olduvai Chron (1.78-1.95 Ma; Scott et al., 1989; Aksu, 1985). If the changeover in the assemblages in the eastern Arctic Ocean was linked to a hiatus or condensed sedimentation it might have been synchronous with that in the Amerasian Arctic Ocean.

4.2.2 HCO of *Bolivina arctica*

https://doi.org/10.5194/egusphere-2025-6290
Preprint. Discussion started: 29 December 2025

Bolivina arctica is endemic to the Arctic Ocean and has a stratigraphic range from the top of lithological Unit A to top of Unit M in the western Arctic Ocean (O´Neil, 1981; Scott et al., 1989). The species likely appeared in the Late Pliocene (Polyak et al., 2013; Dipre et al., 2018) and eventually evolved from *Virgulopsis pygmeus* which was described from Oligocene sediments in the Beaufort-Mackenzie basin (McNeil, 1997) (Appendix A). *Bolivina arctica* is today only a rare component of living assemblages, e.g. at site PS2185 (Wollenburg and Mackensen, 1998; Wollenburg and Kuhnt, 2000), and has a distinct stratigraphic distribution in Pleistocene sediments of the CAO. It is rare in upper Pleistocene to recent sediments and increases to strongly variable relative and absolute abundances downcore from the lower part of the uppermost interval with normal magnetic polarity (Herman, 1973; Scott et al., 1989; Pak et al., 1992; Ishman et al., 1996; Wollenburg et al., 2001b; Wollenburg et al., 2001d, c, a; Polyak et al., 2004; Polyak et al., 2013; Cronin et al., 2014; Lazar and Polyak, 2016).

At the deep-water sites PS72/340 and PS72/396 the youngest maximum of absolute abundance is observed in a lithological sequence consisting of two brown layers interbedded with sediments enriched in detrital dolomite which is visible on split core surfaces only at the Mendeleev Ridge area (Figs. 3, 4). This sequence is assigned to brown beds B 6 and B 7 and pink-white layer PW 2 (Stein et al., 2010b). A pronounced decrease of the absolute abundance occurred close to the base of PW 2 at the top of a brown layer on Northwind, Mendeleev and Alpha Ridges, whereas on the Lomonosov Ridge PW 2 has only been tentatively identified (Fig. 11) (Scott et al., 1989; Cronin et al., 2014; Lazar and Polyak, 2016).

Therefore, a highest common occurrence (HCO) of *B. arctica* (>63 µm size fraction) can be defined for sediment cores from 800 to 2700 m water depth, at the top of the youngest absolute abundance maximum, corresponding to the top of brown bed B7. Absolute abundances of *B. arctica* are consistently low above this stratigraphic level (Fig. 11). Moreover, this bioevent marks the top of lithological Unit L. This offers the possibility to test whether certain layers characteristic for Unit M in the Mendeleev Ridge area may also be found on Lomonosov Ridge. It must be noted that high relative abundances may occur above this stratigraphic level but if absolute abundance were calculated these are low (e.g., Scott et al., 1989, 2009).

Paleomagnetic data indicate that this bioevent is in the middle of the uppermost interval with normal magnetic polarity (Figs. 3, 5), as it has been already observed by Herman (1973). Previously, this stratigraphic level was assigned in core PS2185-6 to MIS 5.5 (Jakobsson et al., 2003; Spielhagen et al., 2004; Backman et al., 2004) but this is untenable because the $^{230}Th_{ex}$ extinction age of 224±56 ka above the HCO is older than MIS 6 (Fig. 5). At the northern Barents Sea continental margin *B. arctica* is rare in in Hole 910A, cores PS2212-3 and PS2138-1 in MIS 6 to MIS 2 sediments (Wollenburg et al., 2001a, b, c, d; Wollenburg, unpubl.) supporting an age older than MIS 6 for the HCO. The HCO is located between two coccolith datums that were correlated from Lomonosov Ridge cores, located close to Greenland, by physical properties to core PS2185-6 (Razmjoeei et al., 2023). This correlation confirms a Middle Pleistocene age, being older than MIS 6 and younger than MIS 12 (Fig. 5). A pink-white layer in core PS115/2-2-2 from the Laptev continental margin that has been dated to 282 ka (Stein et al., 2025) might be coeval with the layer rich in detrital carbonates in core PS2185-6, tentatively assigned to PW 2. This age would perfectly fit into the stratigraphic sequence, located below the $^{230}Th_{ex}$ extinction age of 224±56 ka, suggesting that the HCO has a MIS 9 age (Fig. 5).

At the southwestern Mendeleev Ridge, a tentative interpretation of the $^{230}Th_{ex}$ data (Song et al., 2023) suggests an age older

https://doi.org/10.5194/egusphere-2025-6290
Preprint. Discussion started: 29 December 2025

than MIS 7 and younger than MIS 9/late Termination IV for the HCO in core PS72/396-5 (Fig. 3). If the correlation of a pink-white layer from the Eurasian Basin to the Mendeleev Ridge PW 2 layer holds true (Stein et al., 2025), then an upper MIS 9 age of the HCO of *B. arctica* appears likely for the entire Arctic Ocean.

The calibration of this bioevent cannot be improved in the subarctic realm because *B. arctica* is endemic to the Arctic Ocean. Records of *B. arctica* from the North Atlantic (Scott et al., 1989; Kaminski et al., 1989; Hull et al., 1996; Collins et al., 1996; Wang et al., 2021) are not thoroughly documented to assess a subpolar occurrence.

4.2.3 HO of *Haplophragmoides obscurus*

The HO of the extinct agglutinated *Haplophragmoides obscurus* might be a useful stratigraphic event in the Arctic Ocean but a definite datum cannot be defined with the available data. It disappeared slightly above the HCO of *B. arctica* in a calcareous foraminifer-rich brown layer in core PS2185-6 (Fig. 5), and a few specimens were observed at the top of Unit L in deep-water core PS72/340-5 (Fig. 4). In ACEX Hole M0004C, *H. obscurus* (as *Cyclammina pusilla*) occurs up to the top of the interval with dominant agglutinated benthic foraminifera but agglutinated foraminifers were not determined to species level in the Brunhes Chron (Cronin et al., 2008; O´Regan et al., 2008) preventing to observe the HO. The HO of *H. obscurus* (as *Cyclammina pusilla*) in core PS2200-5 from Morris Jesup Rise is in a planktic foraminifer-rich interval in the Brunhes Chron (Evans and Kaminski, 1998; Spielhagen et al., 2004). This stratigraphic level may correspond to that in core PS2185-6.

In cores from the western Arctic Ocean the HO of *H. obscurus* has been recorded mainly from lower Pleistocene sediments. O`Neill (1981) observed the HO in Unit D of cores from the Mendeleev Ridge area. On Alpha Ridge *H. obscurus* (as *Cyclammina pusilla*) disappeared in lithological Unit H of core CESAR 93-014 at or above the top of the Olduvai Subchron (ca. 1.8Ma; Aksu 1985; Scott et al., 1989). This species is common in Unit I and occurs sporadically up to the top of lithological unit M in Northwind Ridge cores PI88-AR-3 and PI88-AR-5 (Poore et al., 1994; Ishman et al.,1996) but these young occurrences might be reworked.

4.2.4 *Pullenia bulloides*

The occurrence of the genus *Pullenia* spp. or *Pullenia bulloides* has been previously used as stratigraphic marker for MIS 7 in the CAO (Jakobsson et al., 2001; Backman et al., 2004; Nørgaard-Pedersen et al., 2007a; Nørgaard-Pedersen et al., 2007b; Hanslik et al., 2013). However, *P. bulloides* is not restricted to a single stratigraphic interval in Pleistocene sediments from shallow submarine highs in the CAO and at the northern Barents Sea continental margin (Fig. 7; Poore et al., 1994; Wollenburg et al., 2001a, b, c, d; Chauhan et al., 2014; Chauhan et al., 2015; Lazar and Polyak, 2016). This species has been used in the Norwegian-Greenland Sea and Fram Strait as a stratigraphic marker for MIS 5a but in cores located in less than 2000 m water depth, maxima in relative abundance occur during various time intervals in the Late Pleistocene whereas a single maximum has only been observed in deep water sites (e.g., Haake et al., 1992; Struck, 1997; Wollenburg et al., 2001; Chauhan et al.,

https://doi.org/10.5194/egusphere-2025-6290
Preprint. Discussion started: 29 December 2025

2014, 2015). The stratigraphic application is further complicated by the co-occurrence of three closely related *Pullenia* species (*P. bulloides*, *P. quinqueloba*, *P. osloensis*) in the CAO (Figs. 4, 5; Appendix A). These species must be unequivocally distinguished before any of these taxa can further be applied as stratigraphic marker.

4.2.5 *Epistominella exigua* and *E. arctica*

Absolute abundances of *E. exigua* are consistently lower than those of *E. arctica* in Arctic Ocean cores and *E. exigua* is only sporadically present at the deep-water sites PS72/396 and PS72/340 (Figs. 3-5). In the upper Pleistocene a distinct time-transgressive changeover from *E. exigua* to *E. arctica* is observed between PW 1 and PW 2 (Figs. 9, 10; Lazar and Polyak, 2016). In sediments younger than the latter stratigraphic level *E. exigua* is generally rare.

The inconsistent stratigraphic occurrence is, on the one hand, caused by the preferential dissolution of thin shells (Appendix Table B1; Fig. 12). Often the last and largest chamber of *E. arctica* is lost and specimens may be then found preferentially in the size fraction < 63 µm. Selective dissolution of thin-shelled and small (<100 µm) arctic benthic foraminifera may lead to overrepresentation of robust and/or infaunal species such as *Bulimina aculeata* and *Bolivina arctica*.

On the other hand, *E. exigua* may also be difficult to distinguish from *Eilohedra vitrea* (Appendix A). Since *E. exigua* and *E. arctica* differ in their ecological requirements, probably defining different stratigraphic occurrence, both species must be unequivocally distinguished. Both species are feeding on phytodetritus, but *E. arctica* is adapted to the arctic, whereas *E. exigua* is an invasive Atlantic species, demanding a higher, eventually also more frequent particulate organic carbon transfer to depth and eventually higher temperatures (Table B1). Differentiation between *E. exigua* and *E. vitrea* is also essential as only *E. exigua* is a deep-water phytodetritus species, whereas *E. vitrea* is more common at shallower sites and a reproduction following phytodetritus blooms is not mandatory (Table B1).

The turnover from *E. exigua* to *E. arctica* might be a useful stratigraphic event but the age assignment must be evaluated after detailed taxonomic studies were conducted to unequivocally distinguish *E. arctica* and *E. exigua* from *Stetsonia horvathi* and *Eilohedra vitrea*, respectively (Appendix A).

4.2.6 Lowest common occurrence of *Oridorsalis umbonatus*

A range bottom of *O. umbonatus* (as *O. tener)* has been previously defined at the base of a foraminifer-rich brown layer in cores 96/12-1pc, NP26-5 and PI88-AR-P5 and dated to MIS 5.1 (Backman et al., 2004; Polyak et al., 2004). However, this species also occurred sporadically in sediments older than the middle part of the normal polarity interval in the CAO (Fig. 8; Clark et al., 1990; Pak et al., 1992; Ishman et al., 1996; Polyak et al., 2004; Hanslik, 2011; Lazar and Polyak, 2016). In contrast, a distinct oldest absolute abundance maximum can be observed across the CAO in a brown layer above pink-white layer PW 2 (Fig. 8). In sediment cores from shallow submarine highs (< 1700 m water depth) this stratigraphic level coincides with the acme of *B. aculeata* (see below) on Lomonosov Ridge (Fig. 5, PS2185-6; 96/12-1PC, LOMROG07-

https://doi.org/10.5194/egusphere-2025-6290
Preprint. Discussion started: 29 December 2025

PC04; Jakobsson et al., 2001; Lazar & Polyak, 2016) and on Mendeleev Ridge (NP26 composite of cores NP 26-5 and 26-32, HLY0503-6JPC; Polyak et al., 2004; Lazar and Polyak, 2016).

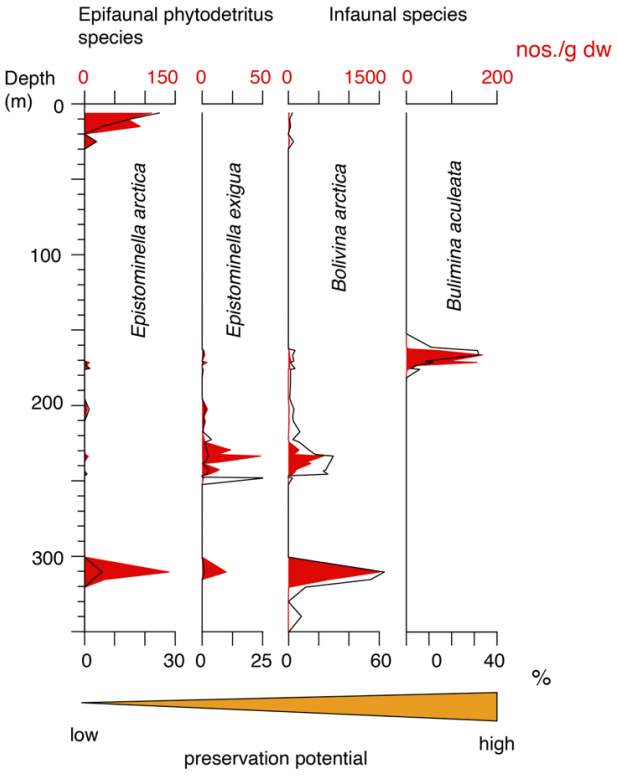

Figure 12: Influence of the preservation potential (non-quantitative assessment) on the formation of absolute abundance maxima in core PS2185-6. The more robust species are successively enriched with increasing selective dissolution

Therefore, based on absolute abundances the LCO of *O. umbonatus* is defined, coeval with the base of the *Bulimina aculeata* acme in sediment cores from water depths shallower than 1700 m. Since *O. umbonatus* generally increases above the HCO of *B. arctica*, it is assumed that the LCO of *O. umbonatus* in both PS72/396-5 and PS72/340-5 is coeval with that in PS2185-6. The LCO is located in core PS2185-6 (Fig. 5) slightly below the $^{230}Th_{ex}$ extinction age of 226±54 ka and distinctly above the correlated $^{230}Th_{ex}$ age of 282 ka (Stein et al., 2025) suggesting an age older than top of MIS 7 and younger than MIS 9. At the southeastern Mendeleev Ridge, the LCO is located slightly above pink-white layer PW 2 in core PS72/396-5 (Fig. 3). This layer has been assigned an age of 282 ka (uppermost MIS 9) based on correlation to core PS115/2-2-2 (Fig. 1) (Stein et al., 2025), and was tentatively dated to older than MIS 7 and younger than MIS 9/late Termination IV by Song et al. (2023). Based on these constraints, the LCO is probably of MIS 7 age.

The LCO is not unequivocally linked to a specific brown layer at Mendeleev and Northwind ridges. The lowest distinct

https://doi.org/10.5194/egusphere-2025-6290
Preprint. Discussion started: 29 December 2025

absolute abundance maximum is associated with brown beds B5 and B4 in the NP26 composite (Polyak et al., 2004). The maximum in B5 is linked to high relative abundances reflecting possibly post-depositional enrichment of this robust species due to selective dissolution of thin-shelled associated species. Comparably, relatively high relative abundances occur in cores PI-88-AR- 3 and -5 at the top of brown bed B5 to B4 (Poore et al., 1994; Ishman et al., 1996). Absolute abundances of *Oridorsalis umbonatus* increase in brown bed B4 in core PS72/340-5 (Fig. 4). An even older age of the LCO cannot be excluded because laminated sediments and absence of calcareous foraminifers in brown bed B5 indicate carbonate-aggressive bottom/pore water conditions at this site. In core PS72/396-5, the oldest absolute abundance maximum is linked to the base of brown bed B6. These differences indicate that an unequivocal correlation of many brown layers is dubious. This may be caused by extensive bioturbation at sites with slow sedimentation such as PS73/396 which is indicated by extensive brown mottling in grayish sediments, the absence of calcareous benthic foraminifers over long intervals at sites such as PS72/340-5 (Fig. 4) and possibly post-depositional changes of redox conditions leading to formation or dissolution of Mn-rich layers (März et al., 2011) causing a variable record of brown layers between sites (see also Stein et al., 2010b).

4.2.7 Acme of *Bulimina aculeata*

The acme of *Bulimina aculeata* in a short stratigraphic interval in upper Pleistocene Arctic Ocean sediments, corresponding to the B. aculeata assemblage zone of Ishman et al. (1996), has previously been used as stratigraphic marker for MIS 5.1 (Jakobsson et al., 2001; Polyak et al., 2004; Nørgaard-Pedersen et al., 2007a; Nørgaard-Pedersen et al., 2007b; Cronin et al., 2014; Xiao et al., 2020). Despite its possible stratigraphic importance this bioevent is rather poorly defined, and often only the occurrence of B. aculeata is noted (e.g. Hanslik et al., 2013; Alexanderson et al., 2014; Cronin et al., 2014; Xiao et al., 2020). Moreover, the interpretation is complicated by sporadic occurrences at other stratigraphic levels in the Pleistocene (Fig. 6; Herman et al., 1989; Poore et al, 1993, 1994; Ishman et al., 1996; Osterman, 1996; Jakobsson et al., 2001; Polyak et al., 2004; Lazar and Polyak, 2016; Wollenburg, unpubl. data of ODP Site 910).

In contrast to relative abundances, absolute abundances depict a distinct single maximum in cores from less than <1700 m water depth across the Arctic Ocean in the Middle Pleistocene (Fig. 6; Jakobsson et al., 2001; Polyak et al., 2004; Lazar and Polyak, 2016). This abundance maximum is located in many cores above a pink-white layer which is assigned to PW 2 (see also Polyak et al., 2004). In core P1-93-AR-P23 from Northwind Ridge the acme is observed even below the inferred PW 2 layer at the HCO of *B. arctica* (Fig. 6) close to the core surface, probably caused by mixing of sediments due to coring disturbance. In contrast, in adjacent cores P1-88-AR-3 and -5, a single maximum in relative abundances occurs distinctly above the HCO of *B. arctica* (>100 µm size fraction, Ishman et al., 1996). The maximum is associated with a brown layer that has been assigned to brown bed B4 in the NP26 composite on Mendeleev Ridge (Polyak et al., 2004). A common feature in many records is the absence of B. aculeata in sediments younger than the acme (Fig. 6).

The *Bulimina aculeata* acme is here defined based on a pronounced maximum in absolute abundances in the >63 µm size fraction, associated with brown bed B 4 on Mendeleev Ridge. This acme is restricted to cores from moderate water depths (<

https://doi.org/10.5194/egusphere-2025-6290
Preprint. Discussion started: 29 December 2025

1700 m) corresponding to the modern habitat depth (200 to 1500 m) of the closely related *B. marginata* which is usually lumped with *B. aculeata* in studies on Norwegian-Greenland Sea sediments (Mackensen et al., 1985; Höglund, 1947; Husum and Hald, 2004; Feyling-Hanssen, 1964; Spezzaferri et al., 2013). *Bulimina aculeata* occurs only sporadically beyond its habitat in deeper waters (Fig. 4). The acme is associated with an absolute abundance maximum of *Cassidulina neoteretis* and *Oridorsalis umbonatus* on the shallow submarine highs (Fig. 5) which can be also recognized in the > 150 µm or > 125 µm size fractions (Jakobsson et al., 2001; Polyak et al.2004; Lazar and Polyak, 2016).

Previously, the acme has been dated to MIS 5.1 but the revision of the coccolith biostratigraphy and $^{230}Th_{ex}$ extinction ages indicate an older age (e.g. Adler et al., 2009; Razmjooei et al., 2023). The $^{230}Th_{ex}$ extinction age of 226±54 kyrs suggests a MIS 7 age for the base of the acme in core PS2185-6 (Fig. 5). The stratigraphic correlation of the LO of E. huxleyi to PS2185-6 (Razmjooei et al., 2023) which is located above the acme indicates an age certainly older than MIS 5 for the top of the acme. Hillaire-Marcel et al. (2017) observe that the maximum of B. aculeata at 70-90 cm in the shipboard data set of core PS87/030-1 (>125 µm size fraction, Stein, 2015) is located between the extinction ages of $^{231}Pa_{excess}$ of ~140 kyrs at about 70 cm and of $^{230}Th_{excess,}$ of ~250±19 kyrs at ~109 cm±44 cm (Song et al., 2023). These authors assume that the base of the event is located at the MIS8/7 transition and in early MIS 7. Therefore, the acme may have occurred in MIS 7, which corresponds to the age for the LCO of *O. umbonatus*. Despite a clear relation to lithology being absent, the LCO in combination with the *B. aculeata* acme appears to be a robust stratigraphic datum in shallow to deep water cores.

4.3 Ecological and taphonomic processes determine formation of bioevents

Since evolutionary turnover does not play a role in the stratigraphic occurrence of most benthic foraminifer species in the Pleistocene of the Arctic Ocean, the composition of assemblages is determined by the complex interaction of ecologic requirements and taphonomic processes (Table B1). Thus, the formation of bioevents is controlled by a set of factors rather than a single environmental variable (Martin, 2003; Loubere et al., 1993; Loubere and Rayray, 2016).

The spatial distribution of living benthic foraminifera and their preference for specific bathyal water depths is essentially controlled by their food and oxygen requirements (Jorissen, 2003; Jorissen et al., 1995). To a lesser extent competition, grain size of sediments, current activity, and bottom water pH determine the bathyal faunal composition (Gooday and Jorissen, 2012). Species like *Lobatula wuellerstorfi* (= *Cibicides wuellerstorfi*) further require a minimum hydrostatic pressure for reproduction (Wollenburg et al., 2015).

However, foraminifera do not exclusively live at the sediment surface but can also survive at significant sediment depths if labile organic matter and oxygen is still available (Jorissen, 2003). Mean modern carbon export in the permanently ice-covered CAO is considered amongst the lowest in the world's oceans (Honjo et al., 2008; Nowicki et al., 2022) resulting inparticulate organic carbon (POC) fluxes of 0.17–1 g C $m^{-2}yr^{-1}$ at depths >1000 m (Harada, 2015; Roca-Martí et al., 2016). The low amount of POC reaching the seafloor in the CAO is usually immediately consumed at the sediment surface and not buried to sustain living foraminifera, or other life, below the surface centimeter under a permanent ice cover (Wollenburg and

https://doi.org/10.5194/egusphere-2025-6290
Preprint. Discussion started: 29 December 2025

Mackensen, 1998b). Therefore, moderate to deep-infaunal living taxa like *Melonis zaandami, Nonionellina labradorica* or various Elphidiids are today only sustained where food flux is high, at the seasonally ice-free upper continental slope and shelf. Species with an even higher food-demand like *Bulimina aculeata* (Jorissen et al., 1995) are absent from the modern Arctic Ocean (Wollenburg and Mackensen, 1998a, b; Wollenburg and Kuhnt, 2000).

Benthic foraminifera have been used to reconstruct past sea ice conditions (Cronin et al., 2008b; Polyak et al., 2013; Seidenkrantz, 2013). However, benthic foraminifera are only indirectly linked to sea-ice conditions because primary production and sedimentation of organic matter is related to light-penetration through sea ice, upwelling processes at the ice margin and release of ballast material from melting sea ice (Anderson et al., 2003; Mar, 2014; Swoboda et al., 2024). The ice-covered bathyal Arctic Ocean is characterized by opportunistic shallow-infaunal and epilithic/-phytic foraminiferal taxa adapted to low to very moderate carbon flux (Wollenburg and Kuhn, 2000). In the seasonally ice-free areas the surplus of labile organic matter provided by algae blooms and the respective algae export (Swoboda et al., 2024) at the ice edge cause an increase in the number of species that dwell on the sea floor in the accumulated phytodetritus. Such species rapidly reproduce after algae export events and are termed phytodetritus species (Gooday, 1988; Gooday and Lambshead, 1989; Thomas et al., 1995; Wollenburg and Kuhnt, 2000; Wollenburg et al., 2001b; Moodley et al., 2002; Wollenburg et al., 2004; Polyak et al., 2013).

Among the taphonomic processes, dissolution strongly affects benthic foraminifer assemblages in the Arctic Ocean and its marginal seas (Hunkins et al., 1971; Herman et al., 1989; Steinsund and Hald, 1994; Wollenburg and Kuhnt, 2000; Wollenburg et al., 2001b; Wollenburg et al., 2004; Loubere and Rayray, 2016). Thus, Hunkins et al. (1971, p.234) assume that foraminifer-poor intervals in CAO sediments indicate conditions more favourable for complete dissolution of calcareous material. In our cores the abundance of thin-shelled specimens and the preservation status of more robust shells indicate when dissolution had a significant impact on the assemblage composition in a specific sample. Many epifaunal taxa, in particular phytodetritus species, which form a major component of living benthic foraminifera in the Arctic Ocean (Wollenburg and Mackensen, 1998a), are thin-shelled and are therefore susceptible to dissolution. These taxa are often lost in the bioturbated uppermost 5 to 10 cm sediments (Loubere and Rayray, 2016). Consequently, the Arctic fossil record usually consists of infaunal taxa and high percentages of epifaunal taxa like *Epistominella exigua* are unusual and cannot be explained with modern geochemical processes in near-surface sediments (Loubere and Rayray, 2016). The extensive loss of thin-shelled epifauna species is often caused by massive sedimentation of labile organic matter after algal blooms (Wollenburg and Kuhnt, 2000). The oxidization of this labile organic matter often leads to lowered pH and carbonate aggressive conditions in near-surface sediments and pore water resulting in a dominance of agglutinated taxa even in the living fauna (Scott and Vilks, 1991; Wollenburg and Mackensen, 1998a; Wollenburg and Kuhnt, 2000; Seidenkrantz, 2013).

As dissolution affects the thin-shelled epifaunal shells first, abundant to dominant robust infaunal species such as *Bolivina arctica*, *Oridorsalis umbonatus*, and especially *Bulimina aculeata* reflect a significant taphonomic loss in associated thin-shelled epi- and shallow-infaunal species (Fig. 13). Such relict assemblages are often preserved in the brown layers. At the termination of warmer climatic conditions or an extended perennial ice cover the taphonomic loss was even higher. Here the

https://doi.org/10.5194/egusphere-2025-6290
Preprint. Discussion started: 29 December 2025

whitish and edged shells of thick-shelled calcareous infaunal taxa are accompanied only by shell fragments of a diminishing number of thin-shelled *Stetsonia horvathi* and *Epistominella arctica* in the small size fraction (Fig. 12).

In the CAO calcareous foraminifera are usually restricted to Quaternary sediments, and were rarely reported from the Pliocene whereas often sediments older than the Brunhes Chron exclusively comprise agglutinated foraminifers (O'Neill, 1981; Mullen and McNeil, 1995; Cronin et al., 2008b; Kaminski et al., 2009; Kender and Kaminski, 2013). Modern assemblages composed exclusively of agglutinated foraminifera occur only where carbonate dissolution is prevalent, in the deep-sea below the CTD, mud-flats or deep shelves (Murray and Alve, 2011; Murray, 2014). Nonetheless, these are residual assemblages resulting from post-depositional dissolution of calcareous shells in an original mixed assemblage due to carbonate-aggressive past bottom- and/or pore water pH values (Murray and Alve, 2011). The transition from agglutinated assemblages or wide-spread barren core sections to dominantly calcareous faunas is characterized by the absence of thin-shelled and corrosion traces on more robust taxa (Fig. 12, 13).

The modern CAO benthic foraminifera fauna is rich in loosely agglutinated taxa like *Crithionina* spp., *Rhizammina* spp., *Aschemonella* spp. that disintegrate soon after death. More robust species, firmly agglutinated with ferruginous cement and often thicker shells like *Rhabdammina* spp., *Saccammina* spp., *Psammosphaera fusca*, *Adercotryma glomerata*, *Glomospira* spp., *Reophax* spp., *Cribrostomoides subglobosum*, *Cyclammina* spp. (Bender, 1989; Schröder, 1988), and the extinct *Haplophragmoides obscurus*, are often the only foraminifera preserved in residual sediment core assemblages. It is assumed that the preservation of agglutinated foraminifera is favoured by a rapid burial and/or exposure of sediments to reducing pore waters. Under oxidizing conditions, the iron in the cement is mobilized and shells disintegrate (Schröder, 1988). High organic bound iron content (Gooday et al., 2008a) is further suggested to be responsible for preservation of organic-walled *Placopsilinella aurantiaca* down to >400 cm depth in core PS2185-6 (this study) and on the Alpha Ridge (Scott et al., 1989). As H. obscurus possess firmly agglutinated thick-shelled tests, we presume that it is the least vulnerable taxon susceptible to disintegration (e.g. in cores PS2185-6 and CESAR 83-014; this study, Scott et al., 1989) explaining their predominance in the intervals with exclusively agglutinated foraminifera. That the original agglutinated residual assemblage with abundant H. obscurus had a higher diversity becomes obvious in some samples where associated agglutinated species are observed. Accordingly, the absence of agglutinated foraminifera in core PS72/396-5 can likely be explained by sedimentation rates being too low to prevent iron mobilization from agglutinating shells. The occurence of *Saccorhiza ramosa* e.g. in laminated sediments of PS72/340-5 can be explained by the species affinity to moderate turbidity water (Schröder, 1988). It is a dominant species in trenches of the Kara Sea and here positively related to organic- and natural radionuclid-rich sediments (Domanov et al., 2017), indicating a preferred preservation at sites/times with increased sedimentation rate. Secondary enrichment in layers by hydrodynamic sorting as in distal turbidital areas, observed in abyssal plains of the Northwest Atlantic, may have happened.

https://doi.org/10.5194/egusphere-2025-6290
Preprint. Discussion started: 29 December 2025

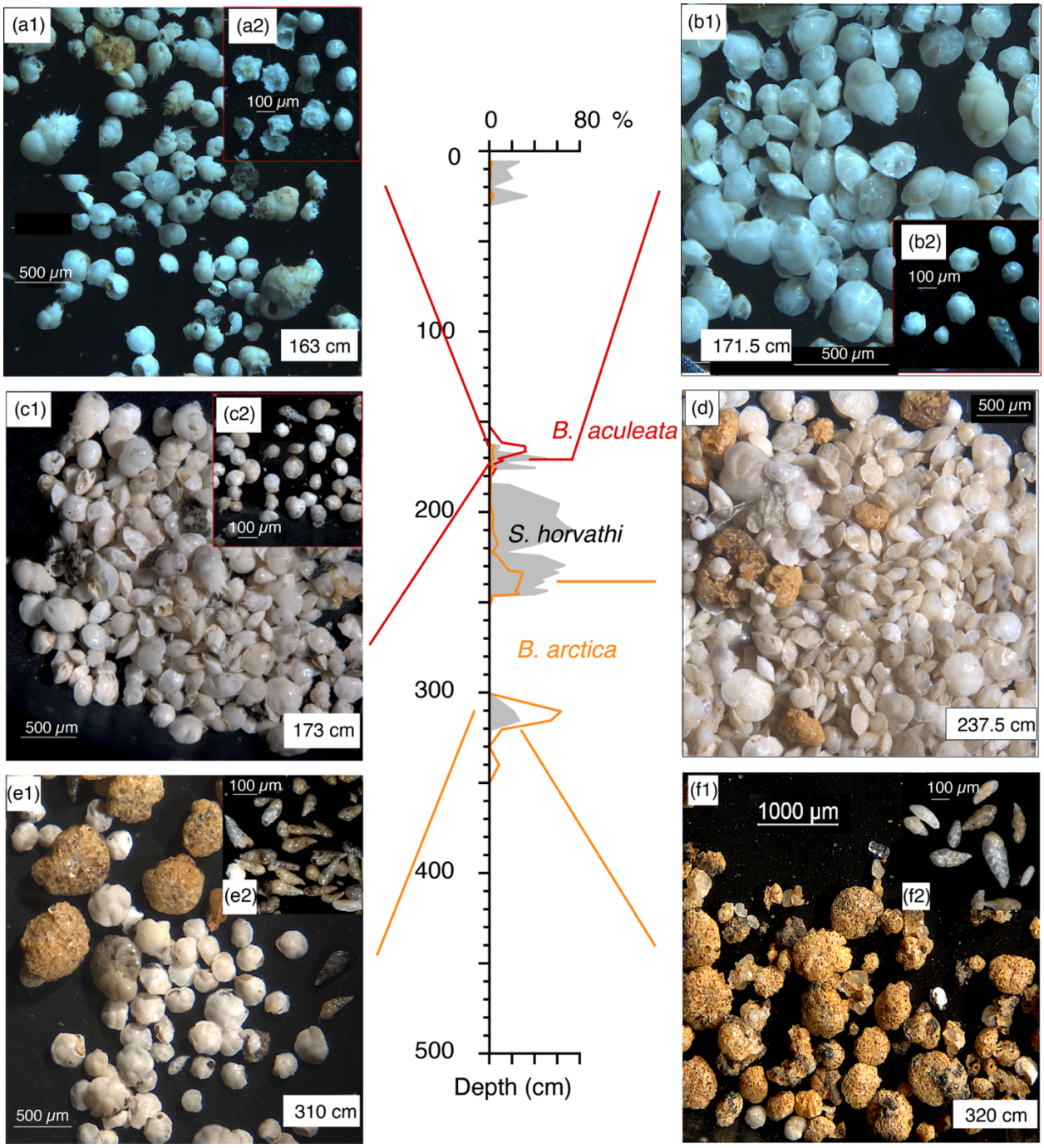

Figure 13: Exemplified preservation of benthic foraminifera in the *Bolivina arctica* and *Bulimina aculeata* bioevents in core PS2185-6. Relative abundance of *B. arctica* and *B. aculeata* vs *Stetsonia horvathi*. (f) 320 cm lower *B. arctica* bioevent, dominated by numerous *H. obscurus* in the lf (f1), mostly well-preserved *B. arctica* in the sf (f2), few corroded calcareous shallow-infaunal

https://doi.org/10.5194/egusphere-2025-6290
Preprint. Discussion started: 29 December 2025

specimens, thin-shelled *S. horvathi* almost absent. (e) 310 cm *B. arctica* bioevent peak, *B. arctica* well preserved, with associated shallow-infauna (e.g. *C. neoteretis*, *S. horvathi*) affected by minor to moderate dissolution (white and partly edged tests) lf (e1) and sf (e2). (d) 237.5 cm termination of the *B. arctica* bioevent peak, sf and lf shells mostly well preserved, partly hyaline, epifaunal species like *L. wuellerstorfi* present. (c) 171.5 cm lower boundary *B. aculeata* bioevent. Almost all shells are whitish but edging in the lf (c1) is minor, in the sf (c2) edging is significant *S. horvathi* becomes rare. (b) 173 cm peak *B. aculeata* event. Shells are progressively affected by dissolution incl. edging (b1), number of *S. horvathi* in the sf (b2) diminishes. (a) 163 cm upper *B. aculeata* bioevent boundary. (a1) cf shells are heavily etched and thin-shelled taxa are extremely rare. (a2) sf consists mainly of shell fragments.

4.4 Recolonization

Environmental conditions changing with time may also cause the sudden formation of benthic foraminifera-rich intervals. The observed abundance maxima often occurred after intervals that are barren or contain only a few individuals. Even if one assumes that episodically most foraminifera were lost due to carbonate dissolution or disintegration of agglutinating foraminifera, recolonization must also have occurred after times of adverse living conditions that have caused death of faunas. Dispersal of foraminifera following e.g. anoxia or extinction is usually rapid on geological time scales (Buzas and Culver, 1991; Alve, 1999; Murray, 2006), however, to restore the full faunal biodiversity after disturbance may take several millenia indicating different species-dependent capabilities of dispersal (Schmiedl et al., 2003). Based on studies on shallow-water foraminifera and occasional net catches, it is assumed that the dispersal and recolonization of foraminifera in the deep realm occurs via propagules, juvenile individuals smaller than 32 µm (Alve and Goldstein, 2010; Alve and Goldstein, 2003; Murray, 2006; Gooday and Jorissen, 2012). As Fram Strait is the only deep-water connection of the Arctic (sill depth ~2500 m) to the world's ocean, any recolonization has to occur through Fram Strait. Propagules are advected by inflow of waters from subpolar latitudes, then circulating anticlockwise as Atlantic Water (~200-600 to 850 m) and Upper Polar Deep Water (Rudels and Carmack, 2022; Timmermans and Marshall, 2020).

The modern Arctic Ocean shares the majority of foraminiferal species with the Norwegian-Greenland Sea (Lagoe, 1977; Mackensen et al., 1985; Scott and Vilks, 1991; Bergsten, 1994; Struck, 1995; Wollenburg and Mackensen, 1998a; Wollenburg and Kuhnt, 2000; Rasmussen et al., 2003b; Rasmussen and Thomsen, 2008; Husum et al., 2015). In pre-Brunhes sediments this was different, e.g. *Oridorsalis umbonatus* occurred in Late Miocene sediments on the Vøring Plateau (Osterman and Qvale, 1989) but much later around the *O. umbonatus* event in the Arctic Ocean. As other calcareous taxa like *E. exigua*, that possess a thinner shell than *O. umbonatus* or *C. teretis/neoteretis* with a approximately similar shell-thickness, are preserved in much older sediments, this indicates that living propagules of *O. umbonatus* had not been advected to the investigated sites for considerable time before the event.

4.5 Paleoceanographic implications of bioevents

https://doi.org/10.5194/egusphere-2025-6290
Preprint. Discussion started: 29 December 2025

In this chapter we consider the processes that were relevant for the formation of the selected bioevents in the Quaternary.

4.5.1 Changeover of agglutinated to calcareous benthic foraminifera

A fundamental change in benthic foraminifer assemblages occurred in upper Pliocene to middle Pleistocene sediments in the CAO (Cronin et al., 2008; this study). This change may be comparable to that observed during the Mid-Pleistocene Transition (MPT) in lower latitudes that was likely driven by a substantial change in food quality and supply (Hayward et al., 2010; Hayward et al., 2012; Mancin et al., 2013). Species adapted to a more continuous food supply, with a long life-span and low number of offspring (k-strategists) (Hayward, 2002; Kawagata et al., 2005; Hayward et al., 2012; Kender et al., 2016) were replaced by opportunistic species adapted to more seasonal primary production and able to immediately react with large offspring to food flux (r-strategists) (Thomas, 2007; Hayward et al., 2012; Mancin et al., 2013; Kender et al., 2016). None of these MPT extinction-group taxa are observed in the Arctic Ocean (O'Neill, 1981; Osterman, 1996) but the shift from a k-strategy to r-strategy dominated foraminiferal assemblage is likely reflected in the change from large-sized agglutinated taxa (considered to be k-strategist (Hottinger, 1983; Linke, 1992) including the dominant *Haplophragmoides obscurus* in core PS2185-6 (Fig. 5) and the miliolid *Pyrgo rotalaria* (Linke, 1992) in core in PS72/396-5 (Fig. 3) to faunas dominated by calcareous r-strategists. Evans et al. (1995) presume that the abundance maxima composed of agglutinated infaunal species with a detritivore life style reflect interglacial conditions, supporting their interpretation as k-strategist species. The fact that agglutinated foraminifera with ferruginous cement can only be preserved in reducing sediments may be indicative of increased past labile organic matter deposition supporting such interpretations.

However, the interpretation is complicated by the unknown loss in calcareous and agglutinated benthic foraminifers in the intervals where only agglutinated foraminifers dominate. In core PS72/396-5, agglutinated taxa are almost negligible, and we assume the common occurrence of *P. rotalaria* below the HCO of *B. arctica* being partly synchronous with the common occurrence of H. obscurus at site PS2185. *Pyrgo rotalaria* is a k-strategist, which is able to ingest large amounts of algae during export events, and to live off its own cytoplasm during periods of starvation (Linke, 1992). It is a long-living species (Wollenburg unpublished observation) without spontaneous reproduction in response to export events. *Pyrgo rotalaria* is common in modern northern high latitude foraminiferal faunas (size fraction >125 µm) dominated by calcareous species such as *Lobatula wuellerstorfi*, *C. neoteretis* or *O. umbonatus* plus the associated agglutinated species *Cribrostomoides subglobosum* (Mackensen et al., 1985; Thies, 1991; Nees, 1997; Wollenburg and Mackensen, 1998a, b). At first glance, this fossil assemblage could be regarded as just a modern-analog assemblage affected by dissolution of calcite and disintegration of agglutinants, however, the preservation potential of *P. rotalaria* is described as being lower than that of *L. wuellerstorfi* and *O. umbonatus* (Corliss and Honjo, 1981). Therefore, the dominance of the k-strategist *P. rotalaria* over the r-strategist L. *wuellerstorfi* and *O. umbonatus* in the >125-fraction is not caused by calcite dissolution but likely reflects a different paleo-export production scenario than today. *Cribrostomoides subglobosum* ingests freshly accumulated phytodetritus within 1-3 days after deposition (Altenbach, 1992; Linke, 1992; Linke and Lutze, 1993; Enge et al., 2011), hereby doubling its

https://doi.org/10.5194/egusphere-2025-6290
Preprint. Discussion started: 29 December 2025

cytoplasmic volume in this time span. As no food-triggered reproduction is reported, this species can be considered a k-strategist that already occurred in some of the oldest sediments of PS2185-6 and at the Alpha Ridge, but till today is a common faunal component and amongst the species with highest preservation potential.

4.5.2 Massive supply of IRD as potential trigger for decrease of *Bolivina arctica*

The youngest absolute abundance maximum of *Bolivina arctica* is terminated by the deposition of the detrital dolomite-rich layer PW 2 in the Arctic Ocean (Figs. 3-5). This represents a massive supply of iceberg-/sea-ice transported material from the Canadian Arctic that might have triggered a fundamental change in the Arctic Ocean ecosystem, possibly linked to grounding of glacial ice on Lomonosov Ridge. Prior to the HCO the assemblages contain well-preserved intermediate thin-shelled specimens of shallow-infaunal *Cassidulina neoteretis* and sometimes of the even more dissolution susceptible, thin-shelled *Stetsonia horvathi* indicating that preservation did not significantly affect these assemblages (Fig. 12). Benthic foraminifers are absent in PW 2 suggesting that the sea floor was recolonized after this event by species from subpolar latitudes. Since B. arctica and H. obscurus are endemic species, their abundance was strongly reduced during this event, and they never regained significant abundances when environmental conditions improved after deposition of the PW 2 diamicton.

4.5.3 The *Bulimina aculeata* acme

The assemblages are characterized by the predominance of robust infaunal species such as *B. aculeata* and *O. umbonatus*. In contrast, especially thin-shelled specimens (*E. arctica*, *E. exigua*), episodically also *S. horvathi* and *C. neoteretis* are thoroughly corroded, indicating extensive dissolution and preservation of only a residual assemblage. Moreover, iron-manganese coatings on shells show that these assemblages were exposed for extended times to sea water, reflecting slow sedimentation during this event. *Bulimina aculeata* is adapted to high carbon fluxes and tolerates a high O_2 depletion (Fontanier et al., 2002; Mackensen et al., 1990; Kaithwar et al., 2020). It is as a deep infaunal living foraminifera restricted today to the seasonally ice-free areas, usually at lower latitudes, water depths <1000 m and high carbon fluxes (Holbourn et al., 2013; Koho et al., 2015; Mackensen et al., 2000). The associated main species do not indicate a higher primary productivity at the sites studied. Therefore, this mixed assemblage is caused by enrichment of robust species and by specific ecological conditions. Nevertheless, the sudden occurrence of *Oridorsalis umbonatus* within this event indicate a substantial ecological change, invasion of the respective species and likely competition.

5 Conclusions

Benthic foraminifer bioevents that were previously used to correlate Pleistocene sediments across the central Arctic Ocean were evaluated by studying three sediment cores from the Lomonosov Ridge and the Amerasian Basin east of the southern

https://doi.org/10.5194/egusphere-2025-6290
Preprint. Discussion started: 29 December 2025

Mendeleev Ridge, and by comparing the results with published records. A standardized methology is applied to define robust bioevents. A stable taxonomy is a prerequisite for any biostratigraphy and therefore the descriptions of previously used taxa are restudied to select those species that can be unequivocally identified. A detailed taxonomic discussion including light and scanning microscope images are provided in the appendix. Published descriptions of some species are controversal and complicate distinguishing *Epistominella exigua* from *Eilohedra vitrea*, *Stetsonia horvathi* from *Epistominella arctica*, *Cassidulina teretis* from *Cassidulina neoteretis*, and different agglutinated taxa. The only taxa that are relatively well-defined are *Bolivina arctica*, *Bulimina aculeata*, species of *Pullenia*, *Oridorsalis umbonatus* and the agglutinated species *Haplophragmoides obscurus*.

If possible, a minimum of 300 specimens were counted in the size fraction of larger than 125 µm <2 mm and depending on diversity >100-300 in the size fraction >63<125 µm in each sample to achieve robust results. The definition of bioevents is based on absolute abundances, i.e. number of specimens per gram dry weight sediment. Relative abundances calculated as dry weight-% are less reliable because taphonomic processes such as bioturbation, dissolution and disintegration overprint assemblage composition. Based on absolute abundances, the stratigraphic occurrences of *Bolivina arctica*, *Bulimina aculeata*, and *Oridorsalis umbonatus* revealed meaningful patterns in the Brunhes Chron. Species of *Pullenia* are too rare in the cores to show interpretable stratigraphic patterns.

We consider the acme of *Bulimina aculeata*, the lowest common occurrence of *Oridorsalis umbonatus*, and the highest common occurrence of *Bolivina arctica* as robust bioevents in the Middle Pleistocene of the central Arctic Ocean. These bioevents are tentatively assigned to marine isotope stages, MIS 7 for *B. aculeata* and *O. umbonatus*, and MIS 9 for *B. arctica*. These bioevents were probably initiated by a more or less coincident advection of respective propagules to the central Arctic Ocean sites where they found suitable environmental conditions to reproduce in high numbers. Other species such as *Epistominella exigua* and *Haplophragmoides obscurus* are restricted to a specific area and water depth.

Agglutinated benthic foraminifer may be additionally useful for stratigraphic correlation in the Arctic Ocean such as the turnover of agglutinated to calcareous benthic foraminifers but based available data it occurred time-transgressive across the Arctic Ocean. *Haplophragmoides obscurus* is probably the only species that became extinct in the Middle Pleistocene of the CAO.

The proposed bioevents require thorough testing in sediment cores that have a robust independent chronostratigraphy, e.g. provided by a sequence of radiometric ages (e.g., ^{14}C, ^{231}Pa, ^{230}Th, ^{10}Be), to accurately calculate numerical ages. Various ecologic and taphonomic processes that may account for the formation of bioevents are discussed.

6 Appendices

Appendix A: Taxonomy of selected benthic foraminifera (Wollenburg)

Appendix A: Table A1 Benthic foraminifera taxa

Appendix B: Table B1 with ecological preferences

https://doi.org/10.5194/egusphere-2025-6290
Preprint. Discussion started: 29 December 2025

Appendix A: Taxonomy of selected benthic foraminifera (J. Wollenburg)

The taxonomy follows the original descriptions deposited in the Ellis and Messina Catalogues (Ellis and Messina, 1940-2025), and deviating generic classification as depicted in The World Foraminifera Database (Hayward et al., 2025), and WoRMS (Worms, 2025) at the date of submission. A total of 236 species was identified in the sediment cores (Table A1). In this appendix, the taxonomy of species that are relevant for this study is described.

Before turning to taxonomy, it is necessary to comment on the shell structure of calcareous species described and illustrated in the work of Herman (1973) and Lagoe (1977). Even at shallow sediment depth the majority of calcareous foraminiferal shells are postmortem affected by authigenic calcite overgrowth resulting in a rough surface texture (Wollenburg et al., 2023). This overgrowth may consist of idiomorphic crystallites or crystals (e.g. the glendonite resembling crystals which grow from the coalescence of idiomorphic crystallites of an overgrowth coating on *Bolivina arctica* in APl. 1, Fig. (c) or, likely due to secondary partial dissolution of authigenic calcite crystallites, an assembly of porous crystallite-remains is left (e.g. APl. 1, Fig. 2c, see also Wollenburg et al. (2023; https://www.pangaea.de/?q=doi:10.1594/PANGAEA.938246).

The 'surface samples' described by Lagoe (1977) comprise the uppermost three cm of piston cores collected from ice island T3. Since the uppermost part of these cores were often lost during coring operations (Clark et al., 1980), most samples may represent an unknown time interval, but not modern conditions. Thus, in Lagoe (1977) common occurrences of *B. arctica* and extensive overgrowth seen on most of the illustrated shells indicate that these samples are substantially older than recent. Authigenic overgrowths seen on SEM images of Lagoe (1977):

Pl. no.	Fig. no.	Species
2	2	Lagena sp.
2	10	*Esosyrinx?*
3	9	*Parafissurina* sp.
3	20-21	*Buliminella hensoni* as *B. elegantissima hensoni*
3	23-24	*Parafissurina* sp.
4	2, 6	*Bolivina arctica*
4	3	*Alabaminella weddellensis* as *Buccella arctica*
4	9, 13, 18	*Nonionella iridea* as *Valvulineria arctica*
4	14, 15, 19	*Epistominella arctica*
4	22	*Stetsonia horvathi*
5	8	*Chilostomella elongata*
5	13	*Ioanella horvathi* as *Eponides tumidulus* subsp. *horvathi*
5	16	*Cassidulina neoteretis* as *C. teretis*
5	17-18	*Islandiella norcrossi* as *C. norcrossi*

https://doi.org/10.5194/egusphere-2025-6290
Preprint. Discussion started: 29 December 2025

5 19-21 *Seabrockia earlandi as C. norcrossi*

***Bolivina arctica* Herman, 1973 emend.**

APl. 1, Figs. (a-d)

Bolivina cf. *B. inflata* Vilks 1969, Pl. 3, Figs. 10a-b.

Bolivina arctica Herman, 1973, Text-Fig. 3, Pl. 1, Figs.1-7

Bolivina arctica Lagoe, 1977, Pl. 4, Figs. 2, 6.

Bolivina arctica Wollenburg, 1992, Pl. 15, Fig. 3.

Original description (Herman, 1973): Test small, elongate, about twice as long as broad. Greatest width formed by the last pair of chambers; initial test narrow and twisted. Chambers are biserial, inflated, and increase gradually in size; they are broad and low in the initial part becoming higher in the last 3 to 4 pairs. The sutures are distinct, and slightly oblique and the aperture is elliptical extending from the base of the final chamber. The wall is calcareous, perforate, composed of numerous closely packed, tapering, hollow tube-like structures illustrated in the scanning electron micrographs. This is the first time that such tube-like structures have been reported in benthic foraminifers to my knowledge. Dimensions: Length of holotype 0.20 mm, greatest width 0.12 mm, greatest thickness 0.90 mm. Paratypes length range 0.30-0.18 mm, greatest width range 0.14-0.10 mm, greatest thickness range 0.07-0.10 mm. Stratigraphic range: Pliocene – Pleistocene.

Emended description: Test biserial either straight throughout or the juvenile test is twisted, test small, elongate, two to three times as long as broad. Up to 10 pairs of chambers have been observed; chamber height and width increase rapidly in size and especially ontogenetic old chambers are often very much inflated. The sutures are depressed and oblique, but each new pair of chambers overlap the previous one slightly creating a ribbon-like suture (APl. 1, Fig. (b3). Well-preserved tests are translucent (APl. 1, Fig. (a1), corroded tests or tests affected by calcite overgrowth opaque to white (APl. 1, Figs. (c1), (d1), (e1). Wall smooth and shiny, with irregularly distributed pores (APl. 1, Figs. (a2-b3), wall thickness 1 to 2 µm. Aperture very variable, sometimes a broad arch (APl. 1, Figs. (c1-2) but more often an elongated basal loop extending within a depression up the apertural face of the last chamber with a serrated bordering lip, internal toothplate missing. Apertural surface covered with tubercles, some tubercles of older apertural surfaces may still be recognizable in the sutures (APl. 1, Figs. (c2).

Dimensions: 20 specimens measured in the size fraction >63 µm: Length mean 200 µm (100-300 µm), largest width 70-400 µm, largest thickness 50-200 µm.

Discussion: In this study, well-preserved specimens lack the closely packed, tapering, hollow tube-like structures, observed by Herman (1973, Pl. 1, Figs. 5-7). These features on the shell surface represent authigenic overgrowth but were included in the original description of *Bolivina arctica* Herman (1973). The majority of Pleistocene *B. arctica* specimens (APl. 1, Figs. (c-e) are indeed covered with authigenic calcite overgrowth (Wollenburg et al., 2023). However, well-preserved specimens are thin-shelled, and have a smooth shell surface and splendid pores (APl. 1, Figs. (a-b). Therefore, the original description

https://doi.org/10.5194/egusphere-2025-6290
Preprint. Discussion started: 29 December 2025

must be emended to include the description of the shell surface of specimens not affected by post mortem precipitation of calcite.

Authigenic overgrowth cover the whole *B. arctica* tests either by a porous sheet (APl. 1, Figs. (c1-3), as has been described by Herman (1973), or in form of solid idiomorphic crystallites (APl. 1, Figs. (d-e). In extreme cases authigenic crystallites grow to large crystals resembling Glendonite (APl. 1, Figs. (d1-2).

The first two whorls of some specimens are rather triserially than twisted biserially arranged (APl. 1, Figs. 3a-b). Except for their shorter triserial test part, their general appearance and their aperture, these specimens resemble *Virgulopsis pygmeus* (3-4 triserial whorls) described from Oligocene sediments in the Beaufort-Mackenzie basin (McNeil, 1997). This may indicate an evolutionary relation of *B. arctica* to *Virgulopsis pygmeus*.

Comparison to other studies: Specimens of *B. arctica* covered by authigenic overgrowth may be easily misidentified as *Siphotextularia rolshauseni* (Wollenburg et al., 2001) or vice versa because of the white agglutinated test with rough surface texture (APl. 2, Fig. (a)) of the latter species. Wang et al. (2021) observed abundant *B. arctica* during MIS 2 in sediment core ARC5-BB01 from the Norwegian Sea. This core is located close to a series of sediment cores which contain abundant *S. rolshauseni* during early MIS 2 but not *B. arctica* (Nees and Struck, 1994). Therefore, it is likely that Wang et al. (2021) assigned specimens of *S. rolshauseni* to *B. arctica*. Scott et al. (2008) illustrated specimens as *B. arctica* (Pl. 5, Figs. 2-9) that may be assigned to the agglutinated taxon *Pseudobolivina antarctica* (Pl. 5, Figs. 2, 3, 6, 7), the calcareous species *Bolivina pseudoplicata* possessing a rough surface texture (Figs. 8, 9) and *Fursenkoina complanata* (Figs. 4, 5). *Bolivina arctica* (Lazar and Polyak, 2016) has been observed in many sediment core studies in the Arctic Ocean that did no document species identification by images (Scott et al., 1989; Wollenburg, 1995a; Wollenburg and Mackensen, 1998c; Mullen and McNeill, 1995; Polyak and Solheim, 1994; Polyak et al., 2013; Adler et al., 2009; Cronin et al., 2014). It is here assumed that *B. arctica* was correctly identified.

Stratigraphic range: ?Pliocene to recent, *B. arctica* became a progressively rare faunal component after the youngest absolute abundance maximum.

Geographic distribution: Arctic Ocean, occurrences outside the Arctic Ocean cannot be validated as they lack images.

Bathymetric comments: continental slope and ridges, more common at lower mesopelagic to bathyal pelagic (600-4000 m) (Lagoe, 1977; Wollenburg and Mackensen, 1998c, a; Wollenburg and Kuhnt, 2000).

***Bulimina aculeata* d'Orbigny, 1826**

APl. 2, Figs. (b-d)

Bulimina aculeata d'Orbigny, 1826, a new species name for *Polymorphium pineïformium* Soldani, 1791 was assigned by him, however, no description and no type figure was provided

Polymorphium pineïformium Soldani, 1791, p. 119, pl. 269, fig. 1; pl. 130, fig. vv. after Holbourn (Holbourn et al., 2013); in Soldani's plates shown in Microtax (Young and B.T., 2025) pl. 127, Figs. I-K .

https://doi.org/10.5194/egusphere-2025-6290
Preprint. Discussion started: 29 December 2025

Bulimina aculeata Parker, Jones and Brady, 1871, p. 172, Pl. 11, Fig. 128. First detailed description and type figure provided.

Bulimina pupoides var. *spinulosa* Williamson, 1858, p. 62, Pl. 5, Fig. 128.

Bulimina aculeata Brady, 1884a, p. 406, Pl. 51, Figs. 7–9.

Bulimina marginata Goës,1894 in parts., Pl. 9, Fig. 444.

Bulimina aculeata van Morkhoven et al., 1986, p. 31, Pl. 7.

Bulimina marginata Höglund, 1947, Figs. 205-209, 215-216.

Bulimina AP. O'Neill, 1981, Pl. 3, Fig. 7.

Bulimina aculeata Chauhan et al., 2015, Pl. C, Fig. 3.

Bulimina marginata Chauhan et al., 2015, Pl. C, Fig. 2.

Original description d'Orbigny, 1826: No descriptions and figures were provided. Instead *Bulimina marginata* was illustrated in his work on recent sediment samples from the Adriatic Sea. In the respective study he also provided a new name, *B. aculeata*, for *Polymorphium pineïformium* Soldani 1789-1799 (see above). Parker, Jones and Brady (1871) later stated that the species would be 'similar to *B. marginata*, but having a series of long spines fringing the outer margins of the chambers in place of the finely serrate edges exhibited by that species.

Taxonomic remarks (Holbourn et al., 2013): 'Test forms an elongate, triserial series; tapered in outline and subcircular in cross-section, with an acute initial portion, and a rounded apertural end; widest in the last whorl. The inflated chambers increase rapidly in height and are separated by distinct, depressed sutures. Chamber walls are calcareous, finely perforate, and often partially translucent and smooth, except at the outer margins of the basal chambers, which are fringed by sturdy spines. These spines may extend halfway up the test. Well-preserved specimens may also have a prominent basal spine. The primary aperture is a loop-shaped opening bordered by a lip and extending up from the base of the final chamber; with an internal toothplate. Geographic distribution: Worldwide. Stratigraphic range: Early Miocene to recent. Bathymetric distribution: Bathyal to abyssal. Dimension: 0.65 to 0.75 mm (Cushman and Parker, 1947).

Discussion: Although *B. aculeata* and *B. marginata* are genetically separated (Tsuchiya et al., 2008), their morphology is extremely variable and intermediate morphotypes often dominate the assemblages. Collins (1989) and Burgess and Schnitker (Burgess and Schnitker, 1990) considered *B. aculeata* and *B. marginata* as distinct species, with an intermediate morphotype representing a morphological variation of *B. marginata*. In contrast, Höglund 1947) suggested that *B. marginata, B. aculeata* and *B. gibba* are morphotypes of the same species. Smith (1964) reported that the number of spines of *B. marginata* f. *denudata* was related to water depth, and loss of spines occurred in relation to increasing water depth. The number and length of spines is extremely variable (Van Morkhoven et al., 1986). Collins (1991) describes an increase in spine length with water depth at sites off Mexico, whereas in the Arctic Ocean specimens from lower deep bathyal water (~2500-3500 m in cores PS72/340-5 and PS72/396-5, this study; O'Neill, 1981) possess shorter but more numerous spines than those from upper bathyal to middle

https://doi.org/10.5194/egusphere-2025-6290
Preprint. Discussion started: 29 December 2025

bathyal water depths (ODP Hole 910A, PS2185-6 (see APL. 1, sp. 2, Fig. (d). In the Arctic Ocean *B. aculeata* and *B. marginata* can be clearly distinguished from each other and usually *B. aculeata* is dominant.

Stratigraphic range: early Miocene to recent (Holbourn et al., 2013)

Geographic distribution: worldwide (Holbourn et al., 2013); absent from the modern Arctic Ocean

Bathymetric comments: upper bathyal to lower abyssal (200-10000 m) (Holbourn et al., 2013).

***Cassidulina neoteretis* Seidenkrantz, 1995**

APl. 2, Figs. (e-i), APl. 3

Cassidulina teretis Lagoe 1977 (Lagoe, 1977), Pl. 5, Figs. 15-16.

Cassidulina teretis Mackensen and Hald, 1988, Pl. 1, Figs. 5-15.

Cassidulina teretis Wollenburg, 1992, Pl. 15, Figs. 6-7.

Cassidulina teretis Wollenburg, 1995, Pl. 3, Figs. 12-13

Cassidulina neoteretis Seidenkrantz, 1995, Pl. 1, Figs. 1-6; Pl. 2, Figs. 1-14; Pl. 3, Figs. 1-8; Pl. 5, Figs. 1-3.

Cassidulina teretis Ishman & Foley 1996, Pl. 2, Fig. 4.

Cassidulina teretis Wollenburg & Mackensen, 1998a, Pl. 3, Figs. 12-13.

Cassidulina neoteretis Wollenburg & Mackensen 2009, Figs. 3.10, 3.15.

Cassidulina neoteretis Chauhan, et al., 2015), Fig. 3.3.

Cassidulina neoteretis Hanslik, 2011, Pl.1, Figs. 5-6.

Cassidulina neoteretis Lazar et al.2016, Fig.8.1-8.6.

Cassidulina teretis Cronin et al., 2019a, b?, Pl. 1, Figs. 9-12.

Cassidulina neoteretis Cage et al., 2021, Figs. 2a, 2d–j, 2o.

For a more detailed list of synonyms see also Cage et al. (2021).

Original description (Seidenkrantz, 1995): Test lenticular, biconvex with an acute, slightly undulating, peripheral margin. Umbilical boss of milky semitranslucent shell material on each side. Eight to ten chambers (frequently 10) in the final whorl, biserial arranged in 4 to 5 alternating pairs, each chamber appearing large, rounded rhomboid to ovate and reaching to the umbilical boss on one side of the test, and small and subtriangular on the other side. Sutures distinct, thickened, but not limbate, slightly depressed and outlining the chamber. Wall calcareous, hyaline or opaque, and optically granular. Surface smooth with relatively small, rounded pores evenly distributed on the chamber walls but with no pores on the umbilical boss or along the sutures. Aperture an elongate, narrow slit extending from the base of the final chamber in a crescent paralleling the outer margin of the chamber, reaching 2/3 to 3/4 the distance from the base of the chamber to the peripheral keel. A subtriangular apertural plate with a smooth edge, formed by the infolded chamber wall, lies along the inner margin and partly covers the aperture. Seldom few very small serrata on the apertural plate are developed. A narrow, serrate ridge lies adjacent to the outer

https://doi.org/10.5194/egusphere-2025-6290
Preprint. Discussion started: 29 December 2025

margin of the aperture. Dimensions: greatest diameter: 230-410 µm (mean 300 µm), greatest thickness: 130-200 µm (mean 150 µm).

Discussion: *Cassidulina teretis* differs from *C. neoteretis* by a usually narrower and crescentic rather than subtriangular-shaped apertural plate. The apertural plate is not almost smooth as in *C. neoteretis* but provided with densely packed serrata (Cage et al., 2021; Seidenkrantz, 1995). *Cassidulina teretis* (360-550 µm) has a larger test size than *C. neoteretis* (200-410 µm) (Cage et al., 2021). Well-preserved specimens may be identified under the light microscope, but SEM analyses may be required to eventually recognize serrata in corroded *C. teretis* specimens (APl. 2, Figs. (i)). However, the majority of corroded *C. neoteretis* specimens can be identified by their broader prominent subtriangular apertural plate. This feature may support species assignment in diagenetically altered specimens even if the edge of the apertural plate has been affected by carbonate dissolution (APl. 3). *Cassidulina teretis* occurs only in trace amounts in the cores examined in this study, while other species that are morphologically similar, such as e.g. *Paracassidulina neocarinata* are absent. For reliable differentiation of *C. neoteretis* from other easily confused species, reference should therefore be made to the study by Cage et al. (2021), which focuses specifically on this topic. Tappan (1951) included in the original description of *C. teretis* only drawings. Neither photographs nor details of the apertural plate edge were shown or mentioned. Subsequently, all specimens resembling *C. teretis* were in studies on sub-Arctic and Arctic sequences assigned to *C. teretis*. Seidenkrantz (1995) later re-studied the *C. teretis* holotype and compared it to ~2000 *Cassidulina* specimens with comparable morphology from high northern latitudes and described *C. neoteretis* as a new species. Yet, most Arctic studies did not differentiate between *C. neoteretis* and *C. teretis* until the early 2000s, and continued to assign all specimens to *C. teretis* (Polyak et al., 2004; Ishman and Foley, 1996; Ishman et al., 1996; Rasmussen and Sheldon, 2003; Rasmussen et al., 2003; Wollenburg and Mackensen, 1998c, a; Wollenburg et al., 2004; Wollenburg and Kuhnt, 2000; Wollenburg et al., 2001; Rasmussen et al., 2014). The first author of this study hesitated to assign specimens to *C. neoteretis* during her early studies when she was searching for the change from *C. teretis* to *C.neoteretis* in calcareous microfossils-bearing sediments of core PS2185-6 that should have recovered the Brunhes/Matyama boundary (Spielhagen et al., 1997). However, SEM analysis did not reveal a strongly serrate apertural plate in any of the roughly 100 specimens. With no significant differences in the toothplate (smooth or with only minor and narrow serrata) of all investigated specimens, the first author, as many others, sticked to *C. teretis* as the species name for specimens in her fossil and modern collection. Her first individuals with distinct serrata as indicative of *C. teretis* were observed in this study from the lowest calcareous foraminifera bearing sediments of core PS72/396-5. While Seidenkrantz describes the extinction of *C. teretis* and substitution by *C. neoteretis* in the Norwegian Sea at 700 ka, Lazar et al. (2016) report a long stratigraphic coexistence of both species in the Brunhes Chron on the Northwind Ridge and the presence of *C. teretis* in almost each sample analysed (Lazar et al., 2016). The images provided are of good quality and support their distinction of *C. teretis* and *C. neoteretis*. In contrast, in the new cores and surface and core samples the first author has previously worked on (older slides were revisited for this study) only *C. neoteretis* specimens were found. The first author analysed hundreds of specimens under the light microscope and conducted more than 100 SEM analyses on *C. neoteretis/teretis* specimens downcore in PS2185-6, and all specimens could be assigned to *C. neoteretis*. In deep-water sites *C. neoteretis/C.teretis* is rare, but most analyzed specimens in cores PS72/396-5

https://doi.org/10.5194/egusphere-2025-6290
Preprint. Discussion started: 29 December 2025

and PS72/340-5 were exclusively specimens of *C. neoteretis*. Only in sample PS72/396-5, 130 cm few *C. teretis* specimens could be identified in sediments dated to the Matuyama Chron (Elkina et al., 2023) which is a stratigraphic interval just below the stratigraphic change to *C. neoteretis* according Seidenkrantz (Seidenkrantz, 1995). In order to gain a better insight into a potential co-occurrence of *C. neoteretis* with C. *teretis* in modern to late Pleistocene sediments on the Mendeleev Ridge I additionally analyzed well-preserved *C. neoteretis* specimens from the upper 5 cm of core PS72/413-3 (1263 m water depth) by light microscope; those specimens including SEM analyses of 20 specimens were also exclusively attributable to *C. neoteretis*. We have no doubt in the species assignment of Lazar et al. (2016) but probably they had also recorded iceberg-rafted specimens in their analyses.

Stratigraphic range: *Cassidulina teretis* was originally described from Pliocene to early Pleistocene sediments of Alaska (Tappan, 1951). It appeared in the Upper and Middle Miocene and became extinct in the North Atlantic shortly after the Gauss/Matuyama boundary and in the Norwegian Sea shortly after the Brunhes/Matuyama boundary (Seidenkrantz, 1995). *Cassidulina neoteretis* had its first occurrence in the North Atlantic around 2.3-2.0 Ma and its first occurrence in the Norwegian Sea at ~700 ka (Seidenkrantz, 1995). *Cassidulina neoteretis* obviously evolved from *C. teretis* and replaced the latter species at progressively younger times with increasing latitude until *C. teretis* finally disappeared after the Brunhes/Matyama boundary in the Norwegian Sea (Seidenkrantz, 1995). Due to the unclear differentiation of *C. teretis* and *C. neoteretis* the first and last occurrence of both taxa in the Arctic Ocean is unclear.

Geographic distribution: Worldwide, common in the subarctic and Arctic (Holbourn et al., 2013)

Bathymetric comments: Bathyal, in the Arctic Ocean most common at depths of 200-1400 m(Wollenburg and Mackensen, 1998c).

***Cribrostomoides subglobosus* (Cushman, 1910)**

APl. 4, Figs. (a-b)

Lituola subglobosa Sars, M., 1868 (1869), p. 250 (Holbourn et al., 2013).

Lituola subglobosa Sars, M., 1871 (1872), p. 253 (Holbourn et al., 2013).

Haplophragmium latidorsatum Brady, 1884, Pl. 34, Figs. 8-10, not figs. 7, 14) (Holbourn et al., 2013).

Haplophragmium latidorsatum Goës, 1894, Pl. 5, Figs. 102-123.

Haplophragmoides subglobosum Cushman, 1910, Figs. 162-163.

Labrospira subglobosa Høglund, 1947, Fig. 126, Pl. 2, Fig. 2.

Alveolophragmium latidorsatum Barker, 1960, Pl. 34, Figs. 7-8, 10, 14.

Cribrostomoides subglobosus Todd and Low, 1980, Pl. 1, Fig. 7.

Cribrostomoides subglobosum Scott and Vilks, 1991, Pl. 1, Figs. 19-20.

Cribrostomoides subglobosum Thies, 1991, Pl. 7, Figs. 4a-b, Pl. 10-11.

Cribrostomoides subglobosus Jones et al, 1993, Pl. 1, Figs 1-5; Pl. 2 Figs. 6-8; Pl. 3, Figs. 1-7.

Cribrostomoides subglobosum Wollenburg, 1995, Pl. 2, Figs. 10-11.

https://doi.org/10.5194/egusphere-2025-6290
Preprint. Discussion started: 29 December 2025

Recurvoides scitulus Ishman and Foley, 1996, Pl. 1, Fig. 11.

Cribrostomoides subglobosum Wollenburg and Mackensen, 1998, Pl. 2, Figs. 10-11.

Original description (Cushman, 1910): Test usually planispiral consisting of two or more coils, involute, depressed at the umbilici, chambers very broad and low, wall arenaceous somewhat roughened but variable, chambers usually seven or eight in the final coil, making the test as a whole subglobose, aperture a more or less elongated slit at the base of the apertural face, simple, colour: grey or brown; diameter 1-2.5 mm.

Taxonomic remarks (Holbourn et al., 2013): Test is involute, initially streptospiral, later planispiral with a subcircular outline and a rounded periphery. Chambers are low and broad, highly inflated, and separated by indistinct sutures. Chamber walls are agglutinated, non-calcareous, and usually smoothly finished. In early chambers the primary aperture is an oval to slit-like areal opening bordered by a narrow lip above the base of the last chamber. In later chambers the primary aperture may become more elongated and the lip may fuse to form multiple openings.

Discussion: O´Neill (1981) described specimens from arctic sediments that are identical to *C. subglobosum* and/or *Cyclammina orbicularis* as *Alveolophragmium polarense* n.sp. but morphological differences to distinguish these species were not discussed. Evans and Kaminski (1998) stated that *A. polarense* from e.g. cores PS2185-6 and PS2212-3 resemble *C. subglobosum* but that alveols in the chamber wall and a planispiral coiling would place these species in *A. polarense*. Having worked on parallel samples from PS2212-3 (Wollenburg et al., 2001a,b,cd?) and PS2185 (this study), the new data suggest that they had assigned all quasi-planispiral *C. subglobosus*-resembling agglutinants to *A. polarense*. At least for core PS2212-3 and the upper 500 cm analyzed in core PS2185-6 this is a misjudgement since all respective specimens analysed under the SEM (>10 from various depths) lack alveoles in their chamber wall, thus, have to be assigned to *C. subglobosus*. If we compare the poor SEM image of the chamber wall of *A. polarense* from Evans and Kaminski (1998) with the wall structure of *C. subglobosus* (Pl. 3 in Jones et al., 1993), it becomes apparent that a tight particle-packing in *C. subglobosus* cannot be observed or expected and that indeed Evans and Kaminski's specimen illustrated in their Pl. 2 Figs. 8-9 should be assigned to *C. subglobosus*. The wall structure of the *Alveolophragmium polarense* specimen shown in Pl. 4, Fig. 1 of Kaminski et al. (2009) with a striking alveolar wall structure, however, is totally alveolar and resembles both in general appearance and wall structure *Cyclammina orbicularis* (Brady, 1884a), (see also their Pl. 1, Figs. 5a-b). *Cyclammina orbicularis* is also found in our samples from PS2185-6 (Pl. 4, Fig. 3). Considering the high morphological variability of *C. subglobosus* (e.g., Goës, 1894; Thies, 1991). I also presume that many specimens assigned by Evans and Kaminski to *Trochammina lomonosovensis* (Evans & Kaminski, 1998) in core PS2212-3, can be regarded as juvenile *C. subglobosum* specimens. Juvenile *C. subglobosum* tests are typically streptospiral coiled and even the holotype SEM images for *T. lomonsovensis* can be regarded as strepto- rather than trochospiral coiled, compare with Evans and Kaminski (1998; Pl. 2, Figs. 7-9) and the *C. subglobosum* illustrations on Plate 9 of Thies (1991). Moreover, in core PS2212-3 the co-occurrence with adult *C. subglobosus* specimens and the absence of otherwise juvenile- *C. subglobosus* specimens supports this assignment. Only clear trochospiral tests co-occurring with *H. obscurus* are here assigned to *T. lomonosovensis.*

https://doi.org/10.5194/egusphere-2025-6290
Preprint. Discussion started: 29 December 2025

Stratigraphic range: Upper Cretaceous to recent (Jones et al., 1993).

Geographic distribution: worldwide (Jones et al., 1993).

Bathymetric comments: shelf to abyssal (Jones et al., 1993), in the Arctic Ocean most abundant between 700 and 3000 m (Wollenburg and Mackensen, 1998c; Husum et al., 2015).

***Cyclammina trullisata* (Brady, 1879)**

APl. 4, Figs. (f1-3).

Trochammina trullisata Brady, 1879, Pl. 5, Figs. 10a, b.

Cyclammina trullisata Barker, 1960, Pl. 40, Figs. 13 a, b, 16.

Cyclammina bradyi Cushman, 1910, p. 113, Text-figs. 174 a,b.

Cyclammina trullisata Schröder-Adams, Pl. 17, Fig. 17.

Original description (Brady, 1879): Test nautiloid, compressed, lenticular, somewhat excavated at the umbilicus; composed of about three convolutions, of which but little more than the latest is visible; peripheral margin acute or somewhat rounded. Segments about nine in each convolution. Septa marked by more or less sinuate lines, only slightly depressed. Exterior smooth, usually smooth, usually polished; interior surface often reticulate; colour brown. Aperture crescentic, situate on the face of the terminal chamber, close to the margin of the previous convolution. Diameter 1/20 inch (1.25 mm). The inner surface of the test of *C. trullissata* sometimes exhibits a slightly raised reticulation, but this in no case, so far as my observation goes, is more than a mere, superficial marking, and never comes to anything resembling the cancellated shelly growths that often nearly fill the chambers of *Cyclammina*. The distribution of the species is wide, but it is by no means abundant in any locality. The best "Challenger" specimens are from two stations in the North Atlantic and two in the South Atlantic, the depth of water varying from 390 to 2200 fathoms.

Taxonomic remarks: The species has a fine-grained test with a smooth surface and an equatorial intermarginal aperture with an almost non-developed inner alveolar wall structure, very uncommon for the genus (Schröder-Adams et al., 1986). Diameter: 0.2-2 mm.

According to Schröder-Adams et al. (1986) who has studied deep-water agglutinated foraminifera of the North Atlantic Ocean in detail, Brady (1884 and collection) describes complete involute specimens and specimens in which up to 2 rarely 3 whorls can be observed. Like in her collection, this variability is also observed in the new cores.

Geographic distribution: Arctic Ocean (O'Neill, 1981).

Stratigraphic range: ?Pliocene to recent (O´Neill, 1981).

Bathymetric distribution: Seamounts, bathyal-abyssal.

https://doi.org/10.5194/egusphere-2025-6290
Preprint. Discussion started: 29 December 2025

***Eilohedra vitrea* (Parker et al., 1953)**

APl. 5, Figs. (d-f).

Epistominella vitrea Parker et al. 1953, Pl. 4; Figs. 34-36, 40-41.

Epistominella vitrea Feyling-Hanssen et al., 1983, Pl. 2, Figs. 7-8.

Epistominella vitrea Feyling-Hanssen & Ulleberg, 1984, Pl. 3, Figs. 25-27.

Epistominella vitrea Murray, 2003, Fig. 7.11-13.

Epistominella vitrea Pawlowsky et al., 2007, Figs. 1a-c.

Original description (Parker et al., 1953): Test small, convex on the dorsal side, depressed toward the umbilicus on the ventral side, periphery rounded, sometimes slightly lobulate, consisting of about three whorls; chambers slightly inflated, six in the last whorl; sutures very slightly depressed and slightly curved on the dorsal side, more depressed on the ventral side, the later ones slightly curved, earlier ones radial; wall smooth, translucent, very finely perforate; aperture long, narrow, slightly curved, with a narrow lip. Maximum diameter 0.27 mm, thickness 0.11 mm.

Taxonomic remarks: The species has a bilamellar shell and an aperture composed of a short extension starting at the base of the chamber from the umbilical side of the periphery to its center then it bends and continues as a slit in the chamber wall (APl. 5, Fig. (f).

Discussion: See under *E. exigua*.

Geographic range: Worldwide except for the Mediterranean (Murray, 1991).

Stratigraphic range: Eocene to recent (Gaździcki & Majewski, 2012).

Bathymetric distribution: Predominantly shelf to upper bathyal, but also reports from abyssal depths (Pawlowski et al., 2007).

***Epistominella arctica* Green, 1959**

APl. 4, Figs. (g-i)

Epistominella arctica Green, 1959, pp. 78-79, Pl. 1, Figs. 4a-b.

Epistominella arctica Green, 1960, Pl. 1, Figs. 4a-b.

Epistominella arctica Lagoe, 1977, Pl. 4, Figs. 14-16.

Epistominella? Lagoe, 1977, Pl. 4, 19-20, 22.

Stetsonia arctica Scott and Vilks, 1991, Pl. 3, Figs. 8-14, not Figs. 6-7.

Epistominella arctica Wollenburg, 1992, Pl. 18, Fig. 7.

Epistominella sp. 1 Wollenburg, 1992, Pl. 18, Figs. 8-9.

Epistominella sp. 2 Wollenburg, 1992, Pl. 18, Fig. 6.

Stetsonia arctica Bergsten, 1994, Pl. 2, Fig. 2, not Fig. 1.

Stetsonia arctica Mullen and McNeil, 1995, no images.

https://doi.org/10.5194/egusphere-2025-6290
Preprint. Discussion started: 29 December 2025

Stetsonia arctica Ishman and Foley, 1996, in parts, no images.

Stetsonia arctica Pak et al., 1992, no images.

Epistominella arctica Wollenburg & Mackensen 1998, Pl. 3, Figs. 16-17.

Epistominella AP. 1 Wollenburg & Mackensen 1998), Pl. 4, Figs. 2-3.

Epistominella AP. 2 Wollenburg & Mackensen 1998, Pl. 4, Figs. 4-5.

Epistominella arctica Wollenburg et al., 2001, 2004, 2007, no images.

Stetsonia arctica Adler et al., 2009, in parts, no images.

Epistominella arctica Polyak et al., 2013

Epistominella arctica Lazar and Polyak, 2016, no images.

Epistominella arctica Jennings et al., 2017, no images.

Epistominella arctica Jennings et al., 2020, Pl. 2, Figs. 8a-b.

Stetsonia horvathi https://byrd.osu.edu/research/groups/paleoceanography/projects/foram/gallery/stetsonia-horvathi

Original description (Green, 1959): Test minute, rotaloid, biconvex, last chamber greatly inflated, test opaque, small; edge broadly rounded; periphery lobate; all chambers slightly inflated, four to five chambers in the last whorl, two whorls visible on the dorsal side; suture depressed slightly; wall finely perforate; aperture elongate in the plane of coiling entrance recurved by an overgrowth of the dorsal wall at times pinching off the aperture before it reaches the base of the chamber leaving the aperture elevated in the face; however, the suture always extends to the base of the last chamber. Diameter of the holotype 0.070 mm, width of the holotype 0.03 mm.

Taxonomic remarks: Different to the description by Green (1959), the shell of living or none-diagenetically altered specimens is fully translucent and not opaque. Thus, the specimens deposited by Green were either affected by calcite dissolution or, affected by authigenic overgrowth like specimens in Lagoe's (1977) work. In contrast, the biogenic shell surface in well-preserved specimens is smooth and irregularly porous. Tests are thin (~0.7 µm shell-thickness) and translucent (APl. 4, Figs. (h-i). The aperture is usually a species-defining aspect, but Green's description includes different morphotypes, one in which the aperture reaches the base of the inflated chamber and another in which the aperture is positioned somewhere in this last chamber on the umbilical side. Following Wollenburg (Wollenburg, 1992) specimens with an inflated last chamber in which the aperture extended to the base of the chamber were counted as *E. arctica* sensu strictu. specimens in which the aperture had no connection to the base in the last inflated chamber were counted as *Epistominella* sp. 1, and specimens in which the aperture was situated within a depression extending from the periphery to the umbilical side were considered *Epistominella* sp. 2 (Wollenburg, 1992). These morphotypes were finally combined as *E. arctica* sensu lato for faunal analyses and environmental/ stratigraphic interpretations (Wollenburg, 1992; Wollenburg, 1995b; Wollenburg and Kuhnt, 2000; Wollenburg et al., 2001; Wollenburg and Mackensen, 1998c; Wollenburg et al., 2004; Wollenburg et al., 2007). The inflated last chamber, described as the prominent feature for the species, is only expressed in the final chamber precipitated by the specimen before reproduction. All previous ontogenetic stages, and thus the majority of specimens, are expressed by specimens

https://doi.org/10.5194/egusphere-2025-6290
Preprint. Discussion started: 29 December 2025

in which the last chamber is completely depressed on from the periphery to the umbilical side (APl. 4, Fig. (i). In this depression a round aperture is situated at the base of the last chamber. These none-terminal ontogenetic stages have been previously described as *Epistominella*? sp. (Lagoe, 1977) and as *Epistominella* sp. 2 (Wollenburg, 1992) (Pl. 18, Fig. 6).

Discussion: Starting with Scott and Vilks (1991) *E. arctica* and the equally small but planispiral *Stetsonia horvathi* were for many years lumped as *S. arctica* (Bergsten, 1994; Adler et al., 2009; Polyak et al., 2010).

In some research groups foraminiferal analyses were or are still limited to the size fractions >150 µm (Polyak et al., 2004; Adler et al., 2009) or >100 µm (Chauhan et al., 2016; Chauhan et al., 2014; Rasmussen et al., 2007; Rasmussen et al., 2014; Sztybor and Rasmussen, 2017). In these studies, the total abundance of the small-sized (mean test size approx. 100 µm) *E. arctica* and *S. horvathi* is not completely recorded.

Geographic distribution: Arctic Ocean, Weddel Sea (Cornelius and Gooday, 2004).

Stratigraphic range: ?Pliocene, Pleistocene to recent (Müllen and Mcneil, 1995). Due to lumping with *Stetsonia horvathi* the first occurrence of *E. arctica* in the CAO? is unclear.

Bathymetric distribution: continental slope to abyssal (Wollenburg and Mackensen, 1998b).

***Epistominella exigua* (Brady, 1884)**

APl. 5, Figs. (a-c).

Pulvinulina exigua Brady, 1884 (Brady, 1884a), Pl. 103, Figs. 13–14.

Eponides exigua Cushman, 1931, P. 44, Pl. 10, Figs. 1-2.

Epistominella exigua Phleger, Parker and Peirson, 1953, PL. 9, Figs. 35-36.

Eponides exiguus Feyling-Hanssen, 1954, P.135, Pl. 2, Fig. 4.

Epistominella exigua Barker, 1960, Pl. 103, Figs. 13–14.

Epistominella exigua Wollenburg, 1992, Pl. 19, Fig. 1.

Epistominella exigua Jones, 1994, P. 103, Pl. 103, Figs. 13–14.

Epistominella exigua Hanslik, 2011, Pl. 1, Figs. 7-8 images shows *E. vitrea* not *E. exigua*

Epistominella exigua Kireenko et al., 2022, Pl. 4, Figs. 48a-b.

Original description of (Brady, 1884a): Test free, rotaliform; both faces convex, the inferior less so than the superior, periphery acute, lobulated; composed of three convolutions, of which the outermost has usually five segments. Sutures non-limbate; marked on the superior face by thickened lines of opaque-white shell-substance; on the inferior by slight depressions. Diameter, 1/65th inch (0.4 mm), or less.

Taxonomic remarks (Holbourn et al., 2013) Test forms a small trochospire; slightly lobulate in outline and unequally biconvex in cross-section, with an evolute, slightly convex spiral side, an involute, convex to nearly conical umbilical side, and an acute, lobulate periphery. The five moderately inflated chambers in the last whorl increase gradually in size, and are separated by flush, oblique, thickened sutures on the spiral side, and by curved, slightly depressed sutures on the umbilical side. Chamber

https://doi.org/10.5194/egusphere-2025-6290
Preprint. Discussion started: 29 December 2025

walls are calcareous, finely perforate, and smooth. The primary aperture is an interiomarginal slit extending up the face of the final chamber on the umbilical side (Holbourn et al., 2013).

Discussion: It is largely unknown that *E. exigua* co-occurs with the visually and genetically closely related *Eilohedra vitrea* (Parker, 1953) (APl. 3, Figs. (a-b) in the marginal Arctic Ocean (Barents Sea continental slope, Yermak Plateau) (Sirenko et al., 2001; Osterman, 1996). Due to the comparable chamber arrangement, *E. vitrea* is easily confused with *E. exigua.* The two species can be best differentiated by the larger chamber number in the last whorl of *E. vitrea* (6 compared to 5 in *E. exigua)*, and the less depressed umbilicus in the latter (APl. 5. Figs. (a-f), and the rather umbilical than peripheral aperture. In detail the aperture of *E. exigua* also lacks the apertural extension along the periphery and its shell wall is monolamellar not bilamellar as in *E. vitrea*. There are many reports of *E. exigua* in sediment cores from the central Arctic Ocean, however, the only illustrated specimen has 6.5 chambers thus, is a *E. vitrea* (Hanslik, 2011). Therefore, the identification of *E. exigua* in other arctic records should be considered with care if these are not confirmed by images or taxonomic descriptions. Both species should be distinguished because *E. exigua* is a Phytodetritus species and therefore is assumed to be indicative of seasonally ice-free conditions with increased carbon transfer to depth, similar observations have not been made for *E. vitrea* (Gooday and Lambshead, 1989; Gooday et al., 2008; Wollenburg et al., 2001).

Moreover, usually *Epistominella exigua* is regarded as deep-water species, and also in the Arctic Ocean usually found at larger water depths >900 m (Wollenburg et al., 2001), *E. vitrea* is regarded a shallow-water species common e.g. on the Yermak Plateau in ODP holes 910C (Osterman, 1996) and 910A (own unpublished observations), here *E. exigua* is absent. However, shallower occurrences of *E. exigua* and much deeper occurrences of *E. vitrea* have also been reported (Pawlowski et al., 2007; Lecroq et al., 2009), and in the Arctic a broad bathymetric range where both species often coexist is found (own unpublished observation). For instance *E. vitrea* usually dominates at 600 m water depth but at site 276 (571 m) of the PS15 expedition of Polarstern in 1987 only *E. exigua* was found (Wollenburg, 1992).

Geographic range: Worldwide except for the Mediterranean (Murray, 1991).

Bathymetric comments: Predominantly lower bathyal to abyssal, but also reports from shallower bathyal depths (Holbourn et al., 2013).

Stratigraphic range: Middle Eocene to recent (Holbourn et al., 2013).

***Haplophragmoides obscurus* O'Neill, 1981**

APl. 2, Fig. (i).

Haplophragmoides obscurus O'Neill, 1981, Pl. 2, Figs. 13, 17.

Cyclammina pusilla Evans et al., 1995, no images.

Cyclammina pusilla Evans and Kaminski, 1998, Pl. 1, Figs. 8-9.

Reticulophragmium pusillum Scott et al.1989, no images.

Cyclammina pusilla Cronin et al., 2008, no images.

https://doi.org/10.5194/egusphere-2025-6290
Preprint. Discussion started: 29 December 2025

Reticulophragmium pusillum Kaminski et al., 2009, Pl. 4, Figs. 4, 6.
Haplophragmoides obscurus Hayward et al.2024

Original description (O'Neill, 1981): Test free, planispiral, involute, compressed, periphery rounded; chambers numerous approximately 10 in the final whorl, sutures indistinct; wall coarsely arenaceous consisting largely of angular quartz grains; aperture an arcuate interiomarginal slit; colour yellowish-brown.
Length of specimen 0.35-0.65 mm, maximum width of specimen 0.30-0.60 mm.
Taxonomic remarks (this study): The specimens chamber walls are thin and usually composed of one-layer of grains and a light brown coloration of the cement. In our specimens only quartz and light-coloured feldspar is used, dark minerals as described by Evans and Kaminski, were not observed. We also observe neither pseudopores nor a labyrinthic wall structure. However, the individual chambers are developed as a high semi-acute arch with a low average height and very long flanks, so that in broken individuals, the side flanks of the chambers can be observed as punctiform depressions.
Discussion: Agglutinated foraminifera are not recorded, or are usually only recorded as a group in most stratigraphic studies of the central Arctic Ocean. Thus, taxonomic studies on agglutinated taxa are limited to the work of O'Neill (1981) and Kaminski and co-workers (Evans et al., 1995; Evans and Kaminski, 1998; Kaminski et al., 2009; Kender and Kaminski, 2013). *Haplophragmoides obscurus* was originally described from the Alpha Ridge where it is restricted to the Pliocene (O'neill, 1981). Later Scott et al. 1989) (without illustrations,) Evans et al. 1995), Evans and Kaminski (1998) and Kaminski et al.(2009) (with illustrations) assigned respective specimens to *Cyclammina pusilla/ Reticulophragmium pusillum* (Brady, 1879). None of these authors discussed why they rejected O'Neill's species concept, but they mentioned that this arctic *C. pusilla* variants are constructed of much coarser grains as described for the species.
Reticulophragmium pusillum uses much smaller grains to construct their tests and is larger in size than *H. obscurus*.
Geographic distribution: Arctic Ocean (O'Neill, 1981).
Stratigraphic range: Pliocene to Pleistocene (O'Neill, 1981).
Bathymetric distribution: bathyal to abyssal (O'Neill, 1981).

***Oridorsalis umbonatus* (Reuss, 1851)**

APl. 5, Figs. (g-k).

Rotalina umbonata Reuss, 1851, Pl. 5, Figs. 35a-c.
Truncatulina tenera Brady, 1884, Pl. 95, Fig. 11a-c.
Pulvinulina umbonata Brady, 1884, Pl. 105, Fig. 2.
Eponides tener Lagoe, 1977, Pl. 5, Figs. 3, 7.
Oridorsalis tenera Herman, 1989, no images.
Oridorsalis tener Belyaeva and Khusid, 1989, no images.
Oridorsalis umbonatus Scott and Vilks, 1991, Pl. 2, Figs. 15-16, Pl. 4, Figs. 4-5.

https://doi.org/10.5194/egusphere-2025-6290
Preprint. Discussion started: 29 December 2025

Oridorsalis umbonatus Bergsten 1994, Pl. 2, Figs. 17-18.
Oridorsalis tener Ishman & Foley 1996, Pl. 2, Fig. 9
Oridorsalis umbonatus Bornmalm 1997, Figs. 24J-k.
Oridorsalis tener Wollenburg & Mackensen 1998, Pl. 5, Figs. 6-8.
Oridorsalis umbonatus/tener Osterman et al., 1999, both names used in different graphs, no images.
Oridorsalis tener Wollenburg & Kuhnt 2000, no images.
Oridorsalis tener Wollenburg et al. 2001, no images.
Oridorsalis tener Wollenburg et al. 2004, no images.
Oridorsalis tener Polyak et al., 2004, no images.
Oridorsalis tener Polyak et al., 2013, no images.
Oridorsalis tener Husum et al., 2015, no images.
Oridorsalis tener Lazar and Polyak 2016, no images.

Original description of *Rotalina umbonata* (Reuss, 1851): Testa suborbiculata, depressa, subtus medio umbonate, superne convexaa, margine lobato-carinata; anfractibus 3, internis obsoletis; loculis 5, subtus oblongis angustis, planis, superne triangularibus, convextusculis, superfiele laevi. Diameter = 0.35-0.45 mm.

Original description of *Truncatulina tenera* (Brady, 1884a): Test regularly rotaliform; both faces convex; peripheral edge acute and lobulated. Consisting of rather more than three convolutions of nearly equal width, the last of which is formed of five or six segments; sutures distinct, slightly depressed, marked on the superior face by nearly straight lines; aperture a curved fissure bordered by a thickened lip, situated at the inner margin of the final segment near the periphery. Diameter= 1/55th inch (0.46 mm).

Discussion: There is a controversial discussion on the taxonomic status of *Oridorsalis tener* and *Oridorsalis umbonatus.* Subtle morphological differences distinguish *O. tener* from *O. umbonatus* and *O. tener* is often considered a junior synonym.

In the Challenger report Brady (1884a) illustrated *O. (Pulvinulina) umbonatus* and the new species *O. (Truncatulina) tenera*. He described that both taxa strongly resemble each other and that they are difficult to differentiate. However, the specimens in the Arctic Ocean with their very acute periphery and reduced shell height, resemble rather Brady´s *T. tenera* than his *P. umbonata*. Moreover, the Arctic *Oridorsalis* specimen, like the Brady's figure of *T. tenera*, usually lack the supplementary spiral sutural apertures characteristic of *O. umbonatus.*

In taxonomic works with illustrations of both morphotypes, *O. umbonatus* has more straight sutures on the spiral side, chambers of equal size in the last whorl, a trochoidal cross-sectional outline, whereas *O. tener* has curved sutures, a more rapid increase in chamber height, and a much more compressed outline (Bornmalm, 1997; Lohmann, 1978; Pflum et al., 1976; Corliss, 1979). It is also stated that *Oridorsalis umbonatus* has a more rounded periphery, is more inflated, and has a smaller rate of whorl expansion than *O. tener* (Lohmann, 1978; Corliss, 1979). Except for the difference in shell height and the lack of visible secondary apertures, none of these differences are supported by the original descriptions of both species (Mead and Kennett,

https://doi.org/10.5194/egusphere-2025-6290
Preprint. Discussion started: 29 December 2025

1987). As both variants usually co-occur it is generally agreed that *O. umbonatus* has a certain morphological variability which includes *O. tener* (Bornmalm, 1997). The Arctic Ocean lacks *Oridorsalis* specimens with rounded periphery, visible supplementary apertures, and only occasionally supplementary apertures 1-2 can be seen under the SEM. They have always a compressed outline, and increase always rapidly in chamber height. Thus, although I agree that the species descriptions of *O. tener* and *O. umbonatus* are very similar, I doubt that the Arctic *Oridorsalis* specimens are genetically identical to the large *O. umbonatus* specimens with significant shell height, small chamber height and rounded periphery found in the Norwegian Seas. However, at present although genetic differences between *O. umbonatus* specimens have recently been observed (Himmighofen et al., 2023), no assignments to different species have been made. Thus, based on today's state of knowledge all records of *O. tener* in the Arctic Ocean are reassigned to *O. umbonatus.*

Geographic distribution: Worldwide (Holbourn et al., 2013).

Stratigraphic range: Middle Paleocene to recent (Holbourn et al., 2013). In the Norwegian-Greenland Sea since the late Miocene (Osterman and Qvale, 1989)

Bathymetric distribution: Lower neritic to abyssal (Holbourn et al., 2013)

***Pullenia bulloides* (d'Orbigny, 1846)**

APl. 4, Figs. (l1-2).

Nonionina bulloides d'Orbigny, 1846, Pl. 5, Figs. 9-10.

Pullenia sphaeroides Brady, 1884a,b?, Pl. 84, Figs. 12-13.

Pullenia sphaeroides Goës, 1894, Pl. 14, Figs. 771-772.

Pullenia bulloides Feyling-Hanssen and Ulleberg, 1984, Pl. 1, Figs. 27-28.

Pullenia bulloides Wollenburg, 1992, Pl. 20, Fig. 2.

Pullenia bulloides Wollenburg & Mackensen 1998, Pl. 5, Figs. 9, 10.

Pullenia bulloides Hanslik, 2011, Pl. 1, Figs. 8-9.

Pullenia bulloides Chauhan et al., 2015, Figs. 3.23-24.

Original description (d'Orbigny, 1846; translated into English): Test spheric, almost as thick as broad, smooth, scope rounded; formed by 4 only very weakly convex, and only by weakly depressions separated chambers, which join in the centre leaving a hardly noticeable umbilical depression; the last flat and halfmoon-curved chamber is penetrated by very long linear opening.

Discussion: In the sediment cores PS2185-6, PS72/340-5 and PS72/396-5, *Pullenia bulloides*, *P. quinqueloba* (Reuss, 1851) and *P. osloensis* Feyling-Hanssen (1954) have been occasionally observed (Figs. 3-5). In contrast, most records from the central Arctic Ocean list only *P. bulloides*. Because of only slight morphological differences, *P. quinqueloba* and *P. osloensis* may have been lumbed with *P. bulloides*. *P. quinqueloba* differs from *P. bulloides* in being much flatter and five-chambered, whereas *P. osloensis* is a small sub-sphaerical five-chambered species (Wollenburg, 1992; Feyling-Hanssen, 1964). Since the observed species *P. bulloides, P. quinqueloba* and *P. osloensis* occupy different habitats in modern Arctic Ocean sediments

https://doi.org/10.5194/egusphere-2025-6290
Preprint. Discussion started: 29 December 2025

(Wollenburg and Mackensen, 1998a), most stratigraphic records from the Arctic Ocean require careful restudy to confirm taxonomic assignments.

Geographic distribution: Worldwide (Holbourn et al., 2013); in the modern Arctic Ocean restricted to areas influenced by the inflow of Atlantic Water close to Fram Strait (Wollenburg and Mackensen, 1998b; Wollenburg et al., 2001).

Stratigraphic range: Latest Paleocene to recent (Holbourn et al., 2013).

Bathymetric distribution: Bathyal to abyssal (Holbourn et al., 2013).

***Pyrgo rotalaria* Loeblich and Tappan, 1953**

APl. 5, Fig. (m).

Pyrgo rotalaria Loeblich and Tappan, 1953, Pl. 6, Figs. 5-6.

Biloculina murrhyna Schwager, Cushman, 1917, Pt. 6, Pl. 29, Figs. 1a-e.

Pyrgo rotalaria Lagoe, 1977, Pl. 2, Fig. 21.

Original description (Loeblich and Tappan 1953): Test free, circular in outline, much inflated, but with a distinctly carinate border, slightly produced at the aboral end; chamber development typically biloculine; wall calcareous, imperforate, surface smooth; aperture nearly circular, with a broad tooth that is slightly notched to give a bifid appearance. Length of holotype 0.55 mm, greatest breadth 0.52 mm, thickness 0.31 mm. Length of figured paratype 0.57 mm, breadth 0.52 mm. Other specimens range from 0.47 to 0.86 mm in length.

Taxonomic remarks: This species resembles *Pyrgo murrhyna* (Schwager) of some authors, but the type specimen of Schwager has two strong spines on either side of an indentation on the basal margin, and the peripheral margin of the test is grooved.

Discussion: As noted by Belanger and Streeter (1980), specimens occur with two varieties of aperture, a round rather small aperture with indistinct bifid tooth as described by Loeblich and Tappan, and a large broad one with broad bifid tooth. Todd and Low (1980) had assigned varieties with a large aperture and large bifid tooth to *P. vespertilio* which, however, is less compressed, has a rounded border and fine rips on the test. In our samples the large aperture is just expressed in some adult tests, whereas all juveniles and also the majority of adult tests show an aperture as described by Loeblich and Tappan. Whether, this is an expression of sexual versus asexual generation is unclear. Size: 0.2-2 mm.

Geographic distribution: Arctic Ocean, Norwegian-Greenland Sea.

Stratigraphic range: In the Arctic Ocean to our knowledge restricted to the Pleistocene, the closely related species has its first occurrence in the middle Miocene (Holbourn et al., 2013).

Bathymetric distribution: Bathyal to abyssal, mostly from depths >600 m (Wollenburg and Mackensen, 1998b; Thies, 1991).

Stetsonia horvathi Green, 1959

APl. 4, Figs. (j-k).

Stetsonia horvathi Green, 1959 (Green, 1959), Pl. 1, Figs. 6a-b.

https://doi.org/10.5194/egusphere-2025-6290
Preprint. Discussion started: 29 December 2025

Stetsonia horvathi Lagoe, 1977, Pl. 4, Figs. 17, 22.

Stetsonia arctica Scott and Vilks, 1991, Pl. 3, Figs. 6-7, not 5, 8-14.

Stetsonia horvathi Wollenburg, 1995, Pl. 4, Figs. 9-11.

Stetsonia arctica Ishman and Foley, 1996, Pl. 2, Fig. 11.

Stetsonia horvathi Wollenburg & Mackensen 1998a, Pl. 4, Figs. 9-11.

Stetsonia arctica Adler et al., 2009, in parts, no images.

Stetsonia horvathi Jennings et al., 2020, Pl. 2, Figs. 3a-4b.

Original description (Green, 1959): Test small, generally quadrate in side view, generally glassy, may be opaque, planispiral involute, four to five chambers in the last whorl, test flat; edge subrounded; periphery smooth; sutures slightly depressed, slightly curved; aperture a high arched opening at the base of the last septal face, somewhat curved, situated in a depression. In the glassy specimens the previous whorls are clearly visible through the outer wall, causing the sutures to appear widen toward the umbilicus. Diameter of the holotype 0.10 mm, width of the holotype 0.04 mm. Diameter of the paratypes 0.07-0.10 mm, width of the paratype 0.03-0.04 mm. Geographic distribution: Arctic Ocean. Stratigraphic range: Pliocene to Pleistocene. Bathymetric distribution: bathyal to abyssal.

Discussion: Scott and Vilks (1991) stated that the trochospiral *E. arctica* and the planispiral *S. horvathi* would represent morphotypes of the same species that they called *S. arctica.* This contrasts with the involute chamber arrangement, one of the basic requirements of the genus *Stetsonia*, that is not expressed in *E. arctica* tests. Moreover, no trochospiral form with a high-arched aperture, and no planispiral form with inflated chamber, that could represent some transitional forms can be identified. In broken *E. arctica* (Apl. 4, Fig. (i) it also becomes obvious that even juvenile *E. arctica* tests are trochospiral and that at no point in ontogeny a high-arched aperture is developed. However, many studies followed the approach of Scott and Vilks lumping both species (Pak et al., 1992; Müllen and McNeil, 1995; Bergsten, 1994). As other groups work on size fractions >150 µm (Polyak et al., 2004; Adler et al., 2009) *Stetsonia horvathi*, like *E. arctica*, are often not recorded in Arctic studies due to its small size?as their mean test size is around 100 µm (Table B1). In shallower cores located at the transition from the Fram Strait to the Arctic Ocean despite working on the size or >100 µm these true arctic species are likely only rare faunal components (Chauhan et al., 2014; Chauhan et al., 2015) .

Geographic distribution: Arctic Ocean, Weddell Sea (Cornelius and Gooday, 2004).

Stratigraphic range: ?Pliocene, Pleistocene to recent (Müllen and McNeil, 1995). Due to lumping with *E. arctica* the first occurrence of *Stetsonia horvathi* is unclear.

Bathymetric distribution: continental slope to abyssal (Wollenburg and Mackensen, 1998b).

https://doi.org/10.5194/egusphere-2025-6290
Preprint. Discussion started: 29 December 2025

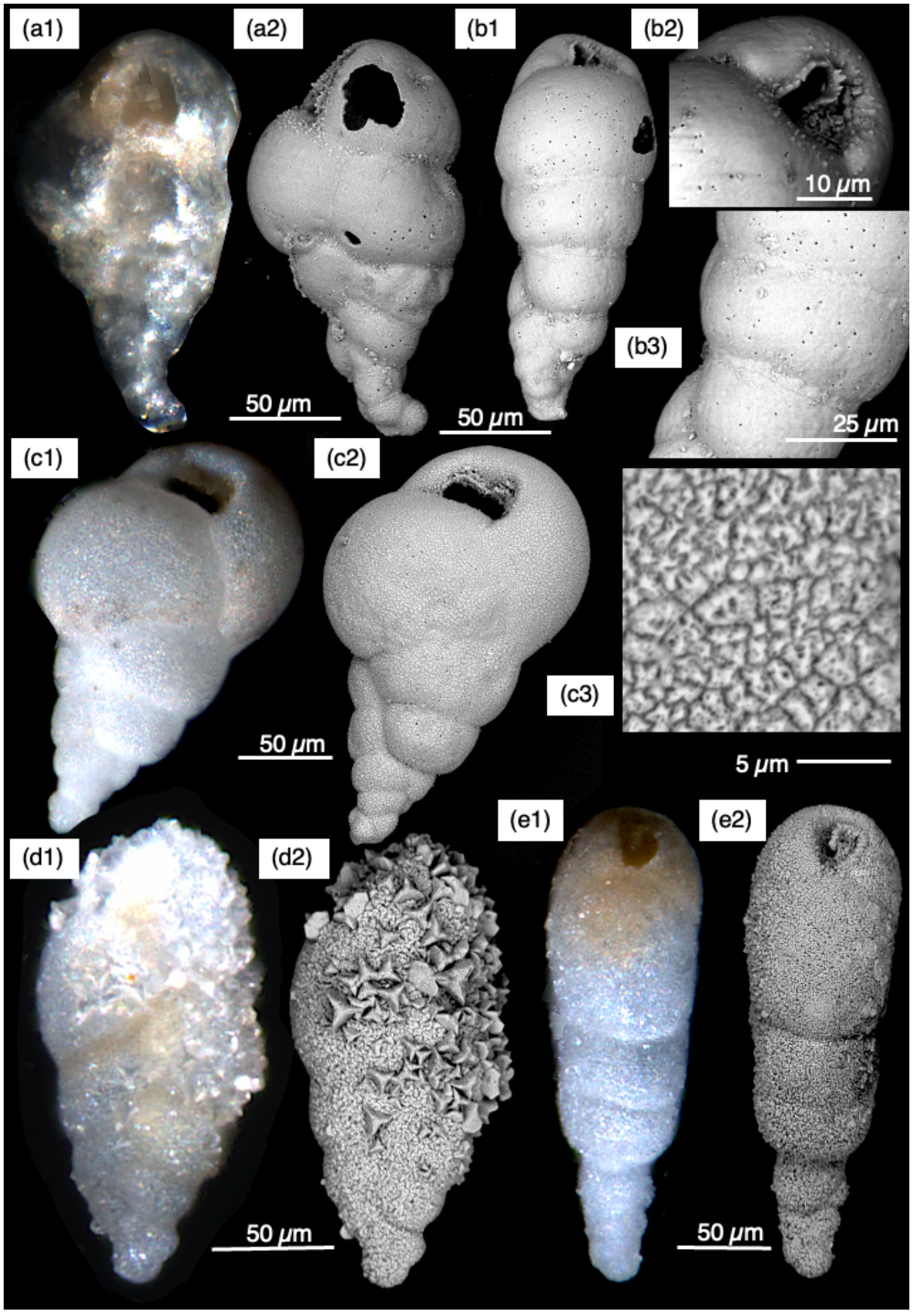

Appendix Plate A1

https://doi.org/10.5194/egusphere-2025-6290
Preprint. Discussion started: 29 December 2025

Figures a – e. *Bolivina arctica*; **Figure (a)**. Same specimen under light (**a1**) and scanning electron microscope (**a2**). (**a1**) Translucent well-preserved specimen; (**a2**) smooth shell surface, covered by unevenly distributed pores; tubercles occur in the apertural face and along some sutures. **Figure (b)**. specimen in side view. (**b1**) Whole specimen; (**b2**) close-up on the aperture situated in a depression, and surrounded by a serrated lip and multiple tubercles; (**b3**) close-up on the overlapping ribbon between two successive chambers. **Figure (c)**. Inflated specimen with triserial juvenile test, wide aperture and a shell covered by a coat of porous calcareous overgrowth. (**c1**) Opaque and dull appearance of the shell caused by authigenic overgrowth; (**c2-3**) details of the porous authigenic overgrowth. **Figure (d)**. Same specimen heavily encrusted by authigenic overgrowth, light (**d1**) and scanning electron microscope images (**d2**). (**d1**) Opaque and dull shell with larger crystals sticking out from the shell; (**d2**) details of large authigenic idiomorphic calcite crystals formed on top of an authigenic overgrowth coat covering the shell, crystals oriented perpendicular to the shell surface. **Figure (e)**. Same specimen covered by small idiomorphic authigenic calcite crystals, light (**e1**) and scanning electron microscope images (**e2**). Figures (a-b). PS2185-4, 0-1 cm; Figure (c). PS72/396-5, 75 cm. Figures (d-e). PS2185-6, 143.5 cm. Figures (a1), (c1), (d1), (e1), Axiozoom images; Figures (a2-b3), (c2-3), (d2), (e2), SEM images.

https://doi.org/10.5194/egusphere-2025-6290
Preprint. Discussion started: 29 December 2025

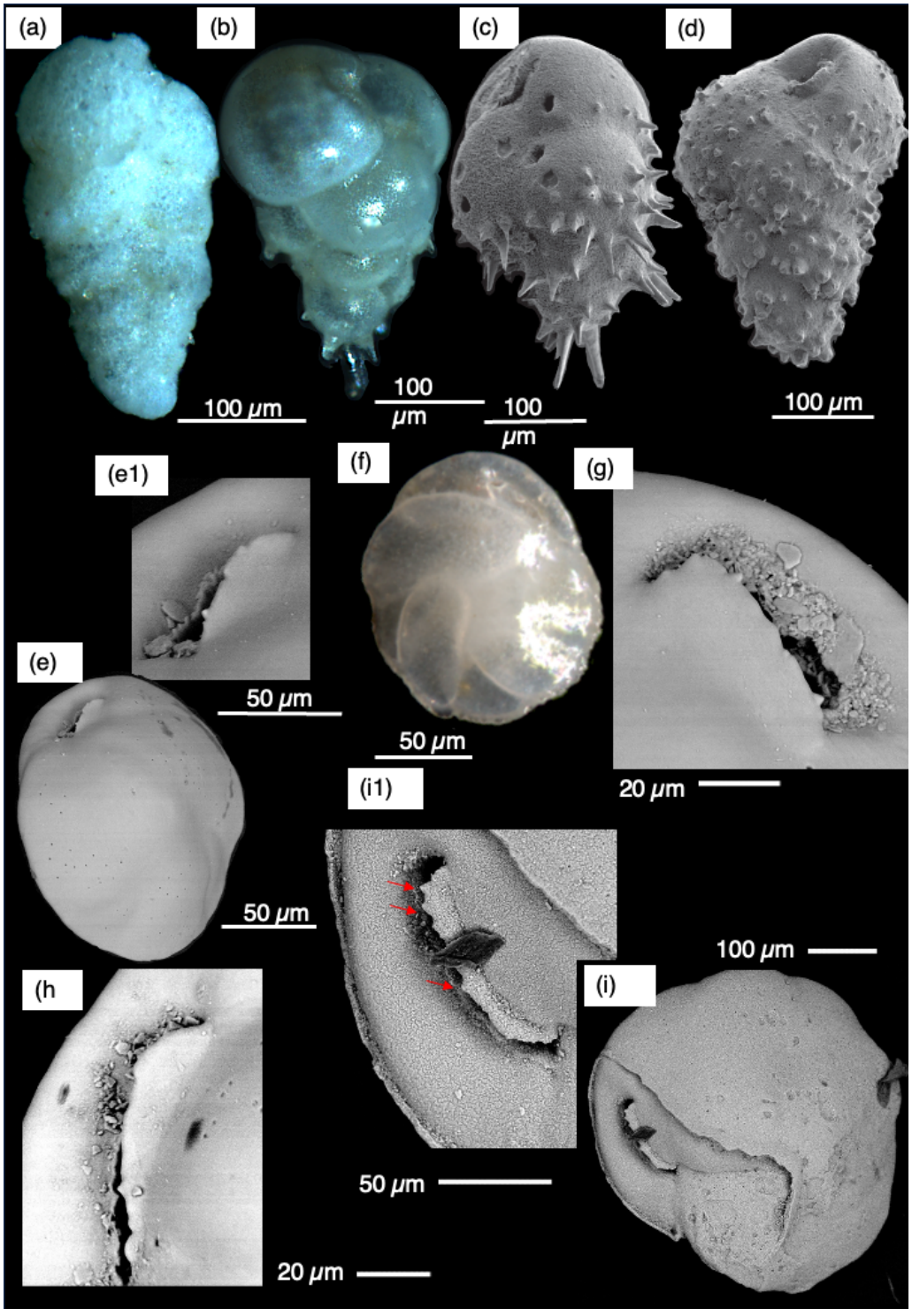

Appendix Plate A2

https://doi.org/10.5194/egusphere-2025-6290
Preprint. Discussion started: 29 December 2025

Figure (a). *Siphotextularia rolshauseni* with its typical white appearance, biserial chamber arrangement, distinct neck, and coarse agglutination. **Figure (b)**. *Bulimina aculeata,* translucent shell of well-preserved specimen with long spines from upper bathyal water depth. **Figure (c)**. *Bulimina aculeata,* corroded specimen with long spines from middle bathyal water depth. **Figure (d)**. *Bulimina aculeata,* corroded specimen with multiple short blunt spines from lower deep bathyal depth. **Figure (e)**. *Cassidulina neoteretis,* well preserved specimens, showing the angular periphery, and slit-like aperture partly covered with a prominent smooth apertural plate; **Figure (e1)**. close-up showing the smooth apertural plate and the opposing serrated ridge. **Figure (f)**. *Cassidulina neoteretis,* well preserved specimens with translucent shell revealing the biserial chamber arrangement and milky umbilical area. **Figures (g-h)**. *Cassidulina neoteretis,* aperture covered by subtriangular apertural plate with a smooth edge, formed by the infolded chamber wall with 1-2 small serrata on the apertural plate. **Figure (i)**. *Cassidulina teretis,* corroded specimen with the last chamber missing; **Figure (i1)**. Close-up of the aperture covered by a crescentic, narrow serrated apertural plate. Red arrows point to the serrata.
Figure (a). PS2212-3, 90 cm (Wollenburg et al., 2001); Figure (b). ODP910A-1H1, 135-136.5; Figure (c). PS2185-6, 163.5 cm; Figure (d). PS72/396-5, 33.5 cm; Figure (e). PS2185-4, 0.5 cm; Figure (f). PS2185-6, 237.5 cm; Figures (g-h). PS2185-6, 223 cm; Figure (i). PS72/396-5, 72.5 cm. Figures (a-b), (f) Axiozoom images; Figures (c-e), (g-i) SEM images.

https://doi.org/10.5194/egusphere-2025-6290
Preprint. Discussion started: 29 December 2025

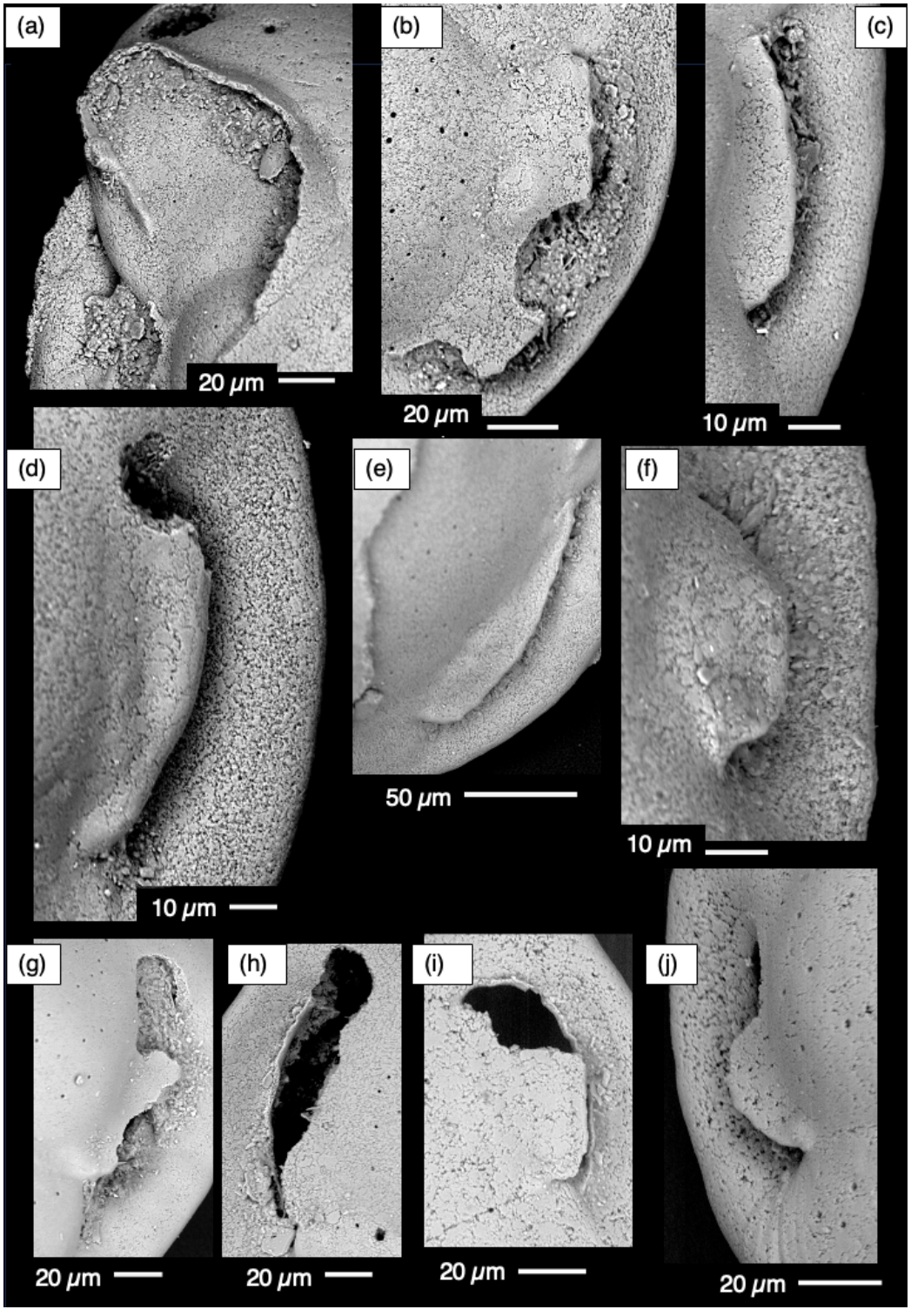

Appendix Plate A3

https://doi.org/10.5194/egusphere-2025-6290
Preprint. Discussion started: 29 December 2025

Cassidulina neoteretis apertural view of all specimens from a sample split of the coarse size fraction >125 µm at 223.5 cm sediment depth in core PS2185-6. All specimens are heavily corroded, revealing the puzzle-like or cogwheel structures caused by dissolution at the borders between neighbouring calcite crystallites of the shell (**Figures (a-d), (f), (h-j)**), and a damaged apertural plate (**Figures (b), (d), (g-j)**. Although the apertural plate of most specimens is damaged, the broader subtriangular apertural plate with smooth rim (compared to *C. teretis*) allows to assign them to *C. neoteretis*. All SEM images.

https://doi.org/10.5194/egusphere-2025-6290
Preprint. Discussion started: 29 December 2025

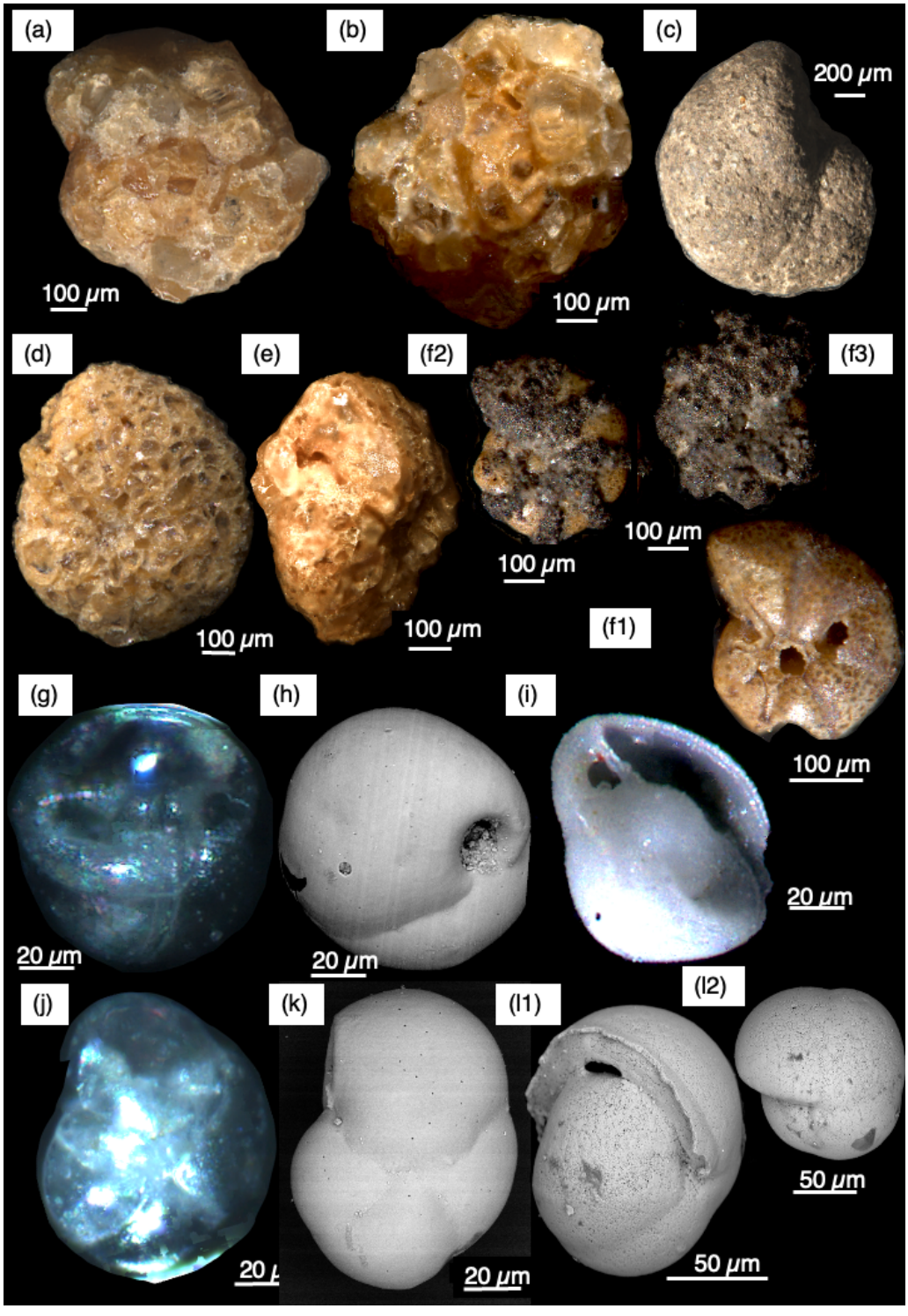

Appendix Plate A4

https://doi.org/10.5194/egusphere-2025-6290
Preprint. Discussion started: 29 December 2025

Figures (a-b). *Cribrostomoides subglobosus* revealing the streptospiral coiling and large variability in grain-size used for agglutination; (**a**) side view; (**b**) apertural view showing the slite-like aperture of young specimen. **Figure (c)**. *Cyclammina orbicularis* side view of the thick planispiral test; agglutination obscured by iron-manganese coating. **Figures (d-e)**. *Haplophragmoides obscurus* revealing the variable grain-size used for agglutination and the numerous indistinct sutures; **Figure (d)** Side view; **Figure (e)** apertural view. **Figures (f1-3)**. *Cyclammina trullisata* with smooth shell surface but progressive coverage by iron-manganese overgrowth (a to c). **Figures (g-i)**. *Epistominella arctica.* **Figures (g-h)** umbilical view of well-preserved specimens, thin, translucent shell; **Figure (g)** with smooth, shiny test. **Figure (h)** irregularly distributed pores. **Figure (i).** Diagenetically altered specimen with broken final chamber revealing that only the final chamber of *E. arctica* is inflated and has a circular aperture on the umbilical side, in earlier chambers the aperture is positioned in a peripheral-umbilical positioned depression. **Figures (j-k)**. *Stetsonia horvathi,* well-preserved specimen; **Figure (j)** translucent shell; **Figure (k)** unevenly distributed pores. **Figures (l1-2)**. *Pullenia bulloides*, images of corroded specimens with visible cogwheel structure, **Figure (m1)** revealing the subglobose 4-chambered shell composed of chambers increasing rapidly in length and width but only little in height, lateral view; **Figure (m2)** apertural view, but slit-like aperture is not visible as last chamber missing.

Figure (a). PS2212-3 90 cm (Wollenburg et al., 2001); Figure (b). PS2185-6, 150 cm; Figures (c-d). PS2185-6, 223 cm; Figure (e). PS2185-4, 379.5 cm; Figures (f-g). PS2185-6, 166.5 cm; Figures (h-k). PS2185-4, 0.5 cm. Figures (a-g), (i-j) Axiozoom photos. Figures (h), (k-l). SEM images.

https://doi.org/10.5194/egusphere-2025-6290
Preprint. Discussion started: 29 December 2025

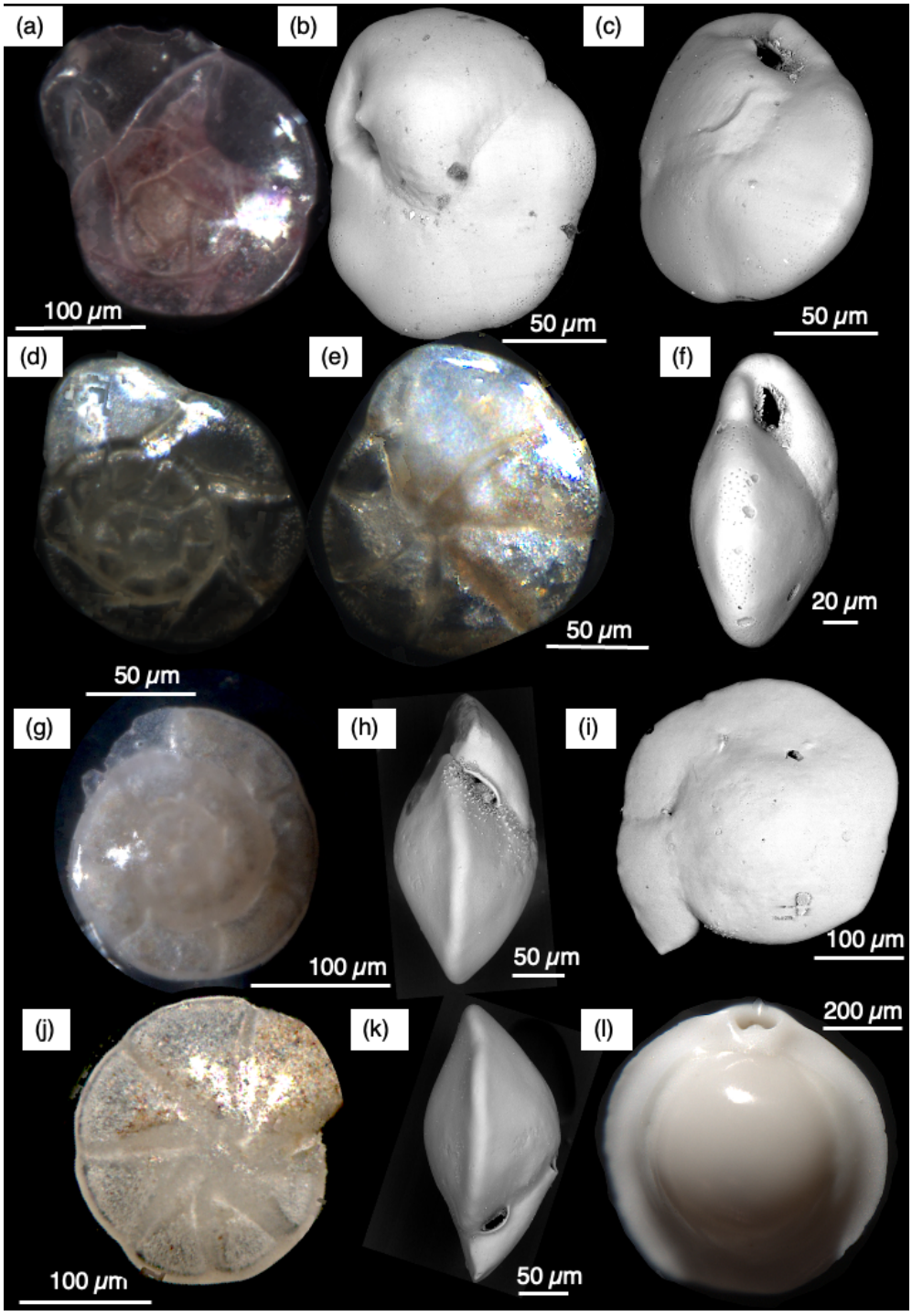

Appendix Plate 5

https://doi.org/10.5194/egusphere-2025-6290
Preprint. Discussion started: 29 December 2025

Figures (a-c). *Epistominella* exigua, well preserved specimens; **Figure (a)**. Dorsal side of a specimen revealing the translucent shell, the curved sutures, and the rapidly increasing chamber size with 5 chambers in the last whorl; **Figure (b)**. umbilical view revealing the lack of a significant depression in the umbilical area, the smooth shell and the increasing porosity towards the periphery; **Figure (c)**. Tilted umbilical view revealing the lack of apertural lips bordering the elongated aperture, peripheral view. **Figures (d-f)** *Eilohedra vitrea*; **Figure (d)**. dorsal view revealing the translucent shell, and 6 chambers in the last whorl separated by straight sutures; **Figure (e)**. umbilical view revealing 6.5 chambers in the last whorl separated by slightly curved sutures, a slightly depressed umbilicus; **Figure (f)**. peripheral view revealing details of the aperture composed of a short basal and elongated slit towards the periphery bordered by serrated lips. **Figures (g-k).** *Oridorsalis umbonatus*; **Figure (g)**. dorsal view revealing the translucent shell with relatively straight sutures; **Figures (I; k)**. peripheral view showing the aperture and an either smooth (k) or granular (h) basal area of the aperture, aperture surrounded by a lip on the last whorl; **Figure (i)**. Dorsal view revealing three Appendix apertures in the last chambers; **Figure (j)**. Umbilical view revealing the only slightly curved sutures and the non-depressed umbilical area. **Figure (l)**. *Pyrgo rotalaria*, specimen with small round aperture and small tooth, apertural view.

Figure (a) sediment surface from site PS2446-2, 2026 m water depth northern Barents Sea continental slope (Wollenburg and Mackensen, 1998c). Figures (b-c) PS2185-6 229.5 cm. Figures (d-f) ODP 910A 1H1 135 cm. Figures (g-k) PS2185-4 0.5 cm

Figures (a), (d-f), (g), (j), (l) Axiozoom photos. Figures (c), (f), (h-i), (j-k). SEM images

A Table A1: Benthic Foraminifera taxa

Adercotryma glomerata (Brady, 1878)
Adelosina pulchella (d'Orbigny, 1826)
Alabaminella weddellensis (Earland, 1936)
Allomorphina fragilis Hofker, 1952

Ammodiscus gullmarensis Höglund, 1948
Ammomarginulina ensis Wiesner, 1931
Archimerismus subnodosus (Brady, 1884)
Aschemonella ramuliformis Brady, 1884

Aschemonella scabra Brady, 1879
Astacolus crepidula (Fichtel and Moll, 1798)
Astacolus hyalacrulus Loeblich and Tappan, 1953

Astrononion hamadaense Asano, 1950 = *A. gallowayi* Loeblich and Tappan, 1953 junior synonym
Bolivina arctica Herman, 1974
Bolivina gramen (d'Orbigny, 1839)
Bolivina sp.
Bolivina robusta (Brady, 1881)
Botuloides ittai (Loeblich & Tappan, 1953)
Buccella floriformis Voloshinova, 1960 = *B. hannai arctica* Voloshinova, 1960 junior synonym (Hayward et al. 2023)
Buccella frigida (Cushman, 1922)
Buccella tenerrima Bandy, 1950

Cyclammina sp.
Cystammina pauciloculata Brady, 1879
Deuterammina (Deuterammina) grisea (Earland, 1934)
Deuterammina (Deuterammina) grahami Brönnimann & Whittaker, 1988
Discorbinella bertheloti (d'Orbigny, 1839)
Discorbis vilardeboanus (d'Orbigny, 1839)
Earlandammina inconspicua (Earland, 1934)
Eggerelloides advenum (Cushman, 1922) = *Verneuilina arctica* (Höglund, 1947) junior synonym
Eilohedra vitrea Parker, in Phleger et al., 1953
Elphidium funderi Feyling-Hanssen, 1990
Elphidiella groenlandica (Cushman, 1933) = *E. gorbunovi* Shchedrina, 1946 junior synonym
Elphidiella rolfi Gudina & Polovova, 1984

Elphidium asklundi Brotzen, 1943
Elphidium bartletti Cushman, 1933
Elphidiella groenlandica (Cushman, 1933)
Emayerella frigida (Cushman, 1933)
Eoeponidella pulchella (Parker, 1952)
Epistominella arctica Green, 1959

Epistominella exigua (Brady, 1884)
Favulina melo (d'Orbigny, 1839)

https://doi.org/10.5194/egusphere-2025-6290
Preprint. Discussion started: 29 December 2025

Bulimina aculeata d'Orbigny, 1826
Buliminella hensoni Lagoe, 1977
Cassidulina reniforme Nørvang, 1945
Cassidulina neoteretis Seidenkrantz, 1995
Cassidulina teretis Loeblich and Tappan, 1953
Cassidulina obtusa Williamson, 1858
Ceratobulimina arctica Green, 1960
Chilostomella elongata Lagoe, 1977
Cibicides refulgens Montfort, 1808
Cornuspira involvens Reuss, 1850
Cornuspira planorbis Schultze, 1854

Cornuspiroides striolata (Brady, 1882)
Cribroelphidium clavatum Cushman, 1930
Cryptoelphidiella asklundi Brotzen, 1943
Cryptoelphidiella bartletti Cushman, 1933
Cryptoelphidiella hallandensis (Brotzen, 1943)
Cryptoelphidiella magellanica (Heron-Allen & Earland, 1932)
Cryptoelphidiella paucilocula (Cushman, 1944) = *C. albiumbilicatum* (Weiss, 1954) junior synonym
Cryptoelphidiella/Cribroelphidium sp.
Cribrostomoides jeffreysii (Williamson, 1858)
Cribrostomoides sphaerilocula (Cushman, 1910)
Cribrostomoides subglobosum (Sars, 1868)
Cuneata arctica (Brady, 1881)
Cyclammina orbicularis Brady, 1881
Cyclammina trullissata (Brady, 1879)
Haynesina orbicularis (Brady, 1881)
Heronallenia sp.
Homalohedra apiopleura (Loeblich & Tappan, 1953)
Hormosinella ovicula (Brady, 1879)
Hormosinelloides guttifer (Brady, 1881)
Hyalinea balthica (Schröter, 1783)
Hyalinonetrion gracillimum (Seguenza, 1862)
Hyperammina elongata Brady, 1878
Hyperammina laevigata Wright, 1891

Hyperammina sp.
Hyperammina/Jaculella/Psammosiphonella fragments
Ioanella tumidula subsp. *horvathi* (Green, 1960)
Islandiella algida (Cushman, 1944) = *I. islandica* (Nørvang, 1945) junior synonym
Islandiella helenae Feyling-Hanssen and Buzas, 1976
Islandiella norcrossi (Cushman, 1933)
Jaculella acuta Brady, 1879
Jaculella obtusa Brady, 1882
Laevidentalina advena (Cushman, 1923)
Laevidentalina baggi (Galloway & Wissler, 1927)

Laevidentalina communis (d'Orbigny, 1826)
Laevidentalina drammenensis (Feyling-Hanssen, 1964)
Laevidentalina frobisherensis (Loeblich & Tappan, 1953)
Laevidentalina elegans (d'Orbigny, 1846) = *D. pauperata* (d'Orbigny, 1846) junior synonym
Laevidentalina sp.
Lagena flatulenta Loeblich & Tappan, 1953
Lagena hispida Reuss, 1863

Fissurina annectens (Burrows & Holland, 1895)
Fissurina bassensis Parr, 1950
Fissurina bimarginata Parr, 1950
Fissurina cucurbitasema Loeblich & Tappan, 1953
Fissurina danica (Madsen, 1895)
Fissurina laevigata (Reus, 1850)
Fissurina lucida (Williamson, 1848)
Fissurina marginata (Montagu, 1803)
Fissurina orbygniana Serguenza, 1862
Fissurina semimarginata (Reuss, 1870)
Fissurina staphyllearia (Schwager, 1866) = *F. kerguelensis* Parr, 1950 junior synonym
Fissurina spp.
Fursenkoina complanata (Egger, 1893)
Galwayella trigonomarginata (Parker & Jones, 1865)
Globobulimina auriculata subsp. *arctica* Höglund, 1947
Globulina glacialis (Cushman & Ozawa, 1930)
Glomospira charoides (Jones & Parker, 1860)

Glomospira gordialis (Jones & Parker, 1860)

Gyroidina subplanulata Echols, 1971
Haplophragmoides bradyi (Schwager, 1883)
Haplophragmoides obscurus O'Neill, 1981
Haplophragmoides pusillum Höglund, 1947
Haplophragmoides sp.
Haynesina nivea (Lafrenz, 1963)
Haynesina orbicularis (Brady, 1881)
Nonionella iridea Heron-Allen & Earland, 1932
Nonionellina labradorica (Dawson, 1860)
Nuttallides umbonifera (Cushman, 1933)
Oolina borealis Loeblich & Tappan, 1954
Oolina caudigera (Wiesner, 1931)
Oolina globosa (Montagu, 1803)
Oolina stelligera (Brady, 1881)
Oolina spp.
Oridorsalis umbonatus (Reuss, 1851) = *O. tener* (Brady, 1884) junior synonym
Parafissurina arctica Green, 1960
Parafissurina fusiformis (Wiesner, 1931)
Parafissurina fusuliformis Loeblich & Tappan, 1953
Parafissurina groenlandica Shchedrina, 1946

Parafissurina lata (Wiesner, 1931)
Parafissurina marginata (Wiesner, 1931)
Parafissurina obtusa (Egger, 1857)
Parafissurina tectulostoma Loeblich & Tappan, 1953
Parafissurina spp.
Paratrochammina challengeri Brönnimann & Whittaker, 1988
Patellina corrugata Williamson, 1858
Placopsilinella aurantiaca Earland, 1934
Polymorphina spp.
Procerolagena meridionalis (Wiesner, 1931)

Psammatodendron arborescens Norman in Brady, 1881
Psammosiphonella cylindrica (Glaessner, 1937)
Psammosphaera fusca Schulze, 1875

https://doi.org/10.5194/egusphere-2025-6290
Preprint. Discussion started: 29 December 2025

Lagena nebulosa Cushmani, 1923
Lagena laevicostata Cushman & Gray, 1946
Lagnea tenuistriatiformis (McCulloch, 1977) = *Fissurina lagenoides tenuistriata*
Lagena sp.
Lagenammina arenulata (Skinner, 1961)
Lagenammina tubulata (Rhumbler, 1931)
Laryngosigma lactea (Walter & Jacob, 1798)
Laryngosigma williamsoni (Terquem, 1878)
Laryngosigma hyalascidea Loeblich & Tappan, 1953
Laryngosigma sp.
Lenticulina sp.
Lepidoparatrochammina lepida Brönnimann & Whitaker, 1986
Lobatula wuellerstorfi (Schwager, 1866)
Lobatula lobatula (Walker & Jacob, 1798)
Lobatula lobatula subsp. grossa Ten Dam & Reinhold, 1941
Marginulina similis d'Orbigny, 1826 = M. glabra (Parker, Jones & Brady, 1865 unaccepted nov. nudum
Marginulinopsis tenuis (Bornemann, 1855)
Melonis zaandami (van Voorthuysen, 1952)
Miliolina pulchella (d'Orbigny, 1826)
Miliolinella subrotunda (Montagu, 1803)
Miliolinella chukchiensis Loeblich & Tappan, 1953
juv. Miliolids
Moncharmontzeiana paradoxa (Sidebottom, 1912)

Nodosaria doliolaris Parr, 1950
Nodosaria sp.
Nonion umbilicatulum (Walker & Jacob, 1798)
Pyrgo williamsoni Silvestri, 1923
Pyrgoella irregularis (d'Orbigny, 1839)
Pyrgoella sphaera (d'Orbigny, 1839)
Pyrulina cylindroides (Roemer, 1838)
Quinqueloculina akneriana d'Orbigny, 1846
Quinqueloculina arctica Cushman, 1933
Quinqueloculina sadkovi (Bogdanowicz in Shchedrina, 1946)
Quinqueloculina seminula (Linnaeus, 1758)
Quinqueloculina stalkeri Loeblich & Tappan 1953
Quinqueloculina venusta Karrer, 1868
Quinqueloculina nitida Nørvang, 1965
Quinqueloculina sp.
Recurvoides laevigatum Höglund, 1947, despite Höglund's argumentation that this species is much more delicate than *R. contortus,* regarded by Kaminski & Gradstein (http://nhm2.uio.no/norges/atlas/index.htm) as being identical
Reophax pilulifer Brady, 1884
Reophax scorpiurus Montfort, 1808
Reophax sp.
Resigella moniliformis (Resig, 1982)
Reussoolina apiculata (Reuss, 1851)
Reusoolina laevis (Montagu, 1803)
Robertinoides charlottense (Cushman, 1925)
Robertinoides pumilum Höglund, 1947
Rosalina sp.
Saccammina socialis Brady, 1884
Saccammina sphaerica Brady, 1871
Saccammina sp.
Saccorhiza ramosa (Brady, 1879)
Seabrokia pellucida Brady, 1890 = jun. Synonym of *S.*

Psammosphaera sp.
Psammossiphonella discreta (Brady, 1881)
Pseudobolivina antarctica Wiesner, 1931

Pseudonodosinella nodulosa Brady, 1879
Pseudopolymorphina dawsoni (Cushmani & Ozawa, 1930)
Pseudopolymorphina novangliae (Cushman, 1923)
Pseudopolymorphina suboblonga Cushman & Ozawa, 1930
Pullenia bulloides (d'Orbigny, 1846)
Pullenia quinqueloba (Reuss, 1851)
Pyrgo rotalaria Loeblich & Tappan, 1953
Pyrgo williamsoni Silvestri, 1923
Pyrgoella irregularis (d'Orbigny, 1839)

Pyrgoella sphaera (d'Orbigny, 1839)
Pyrulina cylindroides (Roemer, 1838)
Pullenia bulloides (d'Orbigny, 1846)
Pullenia quinqueloba (Reuss, 1851)

Pyrgo rotalaria Loeblich & Tappan, 1953
Pyrgo williamsoni Silvestri, 1923
Pyrgoella irregularis (d'Orbigny, 1839)
Pyrgoella sphaera (d'Orbigny, 1839)
Pyrulina cylindroides (Roemer, 1838)
Parafissurina spp.
Paratrochammina challengeri Brönnimann & Whittaker, 1988
Patellina corrugata Williamson, 1858
Placopsilinella aurantiaca Earland, 1934
Pyrgo rotalaria Loeblich & Tappan, 1953
Sorosphaera confusa Brady, 1879
Sphaeroidina sp.
Stainforthia concava Höglund, 1947
Stainforthia feylingi Knudsen & Seidenkrantz, 1994
Stainforthia loeblichi (Feyling-Hanssen, 1954)
Stetsonia horvathi Green, 1959
Subreophax aduncus (Brady, 1882)
Spiroplectammina biformis Parker & Jones, 1865
Textularia earlandi Parker, 1952
Textularia torquata Parker, 1952
Thalamophaga ramosa Rhumbler, 1911
Tholosina confusa (Cushman, 1920)
Thurammina papillata Brady, 1879

Toddinella incerta (Williamson, 1858)
Toddinella ustulata (Todd, 1957)
Tolypammina schaudinni Rhumbler, 1904
Tolypammina vagans (Brady, 1979)
Triloculina elongata d'Orbigny in Fornasini, 1905
Triloculina frigida Lagoe, 1977
Triloculina trigonula (Lamarck, 1804)
Triloculina trihedra Loeblich & Tappan, 1953
Triloculina tricarinata d'Orbigny in Deshayes, 1832
Trochammina japonica Ishiwada, 1950
Trochammina lomonosoviensis Evans & Kaminski, 1998
Trochammina sp.
Trochamminopsis pusilla (Höglund, 1947)
Vaginulinopsis angulata (Noth, 1951)

https://doi.org/10.5194/egusphere-2025-6290
Preprint. Discussion started: 29 December 2025

earlandi Wright, 1891
Sipholagena benevestita (Buchner, 1940)

Valvulineria arctica Green, 1959

https://doi.org/10.5194/egusphere-2025-6290
Preprint. Discussion started: 29 December 2025

Appendix B: Ecology, shell characteristics, and preservation of main calcareous taxa

Species	Habitat depth	Ecology	Size ø µm	No. whorls/Chambers
Epistominella arctica	phytodetritus/surface sediment layer	phytodetritus species, opportunistic, r-strategist	70	2/10
Epistominella exigua	phytodetritus/surface sediment layer	phytodetritus species; Atlantic species, r-strategist opportunistic	390	3/15
Stetsonia horvathi	shallow infaunal	low food demand, opportunistic	100	3/15
Ioanella tumidula subsp. *horvathi*	epifaunal, often epilithic	low to moderate food demand, opportunistic	140	3.5/ca. 20
Nonionella iridea	phytodetritus/surface sediment layer	phytodetritus species, eventually nourishing on associated bacteria, opportunistic, r-strategist	130	2.5/12-14
Eilohedra vitrea	shallow infaunal	able to respond to high food availability, opportunist	150	3/15
Alabaminella weddellensis	phytodetritus/surface sediment layer	phytodetritus species, opportunistic, r-strategist	160	4/20
Pyrgo rotalaria	epi- to shallow infaunal	ingest rapidly phytodetritus and nourish on its own cytoplasm during absent food fall, opportunistic, k-strategist	>600	?not available
Oridorsalis umbonatus	shallow infaunal	low to moderate food demand, opportunistic	400	3.5/ca. 25
Cassidulina neoteretis	shallow infaunal	able to nourish on bacteria associated with phytodetritus, opportunistic, r-strategist	300	8-10 Ch. Last whorl
Bolivina arctica	infauna	Today rare; k-strategist likely adapted to past environmental conditions	200	Biserial/12
Pullenia bulloides	infaunal in seasonally ice-free areas	Atlantic species, opportunistic, r-strategist	500	?/5 in the last whorl
Bulimina aculeata	usually shallow but also deep infaunal	high labile organic carbon demand	2000	?4/?12

https://doi.org/10.5194/egusphere-2025-6290
Preprint. Discussion started: 29 December 2025

Species	Test shape	Shell thickness (µm)	Preservation potential	No. whorls/Chambers
Epistominella arctica	inflated trochospiral, biconvex, chambers increasing rapidly in size with growth	0.47	very low	(9); (18); (21); this study
Epistominella exigua	trochospiral, biconvex, periphery acute, chambers increasing rapidly in size with growth	1.37	low-very low	(3); (27); this study
Stetsonia horvathi	planispiral involute, biconvex	0.77	low	(9); (18); (21); this study
Ioanella tumidula subsp. *horvathi*	trochospiral planoconvex with high dorsal spire	1.45	low	(6); (18); this study
Nonionella iridea	trochospiral, biconvex, periphery rounded, chambers increasing rapidly in size with growth		low	(5); (17); (20); (22); (25); this study
Eilohedra vitrea	trochospiral, biconvex, periphery acute, chambers increasing rapidly in size with growth		low	(7); (13); (25); this study
Alabaminella weddellensis	trochospiral, biconvex	2.25	low-moderate	(6); (16); (20); (21); (23); (25); this study
Pyrgo rotalaria	miliolid, biserial, biconvex, peripheral keel	59.71	moderate-low	(7); (12); (18); this study
Oridorsalis umbonatus	trochospiral, biconvex, periphery acute, chambers increasing moderately in size	2.15	moderate	(4); (18); (19); (25); (26); this study
Cassidulina neoteretis	lenticular, umbilical boss on each side, biserial coiled, peripheral keel	2.64	moderate	(15); (18); (19); (22); this study
Bolivina arctica	elongated biserial, tapered twisted	1.14	moderate	(10); this study
Pullenia bulloides	planispiral involute, biconvex, subglobular, broad rounded periphery	2.59	moderate	(2); (19); this study
Bulimina aculeata	elongated triserial inflated, spinose	5.16	high	(1); (27); (28); (29)

https://doi.org/10.5194/egusphere-2025-6290
Preprint. Discussion started: 29 December 2025

Data availability

All utilized datasets are available via the PANGAEA online repository; they can be accessed through the citations given in the text, with full references provided below. All new benthic foraminifera data presented in this study will be available in the PANGAEA database upon publishing (Felden et al., 2023).

Author contributions

JW and JM conceptualized the study, sampled the sediment cores, interpreted the data set and wrote the manuscript. JW performed the benthic foraminifer analysis.

Competing interests

The authors declare that they have no conflict of interest.

Acknowledgements

We thank the Polarstern Core Repository for providing the samples used in this study. We are gratefull to Stefanie Kaboth-Bahr, Jörg Wagner, Matthias Feldtmann, Matthias Heinze, Leonie Peti who, over the years helped in picking foraminifera from these cores.

References

Adler, R. E., Polyak, L., Ortiz, J. D., Kaufman, D. S., Channell, J. E. T., Xuan, C., Grottoli, A. G., Sellen, E., and Crawford, K. A.: Sediment record from the western Arctic Ocean with an improved Late Quaternary age resolution: HOTRAX core HLY0503-8JPC, Mendeleev Ridge, Glob. Planet. Change, 68, 18-29, https://doi.org/10.1016/j.gloplacha.2009.03.026, 2009.

Aksu, A. E.: Paleomagnetic stratigraphy of the CESAR cores, in: Initial geological report on CESAR - the Canadian expedition to study the Alpha Ridge, Arctic Ocean, edited by: Jackson, H. R., Mudie, P. J., and Blasco, S. M., Geol. Surv. Can. Pap., 101-114, https://doi.org/10.4095/120315, 1985.

Alexanderson, H., Backman, J., Cronin, T. M., Funder, S., Ingólfsson, Ó., Jakobsson, M., Landvik, J. Y., Löwemark, L., Mangerud, J., März, C., Möller, P., O'Regan, M., and Spielhagen, R. F.: An Arctic perspective on dating Mid-Late Pleistocene environmental history, Quat. Sci. Rev., 92, 9-31, https://doi.org/10.1016/j.quascirev.2013.09.023, 2014.

Altenbach, A. V.: Short term processes and patterns in the foraminiferal response to organic flux rates, Mar. Micropaleontol., 19, 119-129, https://doi.org/10.1016/0377-8398(92)90024-E, 1992.

Alve, E.: Colonization of new habitats by benthic foraminifera: a review, Earth Sci. Rev., 46, 167-185, https://doi.org/10.1016/S0012-8252(99)00016-1, 1999.

Alve, E. and Goldstein, S. T.: Propagule transport as a key method of dispersal in benthic foraminifera (Protista), Limnol. Oceanogr., 48, 2163-2170, https://doi.org/10.4319/lo.2003.48.6.2163, 2003.

https://doi.org/10.5194/egusphere-2025-6290
Preprint. Discussion started: 29 December 2025

Alve, E. and Goldstein, S. T.: Dispersal, survival and delayed growth of benthic foraminiferal propagules, J. Sea Res., 63, 36-51, https://doi.org/10.1016/j.seares.2009.09.003, 2010.

Anderson, L. G., Jones, E. P., and Swift, J. H.: Export production in the central Arctic Ocean evaluated from phosphate deficits, J. Geophys. Res. Oceans, 108, 3199, https://doi.org/10.1029/2001JC001057, 2003.

Anthonissen, D. E. and James G. Ogg, J. G.: Appendix 3: Cenozoic and Cretaceous biochronology of planktonic foraminifera and calcareous nannofossils, in: The Geologic Time Scale 2012, edited by Gradstein, F., Ogg, J. G., Schmitz, M. D., and Ogg, G. M., 1083-1127, 2012.

Backman, J., Fornaciari, E., and Rio, D.: Biochronology and paleoceanography of late Pleistocene and Holocene calcareous nannofossil abundances across the Arctic Basin, Mar. Micropaleontol., 72, 86-98, https://doi.org/10.1016/j.marmicro.2009.04.001, 2009.

Backman, J., Jakobsson, M., Løvlie, R., Polyak, L., and Febo, L. A.: Is the central Arctic Ocean a sediment starved basin?, Quat. Sci. Rev., 23, 1435-1454, https://doi.org/10.1016/j.quascirev.2003.12.005, 2004.

Backman, J., Raffi, I., Rio, D., Fornaciari, E., and Pälike, H.: Biozonation and biochronology of Miocene through Pleistocene calcareous nannofossils from low and middle latitudes, Newslett. Stratigr., 45, 221-244, http://dx.doi.org/10.1127/0078-0421/2012/0022, 2012.

Barker, R. W.: Taxonomic notes on the species figured by H. B. Brady in his report on the foraminifera dredged by H. M. S. Challenger during the years 1873-1876, SEPM Spec. Publ., 9, 1-238, 1960.

Bazhenova, E.: Reconstruction of late Quaternary sedimentary environments at the southern Mendeleev Ridge (Arctic Ocean), Phd Thesis, Alfred Wegener Institute, University of Bremen, Bremerhaven, 91 pp., 2012

Bazhenova, E., Fagel, N., and Stein, R.: North American origin of "pink–white" layers at the Mendeleev Ridge (Arctic Ocean): New insights from lead and neodymium isotope composition of detrital sediment component, Mar. Geol., 386, 44-55, https://doi.org/10.1016/j.margeo.2017.01.010, 2017.

Belanger, P. E. and Streeter, S. S.: Distribution and ecology of benthic foraminifera in the Norwegian-Greenland Sea, Mar. Micropaleontol., 5, 401-428, https://doi.org/10.1016/0377-8398(80)90020-1, 1980.

Belyaeva, N. V. and Khusid, T. A.: Benthonic and planktonic foraminifera in the Pleistocene sediments of the Arctic Ocean evolution of communities and of the environment, Dokl. Akad. Nauk SSSR, 309, 1472-1475, 1989.

Bender, H.: Gehäuseaufbau, Gehäusegenese und Biologie agglutinierter Foraminiferen (Sarcodina, Textulariina), Jb. Geol. B.-A., 132, 2, 259-347, 1989.

Bendif, E. M., Probert, I., Archontikis, O. A., Young, J. R., Beaufort, L., Rickaby, R. E., and Filatov, D.: Rapid diversification underlying the global dominance of a cosmopolitan phytoplankton, The ISME Journal, 17, 630-640, https://doi.org/10.1038/s41396-023-01365-5, 2023.

Bergmann, U.: Physical properties of sediment core PS2185-6 [dataset]. PANGAEA, https://doi.org/10.1594/PANGAEA.50137, 1996.

https://doi.org/10.5194/egusphere-2025-6290
Preprint. Discussion started: 29 December 2025

Bergsten, H.: Recent benthic foraminifera of a transect from the North Pole to the Yermak Plateau, eastern central Arctic Ocean, Mar. Geol., 119, 251-267, https://doi.org/10.1016/0025-3227(94)90184-8, 1994.

Bornmalm, L.: Taxonomy and paleoecology of late Neogene benthic foraminifera from the Caribbean Sea and eastern equatorial Pacific Ocean, Fossils Strata, 41, 1-96, https://doi.org/10.18261/8200376664-1997-01, 1997.

Brady, H. B.: Report on the foraminifera collected by H.M.S. Challenger during the years 1873-1876, in: Report on the scientific results of the voyage of H.M.S. Challenger during the years 1873-76: Zoology, 385, 1-21, 21-814, 1884.

Burgess, M. V. and Schnitker, D.: Morphometry of *Bulimina aculeata* Orbigny and *Bulimina marginata* Orbigny, J. Foraminifer. Res., 20, 37-49, https://doi.org/10.2113/gsjfr.20.1.37, 1990.

Buzas, M. A. and Culver, S. J.: Biogeographic and evolutionary patterns of continental margin benthic foraminifera, Paleobiology, 15, 11-19, https://doi.org/10.1017/S0094837300009143, 1989.

Buzas, M. A. and Culver, S. J.: Species diversity and dispersal of benthic foraminifera: Analysis of extant organisms and fossils of the waters around North America, Bio Sci., 41, 483-489, https://doi.org/10.2307/1311806, 1991.

Cage, A., Pieńkowski, A., Jennings, A., Knudsen, K., and Seidenkrantz, M.-S.: Comparative analysis of six common foraminiferal species of the genera *Cassidulina*, *Paracassidulina*, and *Islandiella* from the Arctic–North Atlantic domain, J. Micropalaeontol., 40, 37-60, https://doi.org/10.5194/jm-40-37-2021, 2021.

Carstens, J. and Wefer, G.: Recent distribution of planktonic foraminifera in the Nansen Basin, Arctic Ocean, Deep-Sea Res. I, 39, 507-524, https://doi.org/10.1016/S0198-0149(06)80018-X, 1992.

Chauhan, T., Rasmussen, T., and Noormets, R.: Palaeoceanography of the Barents Sea continental margin, north of Nordaustlandet, Svalbard, during the last 74 ka, Boreas, 45, https://doi.org/10.1111/bor.12135, 2015.

Chauhan, T., Rasmussen, T. L., Noormets, R., Jakobsson, M., and Hogan, K. A.: Glacial history and paleoceanography of the southern Yermak Plateau since 132 ka BP, Quat. Sci. Rev., 92, 155-169, http://dx.doi.org/10.1016/j.quascirev.2013.10.023, 2014.

Clark, D. L., Whitman, R. R., Morgan, K. A., and Mackey, S. D.: Stratigraphy and glacial-marine sediments of the Amerasian Basin, Central Arctic Ocean, Geol. Soc. Am. Spec. Pap., 181, 57, https://doi.org/10.1130/SPE181-p1, 1980.

Clark, D. L., Chern, L. A., Hogler, J. A., Mennicke, C. M., and Atkins, E. D.: Late Neogene climate evolution of the Central Arctic Ocean, Mar. Geol., 93, 69-94, https://doi.org/10.1016/0025-3227(90)90078-X, 1990.

Collins, L. S.: Relationship of environmental gradients to morphologic variation within *Bulimina aculeata* and *Bulimina marginata*, Gulf of Maine area, J. Foraminifer. Res., 19, 222-234, https://doi.org/10.2113/gsjfr.19.3.222, 1989.

Collins, L. S.: Regional versus physiographic effects on morphologic variability within *Bulimina aculeata* and *B. marginata*, Mar. Micropaleontol., 17, 155-170, https://doi.org/10.1016/0377-8398(91)90026-3, 1991.

Corliss, B. H.: Recent deep-sea benthonic foraminiferal distributions in the southeast Indian Ocean: Inferred bottom-water routes and ecological implications, Mar. Geol., 31, 115-138, https://doi.org/10.1016/0025-3227(79)90059-8, 1979.

Corliss, B. H. and Honjo, S.: Dissolution of deep-sea benthonic foraminifera, Micropaleontology, 27, 358-378, 1981.

https://doi.org/10.5194/egusphere-2025-6290
Preprint. Discussion started: 29 December 2025

Cornelius, N. and Gooday, A. J.: 'Live' (stained) deep-sea benthic foraminiferans in the western Weddell Sea: trends in abundance, diversity and taxonomic composition along a depth transect, Deep-Sea Res. II: Top. Stud. Oceanogr., 51, 1571-1602, https://doi.org/10.1016/j.dsr2.2004.06.024, 2004.

Cronin, T., Seidenstein, J., Keller, K., McDougall, K., Ruefer, A., and Gemery, L.: The benthic foraminifera *Cassidulina* from the Arctic Ocean: Application to paleoceanography and biostratigraphy, Micropaleontology, 65, 105-125, https://doi.org/0.47894/mpal.65.2.02, 2019a.

Cronin, T. M., Smith, S. A., Eynaud, F., O'Regan, M., and King, J.: Quaternary paleoceanography of the central Arctic based on Integrated Ocean Drilling Program Arctic Coring Expedition 302 foraminiferal assemblages, Paleoceanography, 23, https://doi.org/10.1029/2007PA001484, 2008.

Cronin, T. M., Polyak, L., Reed, D., Kandiano, E. S., Marzen, R. E., and Council, E. A.: A 600-ka Arctic sea-ice record from Mendeleev Ridge based on ostracodes, Quat. Sci. Rev., 79, 157-167, https://doi.org/10.1016/j.quascirev.2012.12.010, 2013.

Cronin, T. M., DeNinno, L. H., Polyak, L., Caverly, E. K., Poore, R. Z., Brenner, A., Rodriguez-Lazaro, J., and Marzen, R. E.: Quaternary ostracode and foraminiferal biostratigraphy and paleoceanography in the western Arctic Ocean, Mar. Micropaleontol., 111, 118-133, http://doi.org/10.1016/j.marmicro.2014.05.001, 2014.

Cronin, T. M., Keller, K. J., Farmer, J. R., Schaller, M. F., O'Regan, M., Poirier, R., Coxall, H., Dwyer, G. S., Bauch, H., Kindstedt, I. G., Jakobsson, M., Marzen, R., and Santin, E.: Interglacial Paleoclimate in the Arctic, Paleoceanogr. Paleoclimatol., 34, 1959-1979, https://doi.org/10.1029/2019PA003708, 2019b.

Cushman, J. A.: A monograph of the Foraminifera of the North Pacific Ocean. Part I. Astrorhizidae and Lituolidae, U. S. Natl. Mus. Bull., 71, 1-134, https://doi.org/10.5479/SI.03629236.71.I, 1910.

Cushman, J. A.: The Foraminifera of the Atlantic Ocean, U. S. Natl. Mus. Bull., i-ix, 1-179, https://doi.org/10.5479/si.03629236.104.7, 1931.

Cushman, J. A. and Parker, F. L.: *Bulimina* and related foraminiferal genera, U. S. Geol. Surv. Prof. Pap., 210-D, 55-176, https://doi.org/10.3133/pp210D, 1947.

Darby, D. A., Naidu, A. S., Mowatt, T. C., and Jones, G.: Sediment composition and sedimentary processes in the Arctic Ocean, in: The Arctic Seas: Climatology, Oceanography, Geology, and Biology, edited by: Herman, Y., VNR New York, 657-720, https://doi.org/10.1007/978-1-4613-0677-1_24, 1989.

Darby, D. A., Bischof, J. F., Spielhagen, R. F., Marshall, S. A., and Herman, S. W.: Arctic ice export events and their potential impact on global climate during the late Pleistocene, Paleoceanography, 17, 1025, https://doi.org/10.1029/2001PA000639, 2002.

De Schepper, S. and Head, M. J.: Age calibration of dinoflagellate cyst and acritarch events in the Pliocene–Pleistocene of the eastern North Atlantic (DSDP Hole 610A), Stratigraphy, 5, 137–161, https://doi.org/10.29041/strat.05.2.02, 2008.

Dipre, G. R., Polyak, L., Kuznetsov, A. B., Oti, E. A., Ortiz, J. D., Brachfeld, S. A., Xuan, C., Lazar, K. B., and Cook, A. E.: Plio-Pleistocene sedimentary record from the Northwind Ridge: new insights into paleoclimatic evolution of the western Arctic Ocean for the last 5 Ma, Arktos, 4, 1-23, https://doi.org/10.1007/s41063-018-0054-y, 2018.

https://doi.org/10.5194/egusphere-2025-6290
Preprint. Discussion started: 29 December 2025

Domanov, M., Khusid, T., and Libina, N.: Benthic foraminifera in deep trenches of the Kara Sea and the relation of *Saccorhiza ramosa* (Brady) to the distribution of natural radionuclides, Biol. Bull., 44, 187-192, https://doi.org/10.1134/S1062359017020054, 2017.

d'Orbigny, A. D.: Tableu méthodique de la classe des Céphalopodes, Annales des Sciences Naturelles, 1, 245-314, 1826.

Osterman, L. E.: Pliocene and Quaternary benthic foraminiferal biostratigraphy from Site 910, Yermak Plateau, in: Proc. Ocean Drilling Progr., Sci. Res., edited by: Thiede, J., Myhre, A., Firth, J. V., Johnson, G. L., and Ruddiman, W. F., ODP, College Station, 187-195, https://doi.org/10.2973/odp.proc.sr.151.107.1996, 1996.

Dong, L., Polyak, L., Liu, Y., Shi, X., Zhang, J., and Huang, Y.: Isotopic fingerprints of ice-rafted debris offer new constraints on Mid to Late Quaternary Arctic circulation and glacial history, Geochem. Geophys. Geosyst., 21, https://doi.org/10.1029/2020GC009019, 2020.

Ellis, B. F. and Messina, A. R.: Catalogue of foraminifera online, https://doi.org/10.1661/0026-2803(2002)048[0092:EAMCO]2.0.CO;2, 1940-2025.

Elkina, D. V., Piskarev, A.L., and Bezumov, D.V.: Sedimentation in the Central Arctic submarine elevations: Results of comprehensive analysis of paleomagnetic and seismoacoustic data, Geotectonics, 57, Suppl. 1, S100–S111, https://doi.org 10.1134/S0016852123070063, 2023.

Enge, A. J., Nomaki, H., Ogawa, N. O., Witte, U., Moeseneder, M. M., Lavik, G., Ohkouchi, N., Kitazato, H., Kučera, M., and Heinz, P.: Response of the benthic foraminiferal community to a simulated short-term phytodetritus pulse in the abyssal North Pacific, Mar. Ecol. Prog. Ser., 438, 129-142, https://doi.org/10.3354/meps09298, 2011.

Evans, J. R. and Kaminski, M. A.: Pliocene and Pleistocene chronostratigraphy and paleoenvironment of the central Arctic Ocean, using deep water agglutinated foraminifera, Micropaleontology, 44, 109-130, https://doi.org/10.2307/1486065, 1998.

Evans, J. R., Kaminski, M. A., Cronin, T. M., and Fütterer, D. K.: Pleistocene agglutinated foraminifera from the Lomonosov Ridge and Amundsen Basin, Arctic Basin. Initial report on piston cores 2177-5 (KAL) and 2176-3 (KAL), Mar. Micropaleontol., 26, 245-253, https://doi.org/10.1016/0377-8398(95)00016-X, 1995.

Eynaud, F., Cronin, T., Smith, S., Zaragosi, S., Mavel, J., Mary, Y., Mas, V., and Pujol, C.: Morphological variability of the planktonic foraminifer *Neogloboquadrina pachyderma* from ACEX cores: Implications for Late Pleistocene circulation in the Arctic Ocean, Micropaleontology, 55, 2009.

Feyling-Hanssen, R. W.: Late-Pleistocene foraminifera from the Oslofjord Area, Southeast Norway., Norw. J. Geol., 33, 109-151, 1954.

Feyling-Hanssen, R. W.: Foraminifera in Late Quaternay deposits from the Oslofjord area, Norges Geologiske Undersøkelse, 225, 383 pp., 1964.

Feyling-Hanssen, R. W. and Ullberg, K.: A Tertiary-Quaternary section at Sarsbukta, Spitsbergen, Svalbard, and its foraminifera., Polar Res., 2, 77-106, https://doi.org/10.3402/polar.v2i1.6963 1984.

Feyling-Hanssen, R. W., Funder, S., and Petersen, K. S.: The Lodin Elv Formation, a Plio-Pleistocene occurrence in Greenland, Bull. Geol. Soc. Denmark, 31, 81-106, https:/doi.org/10.37570/bgsd-1982-31-07, 1983.

https://doi.org/10.5194/egusphere-2025-6290
Preprint. Discussion started: 29 December 2025

Fontanier, C., Jorissen, F. J., Licari, L., Alexandre, A., Anschutz, P., and Carbonel, P.: Live benthic foraminiferal faunas from the Bay of Biscay: faunal density, composition, and microhabitats, Deep-Sea Res. I: Oceanogr. Res. Pap, 49, 751-785, https://doi.org/10.1016/S0967-0637(01)00078-4, 2002.

Frank, M., Backman, J., Jakobsson, M., Moran, K., O'Regan, M., King, J., Haley, B., Kubik, P., and Garbe-Schönberg, D.: Beryllium isotopes in central Arctic Ocean sediments over the past 12.3 million years: Stratigraphic and paleoclimatic implications, Paleoceanography, 23, PA1S01, doi:10.1029/2007PA001478, 2008.

Gaździcki, A. and Majewski, W.: Foraminifera from the Eocene La Meseta Formation of Isla Marambio (Seymour Island), Antarctic Peninsula, Antarct. Sci., 24, 408-416, https//doi.org/10.1017/S095410201200020X, 2012.

Geibert, W., Matthiessen, J., Stimac, I., Wollenburg, J., and Stein, R.: Glacial episodes of a freshwater Arctic Ocean covered by a thick ice shelf, Nature, 590, 97-102, https://doi.org/10.1038/s41586-021-03186-y, 2021.

Goës, A. T.: A synopsis of Arctic and Scandinavian recent marine Foraminifera hitherto discovered / by Axel Goës, Kungl. Svenska vetenskapsakademiens handlingar, 25, 9, https://doi.org/10.5962/bhl.title.14885, 1894.

Gooday, A. and Lambshead, P. J.: Influence of seasonally deposited phytodetritus on benthic foraminiferal populations in the bathyal northeast Atlantic: The species response, Mar. Ecol. Prog. Ser., 58, 53-67, https://doi.org/10.3354/meps058053, 1989.

Gooday, A., Todo, Y., Uematsu, K., and Kitazato, H.: New organic-walled Foraminifera (Protista) from the ocean's deepest point, the Challenger Deep (western Pacific Ocean), Zool. J. Linn. Soc., 153, 399-423, https://doi.org/10.1111/j.1096-3642.2008.00393.x, 2008a.

Gooday, A. J.: A response by benthic Foraminifera to the deposition of phytodetritus in the deep sea, Nature, 332, 70-73, https://doi.org/10.1038/332070a0, 1988.

Gooday, A. J. and Jorissen, F. J.: Benthic foraminiferal biogeography: Controls on global distribution patterns in deep-water settings, Annu. Rev. Mar. Sci., 4, 237-262, https://doi.org/10.1146/annurev-marine-120709-142737, 2012.

Gooday, A. J., Nomaki, H., and Kitazato, H.: Modern deep-sea benthic foraminifera: a brief review of their morphology-based biodiversity and trophic diversity, Geol. Soc. Spec. Publ., 303, 97, https://doi.org/10.1144/SP303.8, 2008b.

Green, K. E.: Ecology of some Arctic foraminifera. In Bushnell, V.: Scientific Studies at Fletcher's Ice Island, T-3, 1952-1955. Vol. 1. Terrestrial Sciences Laboratory, Geophysics Research Directorate, Air Force Cambridge Research Center, Air Research and Development Command, U.S. Air Force. Geophysical Research Papers no. 63, 1959.

Green, K. E.: Ecology of some Arctic Foraminifera, Micropaleontology, 6, 57-78, https://doi.org/10.2307/1484317, 1960.

Grobe, H. and Fütterer, D. K.: Documentation of sediment core PS2185-6 [dataset], PANGAEA, https://doi.org/10.1594/PANGAEA.115184, 2003.

Gupta Sen, B. K.: Modern Foraminifera, Kluwer Academic Publishers, 368 pp., https://doi.org/10.1007/0-306-48104-9, 2003.

Haake, F.-W., Erlenkeuser, H., and Pflaumann, U.: *Pullenia bulloides* (Orbigny) in sediments of the Norwegian/Greenland Sea and the northeastern Atlantic Ocean: paleo-oceanographic evidence, BENTHOS ´90, Sendai, 235-244.

Hald, M. and Korsun, S.: Distribution of modern benthic foraminifera from fjords of Svalbard, European Arctic, J. Foraminifer. Res., 27, 101-122, https://doi.org/10.2113/gsjfr.27.2.101, 1997.

https://doi.org/10.5194/egusphere-2025-6290
Preprint. Discussion started: 29 December 2025

Hanslik, D.: Late Quaternary biostratigraphy and paleoceanography of the central Arctic Ocean, Phd Thesis, Stockholm IGV, 32 pp., 2011.

Hanslik, D., Löwemark, L., and Jakobsson, M.: Biogenic and detrital-rich intervals in central Arctic Ocean cores identified using x-ray fluorescence scanning, Polar Res., 32, https://doi.org/10.3402/polar.v32i0.18386, 2013.

Harada, N.: Review: Potential catastrophic reduction of sea ice in the western Arctic Ocean: Its impact on biogeochemical cycles and marine ecosystems, Glob. Planet. Change., 136, https://doi.org/10.1016/j.gloplacha.2015.11.005, 2015.

Hayward, B., Kawagata, S., Sabaa, A., Grenfell, H., L, v., Lewandowski, K., and E, T.: The last global extinction (Mid-Pleistocene) of deep-sea benthic foraminifera (Chrysalogoniidae, Ellipsoidinidae, Glandulonodosariidae, Plectofrondicularіidae, Pleurostomellidae, Stilostomellidae), their Late Cretaceous-Cenozoic history and taxonomy, Cush. Found. Spec. Publ., 43, 408 pp., 2012.

Hayward, B. W.: Global deep-sea extinctions during the Pleistocene ice ages, Geology, 29, 599-602, https://doi.org/10.1130/0091-7613(2001)029<0599:GDSEDT>2.0.CO;2, 2001.

Hayward, B. W.: Late Pliocene to middle Pleistocene extinctions of deep-sea benthic foraminifera („*Stilostomella* extinction“) in the southwest Pacific, J. Foraminifer. Res., 32, 274-307, https://doi.org/10.2113/32.3.274, 2002.

Hayward, B. W., Le Coze, F., Vachard, D., and Gross, O.: World Foraminifera Database, https://doi.org/10.14284/305, 2025.

Hayward, B. W., Johnson, K., Sabaa, A. T., Kawagata, S., and Thomas, E.: Cenozoic record of elongate, cylindrical, deep-sea benthic foraminifera in the North Atlantic and equatorial Pacific Oceans, Mar. Micropaleontol., 74, 75-95, https://doi.org/10.1016/j.marmicro.2010.01.001, 2010.

Hayward, B. W., Kawagata, S., Grenfell, H. R., Sabaa, A. T., and O'Neill, T.: Last global extinction in the deep sea during the mid-Pleistocene climate transition, Paleoceanography, 22, 267-291, https://doi.org/10.1016/j.palaeo.2005.03.001, 2007.

Hedley, R. H.: Cement and Iron in the Arenaceous Foraminifera, Micropaleontology, 9, 433-441, https://doi.org/10.2307/1484505, 1963.

Herman, Y.: Temperate water planktonic foraminifera in Quaternary sediments of the Arctic Ocean, Nature, 201, 386-387, https://doi.org/10.1038/201386a0, 1964.

Herman, Y.: *Bolivina arctica*, a new benthonic foraminifera from Arctic Ocean sediments, J. Foraminifer. Res., 3, 137-141, https://doi.org/10.2113/gsjfr.3.3.137, 1973.

Herman, Y.: Arctic Ocean Sediments, Microfauna, and the Climatic Record in Late Cenozoic Time, in: Marine Geology and Oceanography of the Arctic Seas, edited by: Herman, Y., Springer, Berlin, Heidelberg, 283-348, https://doi.org/10.1007/978-3-642-87411-6_13.

Herman, Y., Osmond, J. K., and Somayajulu, B. L. K.: Late Neogene Arctic paleoceanography: Micropaleontology, stable isotopes, and chronology, in: The Arctic Seas, edited by: Herman, Y., Van Nostrand Reinhold Company, New York, 581-655, https://doi.org/10.1007/978-1-4613-0677, 1989.

https://doi.org/10.5194/egusphere-2025-6290
Preprint. Discussion started: 29 December 2025

Hillaire-Marcel, C., Ghaleb, B., de Vernal, A., Maccali, J., Cuny, K., Jacobel, A., Le Duc, C., and McManus, J.: A New chronology of late Quaternary sequences from the central Arctic Ocean based on „extinction ages“ of their excesses in ^{231}Pa and ^{230}Th, Geochem. Geophys. Geosyst, 18, 4573-4585, https://doi.org/10.1002/2017/GC007050, 2017.

Himmighofen, O., Holzmann, M., Barrenechea, I., Pawlowski, J., and Gooday, A.: An integrative taxonomic survey of benthic foraminiferal species (Protista, Rhizaria) from the eastern Clarion-Clipperton Zone, J. Mar. Sci. Eng., 11, https://doi.org/10.3390/jmse11112038, 2023.

Höglund, H. G.: Foraminifera in the Gullmar Fjord and the Skagerrak, Zoolog. bidr. Uppsala, 26, Appelbergs boktrycker, 1947.

Holbourn, A., Henderson, A., and MacLeod, N.: Atlas of Benthic Foraminifera, John Wiley & Sons, 642 pp., https://doi.org/10.1002/9781118452493, 2013.

Honjo, S., Manganini, S. J., Krishfield, R. A., and Francois, R.: Particulate organic carbon fluxes to the ocean interior and factors controlling the biological pump: A synthesis of global sediment trap programs since 1983, Progr. Oceanogr, 76, 217-285, https://doi.org/10.1016/j.pocean.2007.11.003, 2008.

Hottinger, L.: Processes determining the distribution of larger foraminifera in space and time, Utrecht Micropaleontol. Bull., 30, 239-253, 1983.

Hunkins, K., Bé, A. W. H., Opdyke, N. D., and Mathieu, G.: The Late Cenozoic history of the Arctic Ocean, in: The late Cenozoic glacial ages, edited by: Turekian, K.K., New Haven, 215-237, 1971.

Husum, K. and Hald, M.: Modern foraminiferal distribution in the subarctic Malangen Fjord and adjoining shelf, Northern Norway, J. Foraminifer. Res., 34, 34-48, https://doi.org/10.2113/0340034, 2004.

Husum, K., Hald, M., Stein, R., and Weißschnur, M.: Recent benthic foraminifera in the Arctic Ocean and Kara Sea continental margin, Arktos, 1, 5, https://doi.org/10.1007/s41063-015-0005-9, 2015.

Ishman, S. E., Polyak, L. V., and Poore, R. Z.: Expanded record of Quaternary oceanographic change: Amerasian Arctic Ocean, Geology, 24, 139-142, https://doi.org/10.1130/0091-7613(1996)024<0139:EROQOC>2.3.CO;2, 1996.

Ishman, S. E. I. and Foley, K. M.: Modern benthic foraminifer distribution in the Amerasian Basin, Arctic Ocean, Micropaleontology, 42, 206-220, https://doi.org/10.2307/1485871, 1996.

Jakobsson, M., Backman, J., Murray, A., and Løvlie, R.: Optically stimulated luminescence dating supports central Arctic Ocean cm-scale sedimentation rates, Geochem. Geophys. Geosyst., 4, 1016, https://doi.org/1016, 10.1029/2002GC000423, 2003.

Jakobsson, M., Løvlie, R., Al-Hanbali, H., Arnold, E., Backman, J., and Mörth, M.: Manganese and color cycles in Arctic Ocean sediments constrain Pleistocene chronology, Geology, 28, 23-26, https://doi.org/10.1130/0091-7613(2000)28<23:MACCIA>2.0.CO;2, 2000.

Jakobsson, M., Løvlie, R., Arnold, E. M., Backman, J., Polyak, L., Knutsen, J.-O., and Musatov, E.: Pleistocene stratigraphy and paleoenvironmental variation from Lomonosov Ridge sediments, central Arctic Ocean, Glob. Planet. Change, 31, 1-22, https://doi.org/10.1016/S0921-8181(01)00110-2, 2001.

https://doi.org/10.5194/egusphere-2025-6290
Preprint. Discussion started: 29 December 2025

Jennings, A., Reilly, B., Andrews, J., Hogan, K., Walcak, M., Jakobsson, M., Stoner, J., Mix, A., Nicholls, K. W., O'Regan, M., Prins, M. A., and Troelstra, S. R.: Modern and early Holocene ice shelf sediment facies from Petermann Fjord and northern Nares Strait, northwest Greenland, Quat. Sci. Rev., 283, 107460, https://doi.org/10.1016/j.quascirev.2022.107460, 2022.

Jennings, A. E., Andrews, J. T., Ó Cofaigh, C., Onge, G. S., Sheldon, C., Belt, S. T., Cabedo-Sanz, P., and Hillaire-Marcel, C.: Ocean forcing of Ice Sheet retreat in central west Greenland from LGM to the early Holocene, Earth Planet. Sci. Lett., 472, 1-13, https://doi.org/10.1016/j.epsl.2017.05.007, 2017.

Jones, G. A.: The central Arctic Ocean sediment record: Current progress in moving from a litho- to a chronostratigraphy, Polar Res., 5, 309-311, https://doi.org/10.3402/polar.v5i3.6898, 1987.

Jones, R.W. and Bender, H. and Charnock, M.A. and Kaminski, M. A. and Whittaker, J.E.: Emendation of the foraminiferal genus *Cribrostomoides* Cushman, 1910, and its taxonomic implications. J. Micropalaeontol., 12, 181-193. ISSN 0262821X, 12, 10.1144/jm.12.2.181, 1993.

Jones, R. W.: The Challenger Foraminifera, 1995, Oxford University Press, 149 pp., https://doi.org/10.1017/S0025315400018452, 1994.

Jorissen, F. J.: Benthic foraminiferal microhabitats below the sediment-water interface, in: Modern Foraminifera, edited by: Sen Gupta, B. K., Springer Netherlands, Dordrecht, 161-179, https://doi.org/10.1007/0-306-48104-9_10, 2003.

Jorissen, F. J., de Stigter, H. C., and Widmark, J. G. V.: A conceptual model explaining benthic foraminiferal microhabitats, Mar. Micropaleontol., 26, 3-15, https://doi.org/10.1016/0377-8398(95)00047-X, 1995.

Kaithwar, A., Singh, D. P., and Saraswat, R.: A highly diverse living benthic foraminiferal assemblage in the oxygen deficient zone of the southeastern Arabian Sea, Biodiv. Conserv., 29, 3925-3958, https://doi.org/10.1007/s10531-020-02056-9, 2020.

Kaminski, M. A., Silye, L., and Kender, S.: Miocene deep-water agglutinated foraminifera from IODP Hole M0002A, Lomonosov Ridge: faunal constraints for the opening of the Fram Strait, Micropaleontology, 55, 117-135, https://doi.org/10.47894/mpal.55.2.03, 2009.

Kaufman, D. S., Polyak, L., Adler, R., Channell, J. E. T., and Xuan, C.: Dating late Quaternary planktonic foraminifer *Neogloboquadrina pachyderma* from the Arctic Ocean using amino acid racemization, Paleoceanography, 23, PA3224, https://doi.org/10.1029/2008PA001618, 2008.

Kawagata, S., Hayward, B. W., and Kuhnt, W.: Extinction of deep-sea foraminifera as a result of Pliocene–Pleistocene deep-sea circulation changes in the South China Sea (ODP Sites 1143 and 1146), Quat. Sci. Rev., 26, 808-827, https://doi.org/10.1016/j.quascirev.2006.10.011, 2007.

Kawagata, S., Hayward, B. W., Grenfell, H. R., and Sabaa, A.: Mid-Pleistocene extinction of deep-sea foraminifera in the North Atlantic Gateway (ODP sites 980 and 982), Palaeogeogr. Palaeoclimatol. Palaeoecol., 221, 267-291, https://doi.org/10.1016/j.palaeo.2005.03.001, 2005.

Kender, S. and Kaminski, M. A.: Arctic Ocean benthic foraminiferal faunal change associated with the onset of perennial sea ice in the Middle Miocene, J. Foraminifer. Res., 43, 99-109, https://doi.org/10.2113/gsjfr.43.1.99, 2013.

https://doi.org/10.5194/egusphere-2025-6290
Preprint. Discussion started: 29 December 2025

Kender, S., McClymont, E. L., Elmore, A. C., Emanuele, D., Leng, M. J., and Elderfield, H.: Mid Pleistocene foraminiferal mass extinction coupled with phytoplankton evolution, Nature Comm., 7, 11970, https://doi.org/10.1038/ncomms11970, 2016.

Kireenko, L., Tikhonova, A., Kozina, N., and Matul, A.: Image dataset of benthic foraminifera in multicorer and gravity corer sediments from north-western Scotland shelf (North Atlantic Ocean), Biodiv. Data J., 10, e87457, https://doi.org/10.3897/BDJ.10.e87457, 2022.

Kniazeva, O. and Korsun, S.: Seasonal data on Rose Bengal stained foraminifera in the head of Kongsfjorden, Svalbard, Data Brief, 25, 104040, https://doi.org/10.1016/j.dib.2019.104040, 2019.

Koho, K. A., de Nooijer, L. J., and Reichart, G. J.: Combining benthic foraminiferal ecology and shell Mn/Ca to deconvolve past bottom water oxygenation and paleoproductivity, Geochim. Cosmochim. Acta, 165, 294-306, https://doi.org/10.1016/j.gca.2015.06.003, 2015.

Lagoe, M. B.: Recent benthic foraminifera from the central Arctic Ocean, J. Foraminifer. Res., 7, 106-129, https://doi.org/10.2113/gsjfr.7.2.106, 1977.

Lazar, K., Polyak, L., and Dipre, G.: Re-examination of the use of *Cassidulina neoteretis* as a Pleistocene biostratigraphic marker in the Arctic Ocean, J. Foraminifer. Res., 46, 115-123, https://doi.org/10.2113/gsjfr.46.2.115, 2016.

Lazar, K. B. and Polyak, L.: Pleistocene benthic foraminifers in the Arctic Ocean: Implications for sea-ice and circulation history, Mar. Micropaleontol., 126, 19-30, https://doi.org/10.1016/j.marmicro.2016.04.004, 2016.

Lecroq, B., Gooday, A., and Pawlowski, J.: Global genetic homogeneity in the deep-sea foraminiferan *Epistominella exigua* (Rotaliida: Pseudoparrellidae), Zootaxa, 2096, 23-32, https://doi.org/10.11646/zootaxa.2096.1.4, 2009.

Lee, A. J. and Anderson, O. R.: The biology of foraminifera, Academic Press, University of California, 1991.

Linke, P.: Metabolic adaptations of deep-sea benthic foraminifera to seasonally varying food input, Mar. Ecol. Prog. Ser., 81, 51-63, https://doi.org/10.3354/meps081051, 1992.

Linke, P. and Lutze, G. F.: Microhabitat preferences of benthic foraminifera—a static concept or a dynamic adaptation to optimize food acquisition?, Mar. Micropaleontol., 20, 215-234, https://doi.org/10.1016/0377-8398(93)90034-U, 1993.

Lohmann, G. P.: Abyssal benthonic foraminifera as hydrographic indicators in the western South Atlantic Ocean, J. Foraminifer. Res., 8, 6-34, https//doi.org/10.2113/gsjfr.8.1.6, 1978.

Loubere, P. and Rayray, S.: Benthic foraminiferal assemblage formation: Theory and observation for the European Arctic margin, Deep-Sea Research Part I: Oceanogr. Res. Pap., 115, 36-47, https://doi.org/10.1016/j.dsr.2016.05.004, 2016.

Loubere, P., Gary, A., and Lagoe, M.: Generation of the benthic foraminiferal assemblage: Theory and preliminary data, Mar. Micropaleontol., 20, 165-181, https://doi.org/10.1016/0377-8398(93)90031-R, 1993.

Löwemark, L., März, C., O'Regan, M., and Gyllencreutz, R.: Arctic Ocean Mn-stratigraphy: genesis, synthesis and inter-basin correlation, Quat. Sci. Rev., 92, 97-111, http://dx.doi.org/10.1016/j.quascirev.2013.11.018, 2014.

Mackensen, A. and Hald, M.: *Cassidulina teretis* Tappan and *C. laevigata* d'Orbigny; their modern and late Quaternary distribution in northern seas, J. Foraminifer. Res., 18, 16-24, https://doi.org/10.2113/gsjfr.18.1.16, 1988.

https://doi.org/10.5194/egusphere-2025-6290
Preprint. Discussion started: 29 December 2025

Mackensen, A., Sejrup, H. P., and Jansen, E.: The distribution of living benthic foraminifera on the continental slope and rise off southwest Norway, Mar. Micropaleontol., 9, 275-306, https://doi.org/10.1016/0377-8398(85)90001-5, 1985.

Mackensen, A., Grobe, H., Kuhn, G., and Fütterer, D. K.: Benthic foraminiferal assemblages from the eastern Weddell Sea between 68 and 73°S: Distribution, ecology and fossilization potential, Mar. Micropaleontol., 16, 241-283, https://doi.org/10.1016/0377-8398(90)90006-8, 1990.

Mackensen, A., Schumacher, S., Radke, J., and Schmidt, D. N.: Microhabitat preferences and stable carbon isotopes of endobenthic foraminifera: clue to quantitative reconstruction of oceanic new production?, Mar. Micropaleontol., 40, 233-258, http://dx.doi.org/10.1016/S0377-8398(00)00040-2, 2000.

Mancin, N., Hayward, B. W., Trattenero, I., Cobianchi, M., and Lupi, C.: Can the morphology of deep-sea benthic foraminifera reveal what caused their extinction during the mid-Pleistocene Climate Transition?, Mar. Micropaleontol., 104, 53-70, https://doi.org/10.1016/j.marmicro.2013.09.004, 2013.

Mar, F.-M.: Primary productivity in Arctic sea ice and ocean, Phd thesis, Bremerhaven, University Bremen, Bremen, 2014.

Martin, R. E.: Taphonomy and temporal resolution of foraminiferal assemblages, in: Modern Foraminifera, Springer Netherlands, Dordrecht, 281-298, https://doi.org/10.1007/0-306-48104-9_16, 2003.

März, C., Stratmann, A., Matthiessen, J., Meinhardt, A. K., Eckert, S., Schnetger, B., Vogt, C., Stein, R., and Brumsack, H. J.: Manganese-rich brown layers in Arctic Ocean sediments: Composition, formation mechanisms, and diagenetic overprint, Geochim. Cosmochim. Acta, 75, 7668-7687, https://doi.org/10.1016/j.gca.2011.09.046, 2011.

Matthiessen, J., Niessen, F., Stein, R., and Naafs, B. D. A.: Pleistocene Glacial Marine Sedimentary Environments at the Eastern Mendeleev Ridge, Arctic Ocean, Polarforsch. 79, 123-137, 2010.

Matthiessen, J., Schreck, M., De Schepper, S., Zorzi, C., and de Vernal, A.: Quaternary dinoflagellate cysts in the Arctic Ocean: Potential and limitations for stratigraphy and paleoenvironmental reconstructions, Quat. Sci. Rev., 192, 1-26, https://doi.org/10.1016/j.quascirev.2017.12.020, 2018.

Matthiessen, J.: Linescanner images of sediment core PS72/340-5 [dataset], PANGAEA, https://doi.org/10.1594/PANGAEA.817500, 2013a.

Matthiessen, J.: Linescanner images of sediment core PS72/396-5 [dataset], PANGAEA, https://doi.org/10.1594/PANGAEA.817507, 2013b.

McKinney, M. L.: Taxonomic selectivity and continuous variation in mass and background extinctions of marine taxa, Nature, 325, 143-145, https://doi.org/10.1038/325143a0, 1987.

McNeill, D. H.: New foraminifera from the Upper Cretaceous and Cenozoic of the Beaufort-Mackenzie Basin of Arctic Canada, Cushm. Found. Foram. Res. Spec. Publ. 35, 1997.

Mead, G. A. and Kennett, J. P.: The distribution of Recent benthic foraminifera in the Polar Front region, southwest Atlantic, Mar. Micropaleontol., 11, 343-360, https://doi.org/10.1016/0377-8398(87)90006-5, 1987.

https://doi.org/10.5194/egusphere-2025-6290
Preprint. Discussion started: 29 December 2025

Minicucci, D. A. and Clark, D. L. C.: A late Cenozoic stratigraphy for glacial-marine sediments of the eastern Alpha Cordillera, Central Arctic Ocean, in: Glacial-marine sedimentation, edited by: Molnia, B. F., Springer, Boston, MA, 331-365, https://doi.org/10.1007/978-1-4613-3793-5_8, 1983.

Moodley, L., Middelburg, J., Boschker, H., Duineveld, G., Pel, R., Herman, P., and Heip, C.: Bacteria and foraminifera: key players in a short-term deep-sea benthic response to phytodetritus, Mar. Ecol. Prog. Ser., 236, 23-29, https://doi.org/10.3354/meps236023, 2002.

Morris, T. H., Clark, D. L., and Blasco, S. M.: Sediments of the Lomonosov Ridge and Makarov Basin: a Pleistocene stratigraphy for the North Pole, Geol. Soc. Amer. Bull., 96, 901-910, https://doi.org/10.1130/0016-7606(1985)96<901:sotlra>2.0.co;2, 1985.

Mudie, P. J.: Palynology of the Cesar cores, Alpha Ridge, in: Initial geological report on CESAR - the Canadian expedition to study the Alpha Ridge, Arctic Ocean, edited by: Jackson, H. R., Mudie, P. J., and Blasco, S. M., Geol. Surv. Can. Pap., 84-22, 149-174, https://doi.org/10.4095/120315, 1985.

Mudie, P. J. and Blasco, S. M.: Lithostratigraphy of the Cesar cores, in: Initial geological report on CESAR - the Canadian expedition to study the Alpha Ridge, Arctic Ocean, edited by: Jackson, H. R., Mudie, P. J., and Blasco, S. M., Geol. Surv. Can. Pap., 84-22, 59-99, https://doi.org/10.4095/120315, 1985.

Mullen, M. W. and McNeil, D. H.: Biostratigraphic and paleoclimatic significance of a new Pliocene foraminiferal fauna from the central Arctic Ocean, Mar. Micropaleontol., 26, 273-280, https://doi.org/10.1016/0377-8398(96)87758-9, 1995.

Murray, J.: An illustrated guide to the benthic foraminifera of the Hebridean Shelf, west of Scotland, with notes on their mode of life, PE, 5, 31-31, 2003.

Murray, J. and Alve, E.: The distribution of agglutinated foraminifera in NW European seas: Baseline data for the interpretation of fossil assemblages, PE, 14.2, 2011.

Murray, J. W.: Ecology and palaeoecology of benthic Foraminifera, Logman Scientific & Technical, London, 71, 397 pp., 1991.

Murray, J. W.: Ecology and Applications of Benthic Foraminifera, CUP, Cambridge, https.//doi.org/10.1017/CBO9780511535529, 2006.

Nees, S.: High-resolution benthic foraminiferal records of the last glacial termination in the northern North Atlantic, in: Contributions to the Micropaleontology and Paleoceanography of the Northern North Atlantic, edited: Hass, H. C. and Kaminski, M.A., Gryzbowski Found. Spec, Publ., 5, pp. 167-197, https://doi.org/10.1130/0091-7613(1997)025<0659:HRROFR>2.3.CO;2, 1997.

Nees, S. and Struck, U.: The biostratigraphic and paleoceanographic significance of *Siphotextularia rolshauseni* Phleger and Parker in Norwegian-Greenland Sea sediments, J. Foraminifer. Res., 24, 233-240, https://doi.org/10.2113/gsjfr.24.4.233, 1994.

Niessen, F.: Physical properties of sediment core PS72/340-5 [dataset], PANGAEA, https://doi.org/10.1594/PANGAEA.737861, 2010a.

https://doi.org/10.5194/egusphere-2025-6290
Preprint. Discussion started: 29 December 2025

Niessen, F.: Physical properties of sediment core PS72/396-5 [dataset], PANGAEA, https://doi.org/10.1594/PANGAEA.737871, 2010b.

Nørgaard-Pedersen, N., Mikkelsen, N., and Kristoffersen, Y.: Arctic Ocean record of last two glacial-interglacial cycles off North Greenland/Ellesmere Island - Implications for glacial history, Mar. Geol., 244, 93-108, https://doi.org/10.1016/j.margeo.2007.06.008, 2007a.

Nørgaard-Pedersen, N., Mikkelsen, N., Lassen, S. J., Kristoffersen, Y., and Sheldon, E.: Reduced sea ice concentrations in the Arctic Ocean during the last interglacial period revealed by sediment cores off northern Greenland, Paleoceanography, 22, PA1218, https://doi.org/10.1029/2006PA001283, 2007b.

Nowicki, M., DeVries, T., and Siegel, D. A.: Quantifying the Carbon Export and Sequestration Pathways of the Ocean's Biological Carbon Pump, Global Biogeochem. Cycle, 36, e2021GB007083, https://doi.org/10.1029/2021GB007083, 2022.

O'Neill, B. J.: Pliocene and Pleistocene benthic foraminifera from the central Arctic Ocean, J. Paleontol., 55, 1141-1170, 1981.

O'Regan, M., Coxall, H. K., Cronin, T. M., Gyllencreutz, R., Jakobsson, M., Kaboth, S., Löwemark, L., Wiers, S., and West, G.: Stratigraphic Occurrences of Sub-Polar Planktic Foraminifera in Pleistocene Sediments on the Lomonosov Ridge, Arctic Ocean, Front. Earth Sci., 7, https://doi.org/10.3389/feart.2019.00071, 2019.

Osterman, L. E. and Qvale, G.: Benthic foraminifers from the Vøring Plateau (ODP Leg 104), in: Proc. ODP, Sci. Results, edited by: Eldholm, O., Thiede, J., Taylor, E., and al., College Station, TX (ODP), 745–768, https://doi.org/10.2973/odp.proc.sr.104.159.1989, 1989.

Osterman, L. E., Poore, R. Z., and Foley, K. M.: Distribution of benthic foraminifers (>125 μm) in the surface sediments of the Arctic Ocean, U.S. Geol. Surv. Bull. 2164, 1-28, 1999.

Pak, D. K., Clark, D. L., and Blasco, S. M.: Late Pleistocene stratigraphy and micropaleontology of a part of the Eurasian basin (=Fram Basin), central Arctic Ocean, Mar. Micropaleontol., 20, 1-22, https://doi.org/10.1016/0377-8398(92)90006-6, 1992.

Park, K., Kim, J.-H., Asahi, H., Polyak, L., Khim, B.-K., Schreck, M., Niessen, F., Kong, G. S., and Nam, S.-I.: Cyclostratigraphic age constraining for Quaternary sediments in the Makarov Basin of the western Arctic Ocean using manganese variability, Quat. Geochronol., 55, 101021, https://doi.org/10.1016/j.quageo.2019.101021, 2020.

Parker, F. L., Phleger, F. B., and Peirson, J. F.: Ecology of Foraminifera from San Antonio Bay and Environs, Southwest Texas, CFFR, 75 pp., 1953.

Parker W. K, J. T. R. and Brady, H. B.: On the nomenclature of the Foraminifera. Part XIV. The species enumerated by D'Orbigny in the 'Annales des Sciences Naturelles,' 1826, vol. vii. - IV. The species founded upon the figures in Soldani's 'Testaceographia ac Zoophytogeographia'. [Cont. from vol. iv. p. 392.], Ann. Mag. Nat. Hist., 1871.

Pawlowski, J., Bowser, S. S., and Gooday, A. J.: A note on the genetic similarity between shallow- and deep-water *Epistominella vitrea* (Foraminifera) in the Antarctic, Deep-Sea Res. II: Top. Stud. Oceanogr., 54, 1720-1726, https://doi.org/10.1016/j.dsr2.2007.07.016, 2007.

Pflum, C. E., Frerichs, W. E., Pflum, C. E., and Frerichs, W. E.: Gulf of Mexico deep-water foraminifers in: Gulf of Mexico Deep-water Foraminifers, edited by: Sliter, W. V., Cushm. Found. Foramin. Res. Spec. Publ., 14, 124 pp., 1976.

https://doi.org/10.5194/egusphere-2025-6290
Preprint. Discussion started: 29 December 2025

Phillips, R. L. and Grantz, A.: Quaternary history of sea ice and paleoclimate in the Amerasia basin, Arctic Ocean, as recorded in the cyclical strata of Northwind Ridge, Geol. Soc. Am. Bull., 109, 1101-1115, https://doi.org/10.1130/0016-7606(1997)109<1101:QHOSIA>2.3.CO;2, 1997.

Phleger, F. B., Parker, F. L., and Peirson, J. F.: North Atlantic Foraminifera, Scripps Oceanography, La Jolla, California, 7, 1, 122 pp., https://doi.org/10.1306/5ceadc38-16bb-11d7-8645000102c1865d, 1953.

Poirier, R. K., Gaetano, M. Q., Acevedo, K., Schaller, M. F., Raymo, M. E., and Kozdon, R.: Quantifying diagenesis, contributing factors, and resulting isotopic bias in benthic foraminifera using the foraminiferal preservation index: Implications for geochemical proxy records, Paleoceanogr. Paleoclimatol., 36, e2020PA004110, https://doi.org/10.1029/2020PA004110, 2021.

Polyak, L. and Solheim, A.: Late- and postglacial environments in the northern Barents Sea west of Franz Josef Land, Polar Res., 13, 197-207, https://doi.org/10.3402/polar.v13i2.6693, 1994.

Polyak, L., Best, K. M., Crawford, K. A., Council, E. A., and St-Onge, G.: Quaternary history of sea ice in the western Arctic Ocean based on foraminifera, Quat. Sci. Rev., 79, 145-156, https://doi.org/10.1016/j.quascirev.2012.12.018, 2013.

Polyak, L., Curry, W. B., Darby, D. A., Bischof, J., and Cronin, T. M.: Contrasting glacial/interglacial regimes in the western Arctic Ocean as exemplified by a sedimentary record from the Mendeleev Ridge, Palaeogeogr. Palaeoclimatol. Palaeoecol., 203, 73-93, https://doi.org/10.1016/S0031-0182(03)00661-8, 2004.

Polyak, L., Korsun, S., Febo, L. A., Stanovoy, V., Khusid, T., Hald, M., Paulsen, B. E., and Lubinski, D. J.: Benthic foraminiferal assemblages from the southern Kara Sea, a river-influenced arctic marine environment, J. Foraminifer. Res., 32, 252-273, https://doi.org/10.2113/32.3.252, 2002.

Polyak, L., Alley, R. B., Andrews, J. T., Brigham-Grette, J., Cronin, T. M., Darby, D. A., Dyke, A. S., Fitzpatrick, J. J., Funder, S., Holland, M., Jennings, A. E., Miller, G. H., O'Regan, M., Savelle, J., Serreze, M., St. John, K., White, J. W. C., and Wolff, E.: History of sea ice in the Arctic, Quat. Sci. Rev., 29, 1757-1778, https://doi.org/10.1016/j.quascirev.2010.02.010, 2010.

Poore, R. Z., Phillips, R. L., and Rieck, H. J.: Paleoclimatic record for Northwind Ridge, western Arctic Ocean, Paleoceanography, 8, 149-159, https://doi.org/10.1029/93PA00146, 1993.

Poore, R. Z., Ishman, S. E., Phillips, R. L., and McNeil, D. H.: Quaternary stratigraphy and paleoceanography of the Canada Basin, western Arctic Ocean, Bull. U.S. Geol. Surv., 2080, 32 pp., https://doi.org/10.3133/b2080, 1994.

Rasmussen, J. A. and Sheldon, E.: Microfossil biostratigraphy of the Palaeogene succession in the Davis Strait, offshore West Greenland, Mar. Pet. Geol., 20, 1017-1030, https://doi.org/10.1016/S0264-8172(02)00114-9, 2003.

Rasmussen, T. L. and Thomsen, E.: Warm Atlantic surface water inflow to the Nordic seas 34–10 calibrated ka B.P, Paleoceanography., 23, PA1201, https://doi.org/10.1029/2007pa001453, 2008.

Rasmussen, T. L., Thomsen, E., and Nielsen, T.: Water mass exchange between the Nordic seas and the Arctic Ocean on millennial timescale during MIS 4 – MIS 2, Geochem. Geophys. Geosyst., 15, 530-544, https://doi.org/10.1002/2013GC005020, 2014.

https://doi.org/10.5194/egusphere-2025-6290
Preprint. Discussion started: 29 December 2025

Rasmussen, T. L., Oppo, D. W., Thomsen, E., and Lehman, S. J.: Deep sea records from the southeast Labrador Sea: Ocean circulation changes and ice-rafting events during the last 160,000 years, Paleoceanography, 18, 1018, https://doi.org/10.1029/2001pa000736, 2003a.

Rasmussen, T. L., Thomsen, E., Kuijpers, A., and Wastegard, S.: Late warming and early cooling of the sea surface in the Nordic seas during MIS 5e (Eemian Interglacial), Quat. Sci. Rev., 22, 809-821, https://doi.org/10.1016/S0277-3791(02)00254-8, 2003b.

Rasmussen, T. L., Thomsen, E., Slubowska, M. A., Jessen, S., Solheim, A., and Koc, N.: Paleoceanographic evolution of the SW Svalbard margin (76°N) since 20,000 14C yr BP, Quat. Res., 67, 100-114, https://doi.org/10.1016/j.yqres.2006.07.002, 2007.

Razmjooei, M. J., Henderiks, J., Coxall, H. K., Baumann, K.-H., Vermassen, F., Jakobsson, M., Niessen, F., and O'Regan, M.: Revision of the Quaternary calcareous nannofossil biochronology of Arctic Ocean sediments, Quat. Sci. Rev., 321, 108382, https://doi.org/10.1016/j.quascirev.2023.108382, 2023.

Reuss, A. E.: Ueber die fossilen Foraminiferen und Entomostraceen der Septarienthone der Umgegend von Berlin, Zeitschr. Deut. Geol. Gesell., 3, 49-92, 1851.

Roca-Martí, M., Puigcorbé, V., Loeff, M., Katlein, C., Fernández-Méndez, M., Peeken, I., and Masqué, P.: Carbon export fluxes and export efficiency in the central Arctic during the record sea-ice minimum in 2012: a joint $^{234}Th/^{238}U$ and $^{210}Po/^{210}Pb$ study, J. Geophys. Res. Oceans, 121, 5030–5049, https://doi.org/10.1002/2016JC011816, 2016.

Rudels, B. and Carmack, E.: Arctic Ocean water mass structure and circulation, Oceanography, 35, 3-4, 52 - 65, https://doi.org/10.5670/oceanog.2022.116, 2022.

Saidova, K. M.: Deep-water foraminifera communities of the Arctic Ocean, Oceanology, 51, 60-68, https://doi.org/10.1134/S0001437011010152, 2011.

Schmiedl, G., Mitschele, A., Beck, S., Emeis, K.-C., Hemleben, C., Schulz, H., Sperling, M., and Weldeab, S.: Benthic foraminiferal record of ecosystem variability in the eastern Mediterranean Sea during times of sapropel S5 and S6 deposition, Palaeogeogr. Palaeoclimatol. Palaeoecol., 190, 139-164, https://doi.org/10.1016/S0031-0182(02)00603-X, 2003.

Schneider, C. A., Rasband, W. S., and Eliceiri, K. W.: NIH Image to ImageJ: 25 years of image analysis, Nature Meth., 9, 671, https://doi.org/10.1038/nmeth.2089, 2012.

Schoster, F.: Geochemistry of sediment core PS2185-6, PANGAEA [dataset], https://doi.org/10.1594/PANGAEA.227857, 2005.

Schröder, C.: Subsurface preservation of agglutinated foraminifera in the northwest Atlantic Ocean, Abh. Geol. B.-A., 41, 325-336, 1988.

Schröder, C. J.: Deep-water Arenaceous Foraminifera in the Northwest Atlantic Ocean, phD thesis, Canada, 205 pp., 1986.

Schroeder, C.: Subsurface preservation of agglutinated foraminifera in the Northwest Atlantic Ocean, Abh. Geol. B.-A., 41, 325-336, 1988.

https://doi.org/10.5194/egusphere-2025-6290
Preprint. Discussion started: 29 December 2025

Schroeder, C. J., Scott, D. B., and Medioli, F. S.: Can smaller benthic foraminifera be ignored in paleoenvironmental analyses?, J. Foraminifer. Res., 17, 101-105, https://doi.org/10.2113/gsjfr.17.2.101, 1987.

Scott, D. B. and Vilks, G.: Benthic foraminifera in the surface sediments of the deep-sea Arctic Ocean, J. Foraminifer. Res., 21, 20-38, https://doi.org/10.2113/gsjfr.21.1.20, 1991.

Scott, D. B., Schell, T., Rochon, A., and Blasco, S.: Benthic foraminifera in the surface sediments of the Beaufort Shelf and slope, Beaufort Sea, Canada: Applications and implications for past sea-ice conditions, J. Mar. Syst., 74(3-4), 840-863, https://doi.org/10.1016/j.jmarsys.2008.01.008

Scott, D. B., Mudie, P. J., Baki, V., MacKinnon, K. E., and Cole, F. E.: Biostratigraphy and late Cenozoic paleoceanography of the Arctic Ocean: Foraminiferal, lithostratigraphic, and isotopic evidence, Geol. Soc. Am. Bull., 101, 260-277, https://doi.org/10.1130/0016-7606(1989)101<0260:BALCPO>2.3.CO;2, 1989.

Scott, D. B., Schell, T., St-Onge, G., Rochon, A., and Blasco, S.: Foraminiferal assemblage changes over the last 15,000 years on the Mackenzie-Beaufort Sea Slope and Amundsen Gulf, Canada: Implications for past sea ice conditions, Paleoceanography, 24, http://dx.doi.org/10.1029/2007PA001575, 2009.

Seidenkrantz, M.-S.: Benthic foraminifera as palaeo sea-ice indicators in the subarctic realm – examples from the Labrador Sea–Baffin Bay region, Quat. Sci. Rev., 79, 135-144, https://doi.org/10.1016/j.quascirev.2013.03.014, 2013.

Seidenkrantz, M. S.: *Cassidulina teretis* Tappan and *Cassidulina neoteretis* new species (Foraminifera): stratigraphic markers for deep sea and outer shelf areas, J. Micropalaeontol., 14, 145-157, https://doi.org/10.1144/jm.14.2.145, 1995.

Sellén, E., Jakobsson, M., and Backman, J.: Sedimentary regimes in Arctic's Amerasian and Eurasian Basins: Clues to differences in sedimentation rates, Glob. Planet. Change., 61, 275-284, 2008.

Sellén, E., O'Regan, M., and Jakobsson, M.: Spatial and temporal Arctic Ocean depositional regimes: a key to the evolution of ice drift and current patterns, Quat. Sci. Rev., 29(25), 3644-3664, https://doi.org/10.1016/j.quascirev.2010.06.005, 2010.

Sirenko, B. I., Burhinskaja, G. n., Andriashev, A. P., Balushkin, A. V., Neyelov, A. V., Markhaseva, E. L., Stepanjants, S. D., and Lukina, T. G., Alimov, A. F. (Ed.): List of species of free-living invertebrates of Eurasian Arctic Seas and adjacent deep water, Explorations of the fauna of the seas, 52(59), ISSN 0386 - 077X, St.-Petersburg, 2001.

Song, T., Hillaire-Marcel, C., Liu, Y., Ghaleb, B., and de Vernal, A.: Cycling and behavior of ^{230}Th in the Arctic Ocean: Insights from sedimentary archives, Earth Sci. Rev., 244, 104514, https://doi.org/10.1016/j.earscirev.2023.104514, 2023.

Spezzaferri, S., Rüggeberg, A., Stalder, C., and Margreth, S.: Benthic Foraminifer Assemblages from Norwegian cold-water coral reefs, J. Foraminifer. Res., 43, 21-39, https://doi.org/10.2113/gsjfr.43.1.21, 2013.

Spielhagen, R. F., Baumann, K.-H., Erlenkeuser, H., Nowaczyk, N. R., Norgaard-Pedersen, N., Vogt, C., and Weiel, D.: Arctic Ocean deep-sea record of northern Eurasian ice sheet history, Quat. Sci. Rev., 23, 1455-1483, https://doi.org/10.1016/j.quascirev.2003.12.015, 2004.

Spielhagen, R. F., Bonani, G., Eisenhauer, A., Frank, M., Frederichs, T., Kassens, H., Kubik, P. W., Mangini, A., Nørgaard-Pedersen, N., Nowaczyk, N. R., Schäper, S., Stein, R., Thiede, J., Tiedemann, R., and Wahsner, M.: Arctic Ocean evidence

https://doi.org/10.5194/egusphere-2025-6290
Preprint. Discussion started: 29 December 2025

for late Quaternary initiation of northern Eurasian ice sheets, Geology, 25, 783-786, https://doi.org/10.1130/0091-7613(1997)025<0783:AOEFLQ>2.3.CO;2, 1997.

Stärz, M.: Stratigraphie und Paläoumwelt im Arktischen Ozean während des mittleren Pleistozäns: Rekonstruktion aus Sedimentabfolgen vom Lomonosov-Rücken, Fakultät für Geowissenschaften, Geotechnik und Bergbau der Technischen Universität Bergakademie Freiberg, 105 pp., 2008.

Stein, R., Matthiessen, J., and Niessen, F.: Re-coring at Ice Island T3 site of key core FL-224 (Nautilus Basin, Amerasian Arctic): sediment characteristics and stratigraphic framework, Polarforsch., 79, 81-96, https://doi.org/10.2312/polarforschung.79.2.81, 2010a.

Stein, R., Matthiessen, J., Niessen, F., Krylov, R., Nam, S., and Bazhenova, E.: Towards a better (litho-) stratigraphy and reconstruction of Quaternary paleoenvironment in the Amerasian Basin (Arctic Ocean), Polarforsch., 79, 97-121, 2010b.

Steinsund, P. I. and Hald, M.: Recent calcium carbonate dissolution in the Barents Sea: Paleoceanographic applications, Mar. Geol., 117, 303-316, https://doi.org/10.1016/0025-3227(94)90022-1, 1994.

Struck, U.: Stepwise postglacial migration of benthic foraminifera into the abyssal northeastern Norwegian Sea, Mar. Micropaleontol., 26, 207-213, https://doi.org/10.1016/0377-8398(95)00034-8, 1995.

Swoboda, S., Krumpen, T., Nöthig, E.-M., Metfies, K., Ramondenc, S., Wollenburg, J., Fahl, K., Peeken, I., and Iversen, M.: Release of ballast material during sea-ice melt enhances carbon export in the Arctic Ocean, PNAS Nexus, 3, https://doi.org/10.1093/pnasnexus/pgae081, 2024.

Sztybor, K. and Rasmussen, T.: Late glacial and deglacial palaeoceanographic changes at Vestnesa Ridge, Fram Strait: Methane seep versus non-seep environments, Palaeogeogr. Palaeoclimatol. Palaeoecol., 476, 77-89, https://doi.org/10.1016/j.palaeo.2017.04.001, 2017.

Thies, A.: Die Benthos-Foraminiferen im Europäischen Nordmeer, Ber. SFB 313, Kiel, Germany, 144, https://doi.org/10.2312/reports-sfb313.1991.31, 1991.

Thomas, E.: Cenozoic Mass Extinctions in the Deep Sea; What Disturbs the Largest Habitat on Earth?, D-III Fac. Publ., 424, 23, https://doi.org/10.1130/2007.2424(01), 2007.

Thomas, E., Booth, L., Maslin, M., and Shackleton, N. J.: Northeastern Atlantic benthic foraminifera during the last 45,000 years: Changes in productivity seen from the bottom up, Paleoceanography, 10, 545-562, https://doi.org/10.1029/94PA03056, 1995.

Timmermans, M.-L. and Marshall, J.: Understanding Arctic Ocean circulation: A review of ocean dynamics in a changing climate, J. Geophys. Res. Oceans, 125, https://doi.org/10.1029/2018JC014378, 2020.

Todd, R. and Low, D.: Foraminifera from the Kara and Greenland Seas, and review of arctic studies, U.S. Geol. Surv. Prof. Paper 1070, pages, GPO, https://doi.org/ 10.3133/pp1070, 1980.

Tsuchiya, M., Tazume, M., and Kitazato, H.: Molecular characterization of the non-costate morphotypes of buliminid foraminifers based on internal transcribed region of ribosomal DNA (ITS rDNA) sequence data, Mar. Micropaleontol., 69, 212-224, https://doi.org/10.1016/j.marmicro.2008.07.008, 2008.

https://doi.org/10.5194/egusphere-2025-6290
Preprint. Discussion started: 29 December 2025

Van Morkhoven, F. P. C. M., Berggren, W. A., Edwards, A. S., and Oertli, H. J.: Cenozoic Cosmopolitan Deep-water Benthic Foraminifera, Elf Aquitaine, 1986.

Vermassen, F., O'Regan, M., West, G., Cronin, T. M., and Coxall, H. K.: Testing the stratigraphic consistency of Pleistocene microfossil bioevents identified on the Alpha and Lomonosov Ridges, Arctic Ocean, AAAR?, 53, 309-323, https:/doi.org/10.1080/15230430.2021.1988356, 2021.

Wang, R., Polyak, L., Xiao, W., Wu, L., Zhang, T., Sun, Y., and Xu, X.: Late-Middle Quaternary lithostratigraphy and sedimentation patterns on the Alpha Ridge, central Arctic Ocean: Implications for Arctic climate variability on orbital time scales, Quat. Sci. Rev., 181, 93-108, https://doi.org/10.1016/j.quascirev.2017.12.006, 2018.

Wang, W., Zhao, M., Yang, J., Xiao, W., Wang, H., and Liu, Y.: The marine environmental evolution in the northern Norwegian Sea revealed by foraminifera during the last 60 ka, Adv. Polar Sci., 32, 210-220, https://doi.org/10.13679/j.advps.2021.0020, 2021.

West, G., Kaufman, D., Jakobsson, M., and O'Regan, M.: Amino acid racemization in *Neogloboquadrina pachyderma* and *Cibicidoides wuellerstorfi* from the Arctic Ocean and its implications for age models, Geochronology, 5, 285-299, https://doi.org/10.5194/gchron-2022-25, 2023.

Williamson, W. C.: On the recent Foraminifera of Great Britain, The Ray Society, London, 1-107, 1858.

Wollenburg, J.: Taxonomic notes on recent benthic foraminifera from Nansen Basin, Arctic Ocean, Ber. Polarforsch., 112, 136 pp., https://doi.org/10.2312/BzP_0112_1992 1992.

Wollenburg, J. E.: Benthic foraminiferal assemblages in the Arctic Ocean: indicators for water mass distribution, productivity, and sea ice drift, Ber. Polar., Alfred-Wegener-Institut, Bremerhaven, 227 pp., https://doi.org/10.2312/BzP_0179_1995, 1995.

Wollenburg, J. E. and Kuhnt, W.: The response of benthic foraminifers to carbon flux and primary production in the Arctic Ocean, Mar. Micropaleontol., 40, 189-231, https://doi.org/10.1016/S0377-8398(00)00039-6, 2000.

Wollenburg, J. E. and Mackensen, A.: Living benthic foraminifers from the central Arctic Ocean: faunal composition, standing stock and diversity, Mar. Micropaleontol., 34, 153-185, https://doi.org/10.1016/S0377-8398(98)00007-3, 1998a.

Wollenburg, J. E. and Mackensen, A.: On the vertical distribution of living (rose bengal stained) benthic foraminifers in the Arctic Ocean, J. Foraminifer. Res., 28, 268-285, https://doi.org/10.2113/gsjfr.28.4.268, 1998b.

Wollenburg, J. E. and Mackensen, A.: The ecology and distribution of benthic foraminifera at the Håkon Mosby mud volcano (SW Barents Sea slope), Deep Sea Res. Part I: Oceanographic Res. Pap., 56, 1336-1370, https://doi.org/10.1016/j.dsr.2009.02.004, 2009.

Wollenburg, J. E., Knies, J., and Mackensen, A.: High-resolution paleoproductivity fluctuations during the past 24 kyr as indicated by benthic foraminifera in the marginal Arctic Ocean, Palaeogeogr. Plaeoclimatol. Paleoecol., 204, 209-238, https://doi.org/10.1016/S0031-0182(03)00726-0, 2004.

Wollenburg, J. E., Kuhnt, W., and Mackensen, A.: (Table 2) Distribution of benthic foraminifers of sediment core PS2138-1, PANGAEA [dataset], https://doi.org/10.1594/PANGAEA.56208, 2001a.

https://doi.org/10.5194/egusphere-2025-6290
Preprint. Discussion started: 29 December 2025

Wollenburg, J. E., Kuhnt, W., and Mackensen, A.: Changes in Arctic Ocean paleoproductivity and hydrography during the last 145 kyr: the benthic foraminiferal record, Paleoceanography, 16, 65-77, https://doi.org/10.1029/1999PA000454, 2001b.

Wollenburg, J. E., Kuhnt, W., and Mackensen, A.: (Table 4a) Distribution of benthic foraminifera of sediment core PS2212-3, PANGAEA [dataset], https://doi.org/10.1594/PANGAEA.56209, 2001c.

Wollenburg, J. E., Kuhnt, W., and Mackensen, A.: (Table 4b) Distribution of benthic foraminifera of sediment core PS2212-3, PANGAEA [dataset], https://doi.org/10.1594/PANGAEA.56213, 2001d.

Wollenburg, J. E., Mackensen, A., and Kuhnt, W.: Benthic foraminiferal biodiversity response to a changing Arctic palaeoclimate in the last 24.000 years, Palaeo3, 255, 195-222, https://doi.org/10.1016/j.palaeo.2007.05.007, 2007.

Wollenburg, J. E., Raitzsch, M., and Tiedemann, R.: Novel high-pressure culture experiments on deep-sea benthic foraminifera — Evidence for methane seepage-related δ13C of *Cibicides wuellerstorfi*, Mar. Micropaleontol., 117, 47-64, https://doi.org/10.1016/j.marmicro.2015.04.003, 2015.

Wollenburg, J. E., Matthiessen, J., Vogt, C., Nehrke, G., Grotheer, H., Wilhelms-Dick, D., Geibert, W., and Mollenhauer, G.: Omnipresent authigenic calcite distorts Arctic radiocarbon chronology, Commun. Earth Environ., 4, 136, https://doi.org/10.1038/s43247-023-00802-9, 2023.

WoRMS, E. B. o.: World Register of Marine Species (WoRMS), https://doi.org/10.14284/170, 2025.

Xiao, W., Polyak, L., Wang, R., Löwemark, L., Mei, J., You, D., Wang, W., Wu, L., and Jin, X.: Middle to Late Pleistocene Arctic paleoceanographic changes based on sedimentary records from Mendeleev Ridge and Makarov Basin, Quat. Sci. Rev., 228, 106105, https://doi.org/10.1016/j.quascirev.2019.106105, 2020.

Yurco, L. N., Ortiz, J. D., Polyak, L., Darby, D. A., and Crawford, K. A.: Clay mineral cycles identified by diffuse spectral reflectance in Quaternary sediments from the Northwind Ridge: implications for glacial–interglacial sedimentation patterns in the Arctic Ocean, Polar Res., 29, 176-197, https://doi.org/10.1111/j.1751-8369.2010.00160.x, 2010.

bforams@mikrotax website: http://www.mikrotax.org/bforams, last access: 2025-11-17.?????

Zhao, S., Dong, L., Shi, X., Polyak, L., Zou, X., Wang, W., and Wu, D.: Sedimentary record of glacial impacts and melt water discharge off the East Siberian Continental Margin, Arctic Ocean, J. Geophys. Res. Oceans, 127, https://doi.org/10.1029/2021JC017650, 2022.